



**The pathogenic role of endogenous antibodies in a mouse model for
Charcot-Marie-Tooth 1B neuropathy**

**Die pathogenetische Funktion von endogenen Antikörpern in einem
Maus-Modell der Charcot-Marie-Tooth 1B Neuropathie**

**Doctoral thesis for a doctoral degree
at the Graduate School of Life Sciences,
Julius-Maximilians-Universität Würzburg,
Section Neuroscience**

submitted by

Dennis Klein

from

Alzenau i. Ufr.

Würzburg 2015

Submitted on:

Members of the *Promotionskomitee*:

Chairperson: Prof. Dr. Utz Fischer

Primary Supervisor: Prof. Dr. Rudolf Martini

Supervisor (Second): Prof. Dr. Wolfgang Rössler

Supervisor (Third): Prof. Dr. Claudia Sommer

Date of Public Defence:

Date of Receipt of Certificates:

Affidavit

I hereby confirm that my thesis entitled “The pathogenic role of endogenous antibodies in a mouse model for Charcot-Marie-Tooth 1B neuropathy” is the result of my own work. I did not receive any help or support from commercial consultants. All sources and / or materials applied are listed and specified in the thesis.

Furthermore, I confirm that the thesis has not yet been submitted as part of another examination process neither in identical nor in similar form.

Place, Date

Signature

Eidesstattliche Erklärung

Hiermit erkläre ich an Eides statt, die Dissertation „Die pathogenetische Funktion von endogenen Antikörpern in einem Maus-Modell der Charcot-Marie-Tooth 1B Neuropathie“ eigenständig, d.h. insbesondere selbstständig und ohne Hilfe eines kommerziellen Promotionsberaters, angefertigt und keine anderen, als die von mir angegebenen Quellen und Hilfsmittel verwendet zu haben.

Ich erkläre außerdem, dass die Dissertation weder in gleicher noch in ähnlicher Form bereits in einem anderen Prüfungsverfahren vorgelegen hat.

Ort, Datum

Unterschrift

Table of contents

1. Abstract	6
2. Zusammenfassung	7
3. Introduction	9
3.1. Charcot-Marie-Tooth neuropathies	9
3.2. Rodent models for CMT1	10
3.3. Low grade inflammation as an important amplifier in the pathogenesis of CMT1.....	11
3.3.1. The innate immune system	11
3.3.2. The adaptive immune system	13
3.4. Aim of the study	15
4. Material and methods	16
4.1. Equipment, buffers and solutions, antibodies, and primer sequences	16
4.2. Animals and genotyping	16
4.3. Sciatic nerve crush injury	16
4.4. Dissection and tissue processing	17
4.5. Immunohistochemistry	18
4.6. RNA extraction and semi-quantitative real-time PCR	20
4.7. Western blot analysis.....	21
4.8. Electron microscopy and morphological analysis	22
4.9. Reconstitution experiments	22
4.10. Nerve conduction studies.....	22
4.11. Statistical analysis.....	23
5. Results	24
5.1. Antibodies accumulate in peripheral nerves of P0het myelin mutant mice	24
5.2. Lack of evidence for complement deposition.....	28
5.3. Reduced macrophage numbers in peripheral nerves of 6-month-old P0het JHD ^{-/-} mice	30
5.4. JHD deficiency ameliorates the demyelinating phenotype in 6-month-old P0het mutant mice	34
5.5. Passive transfer of antibodies reverts the ameliorated demyelinating phenotype in 6-month-old P0het JHD ^{-/-} mice	35

5.6. Increased macrophage numbers in peripheral nerves of 12-month-old P0het JHD-/-	38
5.7. JHD deficiency aggravates the demyelinating phenotype in 12-month-old P0het mutant mice	40
5.8. Altered numbers of immune-related cells in 12-month-old P0het JHD-/- mice	45
6. Discussion	52
6.1. Endogenous antibodies accumulate in peripheral nerves of P0het myelin mutant mice	52
6.2. Crucial role for endogenous antibodies in early macrophage-mediated demyelination	54
6.3. JHD deficiency triggers increased immune reactions and disease aggravation in 12-month-old P0het mice	56
6.4. The immune system as a therapeutic target for CMT1	60
6.5. Synopsis.....	62
7. References	64
8 Appendices	74
8.1 Technical equipment.....	74
8.2. Reagents.....	75
8.3. Buffers and solutions	77
8.4. Primer sequences for genotyping	80
8.5. Antibodies used in immunohistochemistry	81
9. Abbreviations	83
10. Curriculum vitae	86
11. Publications	87
12. Danksagung	90

Parts of the results presented in this thesis have been published:

Klein D, Groh J, Weishaupt A, Martini R (2015) Endogenous antibodies contribute to macrophage-mediated demyelination in a mouse model for CMT1B. *J Neuroinflammation* 12:267.

The published manuscript and this thesis contain similar text passages in adapted form in some sections.

1. Abstract

Charcot-Marie-Tooth (CMT) type 1 neuropathies are a genetically heterogeneous group of non-treatable inherited disorders affecting the peripheral nervous system that lead to sensory and motor dysfunction. Secondary low grade inflammation, implicating the innate and adaptive immune system, could previously be identified as a substantial disease modifier in two mouse models for CMT1, CMT1B and 1X, respectively. However, the exact mechanism how the adaptive immune system contributes to disease pathogenesis is not completely understood. Based on observations that the accumulation of endogenous antibodies to myelin components is important for rapid myelin clearance after nerve injury during Wallerian degeneration, a possibly similar mechanism was considered for endogenous antibodies as disease amplifier in mice heterozygously deficient for P0 (P0het), mimicking some typical features of CMT1B.

In this study an increased antibody deposition was detected in the affected peripheral nerves of P0het myelin mutant mice. By crossbreeding P0het mutants with mice specifically lacking B-lymphocytes, and therefore antibodies (JHD^{-/-}), a decline of endoneurial macrophages together with a substantially ameliorated demyelination could be demonstrated in 6-month-old mutant mice. Moreover, reconstitution with murine IgGs reverted the neuropathic phenotype, substantiating that endogenous antibodies are potentially pathogenic at this early stage of disease. Unexpectedly, in 12-months-old P0het mutants, JHD deficiency resulted in disease aggravation accompanied by an increased inflammatory reaction and M2-polarized macrophage response.

These observations suggest that in a mouse model for CMT1B, the lack of endogenous antibodies has a dichotomous effect: ameliorating early macrophage-mediated demyelination, as opposed to increasing inflammatory reactions leading to disease aggravation at older ages.

2. Zusammenfassung

Als Charcot-Marie-Tooth (CMT) Typ 1 Erkrankungen bezeichnet man eine genetisch heterogene Gruppe von nicht behandelbaren, erblichen Neuropathien, die das periphere Nervensystem betreffen und letztendlich zu starken motorischen und sensorischen Defiziten führen. Anhand verschiedener Studien konnte gezeigt werden, dass sekundäre Entzündungsreaktionen, insbesondere des angeborenen und adaptiven Immunsystems, eine entscheidende Rolle bei der Pathogenese von zwei verschiedenen CMT1-Mausmodellen (CMT1B und CMT1X) spielen. Jedoch ist der genaue Mechanismus, in dem das adaptive Immunsystem zur Pathogenese beiträgt, nicht komplett bekannt. In einer veröffentlichten Studie wurden gebundenen endogenen Antikörpern eine wichtige Rolle beim raschen Myelinabbau nach Nervläsion während der Waller'schen Degeneration zugeschrieben. In Mäusen, die heterozygot defizient für P0 (P0het) sind und einige typische Merkmale der CMT1B Neuropathie aufweisen, sollte ein möglicherweise ähnlicher Mechanismus von endogenen Antikörpern untersucht werden, der zur Verstärkung der Krankheitsentwicklung führt.

In dieser Studie konnte eine vermehrte Antikörperbindung in den betroffenen peripheren Nerven von P0het Myelinmutanten beobachtet werden. Anhand von Verkreuzungs-Experimenten von P0het Mutanten mit Mäusen, die keine B-Lymphozyten besitzen und daher keine Antikörper bilden können (JHD-/-), konnte zudem in den untersuchten 6 Monate alten Doppelmutanten eine verringerte Anzahl endoneuraler Makrophagen und eine deutliche Verbesserung der Demyelinisierung aufgezeigt werden. Zusätzlich konnte anhand von Rekonstitutions-Experimenten mit mausspezifischen-IgGs der neuropathische Phänotyp in peripheren Nerven wiederhergestellt werden, was die mögliche pathogenetische Rolle endogener Antikörper im frühen Stadium der Erkrankung bekräftigt. Unerwarteterweise führte die JHD-Defizienz jedoch in 12 Monate alten P0het Mausmutanten eher zu einer Verschlechterung der Neuropathie, zusammen mit einer verstärkten Entzündungsreaktion und M2-polarisierten Makrophagen-Aktivierung.

Diese Beobachtungen deuten darauf hin, dass das Fehlen von Antikörpern in einem etablierten Mausmodell für CMT1B unterschiedliche Folgen hat, da dies zu einer verringerten Makrophagen-vermittelten Demyelinisierung im frühen Erkrankungsverlauf

führt, gleichzeitig aber im späteren Alter in einer verstärkten Entzündungsreaktion und einem vermehrten Nervschaden resultiert.

3. Introduction

3.1. Charcot-Marie-Tooth neuropathies

Charcot-Marie-Tooth (CMT) disease, also known as hereditary motor and sensory neuropathy (HMSN), is a genetically heterogeneous group of non-treatable hereditary neuropathies with a prevalence of 1:2500 affecting the peripheral nervous system (PNS). They are named after Jean-Martin Charcot, Pierre Marie, and Howard Tooth, who first described the disease in 1886. CMT is divided into demyelinating (CMT1 and CMT4) and axonal neuropathies (CMT2), whereas severely affected patients diagnosed with congenital hypomyelinating neuropathies (CHN) or Dejerine-Sottas neuropathies (DSN) are designated as CMT3 (Reilly and Shy, 2009; Patzko and Shy, 2011). Usually nerve conduction velocity (NCV) measurements are used as a diagnostic tool to distinguish between demyelinating (<38 m/s) or axonal forms (>38 m/s) (Reilly and Shy, 2009; Patzko and Shy, 2011). The age of onset can vary from early childhood to adulthood. Patients are clinically characterized by progressive distal muscle weakness, muscle wasting, sensory dysfunction, skeletal abnormalities (scoliosis) and foot deformities (pes cavus), as well as the classical 'steppage' gait (Saporta and Shy, 2013; Brennan et al., 2015). To date no causative cure is available and only rehabilitative strategies or surgeries are available as therapeutic approaches for CMT patients (Schenone et al., 2011).

In the last years new diagnostic tools (high-throughput sequencing) in research made it possible to discover underlying genetic causes and new mutations in CMT. So far, mutations in over 80 disease-causing genes have been described (Timmerman et al., 2014) and the most common forms are described below. A 1.4-Mb duplication on chromosome 17, containing the peripheral myelin protein 22 (PMP22) gene, is responsible for the most frequent form of CMT, CMT1A (Reilly et al., 2011). The X-chromosomal dominant form of CMT, CMT1X, is the second most common subtype and caused by mutations in the gene encoding the gap junction protein Connexin 32 (Cx32/Gjb1). More than 300 causative mutations have been described in this gene (Kleopa and Scherer, 2006; Reilly et al., 2011). CMT1 type B comprises about 5-10% of all CMT1 patients and is caused by mutations in myelin protein zero (MPZ/P0). Some mutations in the MPZ/P0 gene are also associated with the severe early onset neuropathy CMT3 (Shy et al., 2004). Thirteen genes have been identified to cause the autosomal recessive form of CMT, CMT4. Among these are mutations in myotubularin-related protein (MTMR2), periaxin or EGR2, also known as

KROX20 (Reilly et al., 2011; Brennan et al., 2015). Most of these cause a demyelinating neuropathy. The axonal subtype CMT2 can result - among others - from mutations in mitofusin 2 (MFN2) or the neurofilament light polypeptide gene (NEFL). They can affect mitochondrial function and energy support, neurofilament assembly, as well as axonal transport (Shy and Patzko, 2011; Jerath and Shy, 2015).

3.2. Rodent models for CMT1

In the past years a series of genetically modified rodent models have been generated in CMT1 research (Fledrich et al., 2012). Similar to patient biopsies, peripheral nerves of mouse models show typical hallmarks such as segmental demyelination, axonal degeneration, and formation of ‘onion bulbs’. The latter are supernumerary Schwann cells (SCs) that share the expression of molecules typical for immature SCs (Guenard et al., 1996; Klein et al., 2014) and possibly develop from consecutive episodes of de- and remyelination (Suter and Scherer, 2003; Casasnovas et al., 2008).

In mouse models for CMT1A it was demonstrated that the degree of nerve fiber damage correlates with the level of PMP22 expression. For instance, PMP22 overexpressing mice with seven copies of the human gene (strain C22) develop an obvious neuropathic phenotype with pronounced demyelination. In contrast, heterozygous C61 mice with only four copies of PMP22 are characterized by a milder neuropathic phenotype (Huxley et al., 1996; Huxley et al., 1998). Moreover, homozygous transgenic rats with three extra copies of the murine PMP22 gene develop a severe phenotype, whereas heterozygous rats are less affected and characterized by motor impairment and demyelination, resembling human CMT1A patients (Sereda et al., 1996).

Although more than 300 mutations have been described for the X-linked form of CMT1, most of them result in a rather uniform clinical phenotype. Therefore, CMT1X is considered to be caused by loss of function mutations (Kleopa and Scherer, 2006; Reilly et al., 2011). Corresponding mice with deleted Cx32/Gjb1 alleles (Cx32def) develop a progressive, demyelinating peripheral neuropathy beginning at approximately 3 months of age comparable to those abnormalities associated with human CMT1X (Anzini et al., 1997; Scherer et al., 1998).

To date, more than 100 different mutations in the MPZ/P0 gene are known which result in a variable outcome (Gabreels-Festen et al., 1996). Several point mutations and deletions are associated with human CMT1B (Hayasaka et al., 1993c; Hayasaka et al., 1993b; Hayasaka et al., 1993a; Himoro et al., 1993; Kulkens et al., 1993; Nelis et al., 1994). Among these mutations, a deletion of serine 63 was identified to cause CMT1B (Kulkens et al., 1993) and the corresponding MpzS63del model exhibits demyelination and reduced NCV. Moreover, it was shown that the mutated protein is retained in the endoplasmic reticulum and activates the unfolded protein response (UPR) (Wrabetz et al., 2006). On the other hand heterozygous knockout mice (P0het) that were used in this study, show mainly normal myelin until postnatal week 10, but develop a mild, progressive neuropathy and are characterized by demyelination, formation of onion bulbs and a reduced motor NCV (Giese et al., 1992; Martini et al., 1995; Shy et al., 1997). Of note, mainly motor axons are affected in most of the described animal models, which is in contrast to affected human sensory sural nerve biopsies (Martini, 1997).

It has been reported that P0het, Cx32def, and PMP22tg (C61) mice develop characteristic molecular abnormalities (Klein et al., 2014). However, despite the different nature and function of mutated proteins, corresponding mouse models develop a similar disease outcome. These similarities in the nerve phenotype might suggest the activation of common pathomechanisms that will be described in the following part.

3.3. Low grade inflammation as an important amplifier in the pathogenesis of CMT1

3.3.1. The innate immune system

Several previous studies could demonstrate that chronic low grade inflammation acts as a substantial disease modifier in the pathogenesis of distinct CMT1 mouse models (Martini et al., 2008; Martini et al., 2013). An age-dependent increase in the number of endoneurial macrophages - as a part of the innate immune system - has been described in peripheral nerves of mutant mice compared to wildtype littermates (Schmid et al., 2000; Carenini et al., 2001; Kobsar et al., 2002; Kobsar et al., 2005). Moreover, macrophages in myelin mutant mice enter endoneurial tubes and often acquire a 'foamy' appearance due to increased myelin phagocytosis and subsequent degradation (Ip et al., 2006). Interestingly, the dynamic in the increase of macrophages numbers differs between distinct CMT1

mouse models. P0het and Cx32def myelin mutant mice are characterized by gradually increasing macrophage numbers beginning at 3 months of age (Schmid et al., 2000; Carenini et al., 2001; Kobsar et al., 2002), whereas PMP22tg mice show an initial elevation of macrophage numbers that only moderately increase during aging (Kobsar et al., 2005; Kohl et al., 2010a). This correlates also with the course of the disease, as PMP22tg mice exhibit already early signs of pathological alterations compared to the other two models (Klein et al., 2014).

To date, at least two important mediators of macrophage activation have been identified in mouse models for CMT1. These are the Schwann cell derived chemokine CCL2 (also known as MCP-1: monocyte chemoattractant protein-1) and the fibroblast derived colony stimulating factor-1 (CSF-1/M-CSF) (Groh et al., 2010; Groh et al., 2012). It could be shown that the expression of both cytokines is elevated in peripheral nerves of myelin mutant mice compared to wildtype littermates (Fischer et al., 2008b; Groh et al., 2010; Groh et al., 2012). CSF-1 is the pivotal regulator of macrophage function and survival (Chitu and Stanley, 2006) and it was shown that CSF-1 stimulates the proliferation of nerve-resident macrophages (Müller et al., 2007). Moreover, crossbreeding experiments with osteopetrotic (op) mice that have an inactivating mutation in the coding region of CSF-1 (Yoshida et al., 1990) demonstrated for the first time that macrophages actively contribute to the pathological alterations seen in CMT1 mutant mice (Carenini et al., 2001; Groh et al., 2012). In P0het and Cx32def mice, the lack of CSF-1 prevented the increase in macrophage numbers in peripheral nerves and led to a robust and persistent amelioration of the demyelinating phenotype, preservation of axons, and reduced muscle denervation (Carenini et al., 2001; Groh et al., 2012; Groh et al., 2015). Similar consequences of CSF-1 deficiency were observed in PMP22tg mutant mice (Groh and Martini, unpublished observations). In contrast, bone marrow transplantation studies in the corresponding CMT1 mouse models revealed that CCL2 is important for the infiltration of macrophages into peripheral nerves in P0het and Cx32def mice (Fischer et al., 2008b; Groh et al., 2010) and crossbreeding experiments with CCL2-deficient mice gave further evidence for a functional role of macrophages in the pathogenesis of CMT1 mouse models. P0het, Cx32def, and PMP22tg mice that were heterozygously deficient for CCL2 - and therefore expressed only half the dose of the chemokine - showed substantially attenuated macrophage recruitment and an ameliorated demyelinating phenotype. Moreover, axonal properties were significantly improved in the CMT1X mouse model (Groh et al., 2010).

Interestingly, the complete absence of CCL2 did not attenuate macrophage numbers and ameliorate the demyelinating phenotype in peripheral nerves of P0het and Cx32def mice. A likely compensatory upregulation of CSF-1 expression and subsequent proliferation of nerve-resident macrophages counteracts the reduced infiltration of macrophages from the periphery, revealing a correlation between the total number of endoneurial macrophages and subsequent nerve damage (Fischer et al., 2008b; Groh et al., 2010). Additionally, by crossbreeding P0het mutants with mice lacking the macrophage-restricted adhesion molecule sialoadhesin (Siglec-1) (Oetke et al., 2006), the corresponding double mutants had reduced numbers of endoneurial macrophages together with an ameliorated demyelinating phenotype (Kobsar et al., 2006).

Together these results demonstrate that macrophages are actively involved in disease development, however, the exact mechanisms that contribute to macrophage-mediated demyelination and axonal perturbation in CMT1 mouse models need to be further investigated.

3.3.2. The adaptive immune system

Other studies showed that - in addition to the innate immune system - the adaptive immune system is involved in the pathogenesis of CMT1 mouse models. First evidence for a contribution of the adaptive immune system was gained by observations that some patients responded positively upon immunomodulation (Dyck et al., 1982). Moreover, lymphocytes were elevated in the blood of CMT patients (Williams et al., 1987; Williams et al., 1993) and peripheral nerves of myelin mutant mice (Shy et al., 1997; Schmid et al., 2000). A detrimental role of the adaptive immune system could be demonstrated, when RAG1-deficient mice that lack both mature T- and B-lymphocytes (Mombaerts et al., 1992) were crossbred with P0het and Cx32def mice. This caused a persistent and substantial amelioration of demyelination and axonal perturbation together with a reduction of macrophages (Schmid et al., 2000; Kobsar et al., 2003). However, no beneficial effect was detectable in PMP22tg mutant mice that were RAG1-deficient (Kohl et al., 2010b). Further crossbreeding experiments of P0het mutant mice with TCR- α -deficient mice (Philpott et al., 1992), lacking $\alpha\beta$ T-lymphocytes, but with normal B-lymphocytes, resulted also in an amelioration of the demyelinating phenotype (Schmid et al., 2000). In a reciprocal experiment, P0het mice deficient for the co-inhibitory molecule programmed cell death-1 (PD-1), which is expressed on the surface of activated T- and B-lymphocytes, showed an

increased inflammatory reaction and aggravated neuropathy, corroborating the impact of the adaptive immune system (Kroner et al., 2009). Furthermore, transplantation of wildtype bone marrow into RAG1-deficient P0het mice reverted the beneficial effect of RAG1 deficiency, confirming the direct pathogenic role of lymphocytes (Mäurer et al., 2001). Based on these results and the observations that T-lymphocytes, but not B-lymphocytes, are present in peripheral nerves and increase in numbers during disease progression, CD8-positive T-lymphocytes were considered to be the culprit cells contributing to the pathogenic process (Schmid et al., 2000; Mäurer et al., 2001). However, by means of further bone marrow reconstitution experiments into P0het RAG1^{-/-} mice, neither CD8- nor CD4-positive T-lymphocytes could be unequivocally identified as the only pathogenic mediators (Kroner and Martini, unpublished observations).

The search for an alternative explanation for these latter observations and for the beneficial effect of RAG1 deficiency in myelin mutants shifted the focus on B-lymphocytes. They can give rise either to antigen-presenting cells or to plasma cells, the main source for antibody production (Mauri and Bosma, 2012). Favoring the possibility of antibodies, a recent study could reveal an important role of immunoglobulins following peripheral nerve injury during Wallerian degeneration (Vargas et al., 2010). The authors detected that endogenous antibodies rapidly accumulate after crush injury along myelinated fibers distal to the lesion site and contribute to the recruitment of macrophages. Furthermore, they demonstrated that mice deficient for B-lymphocytes, and therefore lacking antibodies, exert a reduced macrophage activation leading to delayed removal of myelin debris and compromised regeneration after nerve injury (Vargas et al., 2010).

In the present study the hypothesis was tested whether endogenous antibodies could function as potential recognition signals for phagocytosing macrophages in peripheral nerves of a CMT1B mouse model (P0het) and thereby contribute to disease pathogenesis.

3.4. Aim of the study

Immune reactions, implicating the innate and adaptive immune system, are functionally important modulators in mouse models for CMT1, representing non-treatable, inherited disorders affecting the peripheral nervous system. However, the exact mechanism how the adaptive immune system contributes to disease pathogenesis is not completely understood. Since antibodies have recently been shown to contribute to myelin clearance during Wallerian degeneration, the aim of this study was to analyze the impact of endogenous antibodies in a mouse model for CMT1B (P0het) by addressing the following issues:

- Investigating if antibodies are deposited in peripheral nerves of myelin mutant mice.

- Studying the pathological relevance of antibody depositions:
 - by investigating macrophage activation and nerve pathology when antibodies are genetically depleted in P0het mice.

 - by scoring the effect of antibody reconstitution in genetically depleted P0het mice.

4. Material and methods

4.1. Equipment, buffers and solutions, antibodies, and primer sequences

Technical equipment (Appendix 8.1), reagents (Appendix 8.2), buffers and solutions (Appendix 8.3) as well as primer sequences for genotyping (Appendix 8.4) and antibodies for immunohistochemistry (Appendix 8.5) are listed in detail in the appendices. Unless mentioned otherwise, standard material was used for laboratory work.

4.2 Animals and genotyping

Mice heterozygously deficient for P0 (P0het) (Giese et al., 1992) were crossbred with animals specifically lacking B-lymphocytes (JHD^{-/-}) (Chen et al., 1993) according to previously published protocols (Schmid et al., 2000) and investigated at 6 and 12 months of age with the corresponding littermates of both gender. Additionally, RAG1-deficient mice, lacking both B- and T-lymphocytes, were analyzed (Mombaerts et al., 1992). All mice were on a C57BL/6N background and genotypes were identified after purification of genomic DNA from ear biopsies using DNeasy blood & tissue kit (Qiagen) according to the manufacturer's guidelines. Genotypes were determined by conventional PCR (respective primer sequences listed in appendix 8.4). Animals were kept in the animal facility of the Department of Neurology, University clinic of Wuerzburg, in a 12h/12h day (<300 lux)/night rhythm under barrier conditions using individually ventilated cages. All animal experiments were approved by the local authority, the Government of Lower Franconia, Germany.

4.3. Sciatic nerve crush injury

Wildtype mice were deeply anesthetized by an intraperitoneal injection of a mixture of ketavet and xylavet (10 µl per g body weight). The right sciatic nerve was exposed and crushed at the region of the sciatic notch by using a non-serrated clamp with a constant pressure for 15 s. This resulted in a completely translucent appearance of the crushed area of the nerve. After 3 days, the mice were sacrificed and lesioned nerves were removed for analysis of complement deposition (see below). All operations were performed by Dr. Chi Wang Ip.

4.4 Dissection and tissue processing

For preparation of fresh frozen spleens, flexor digitorum brevis muscles and femoral nerves, animals were killed by asphyxiation with CO₂ (according to guidelines by the State Office of Health and Social Affairs Berlin), blood was transcardially rinsed with phosphate-buffered saline (PBS) containing heparin, followed by harvesting and embedding nerves in O.C.T. medium and frozen in liquid nitrogen-cooled methyl butane. For isolation of total RNA and protein, tissue was snap frozen in liquid nitrogen and stored at -80°C.

In case of preparation for fixed femoral nerves, blood was transcardially rinsed with PBS/heparin and a perfusion with 4% paraformaldehyde (PFA) in PBS for 10 min was performed. Dissected nerves were post-fixed in the same solution for 2 h, stored in 30% sucrose/PBS over night at 4°C, and embedded in O.C.T. medium. Fresh frozen and fixed peripheral nerves were cut into 10 µm-thick cross-sections on a cryostat (Leica) and stored at -20°C before further processing.

For single teased fiber preparations, blood was transcardially rinsed with PBS/heparin followed by perfusion with 2% PFA in PBS for 10 min. Femoral quadriceps and sciatic nerves were dissected, the perineurium removed and single fibers were separated by forceps on glass slides. Alternatively, blood was transcardially rinsed with PBS/heparin and unfixed sciatic nerves were separated into small fiber bundles followed by incubation in PBS in a 96-well plate (free floating).

For electron microscopy, mice were transcardially rinsed with PBS/heparin followed by perfusion with 4% PFA and 2% glutaraldehyde in 0.1M cacodylate buffer for 15 min. Dissected nerves were post-fixed in the same solution over night at 4°C. After osmification with 2% osmiumtetroxide in 0.1M cacodylate buffer (2 h) and dehydration in ascending acetone concentrations samples were embedded in Spurr's medium. Semithin sections (0.5 µm) were stained with alkaline methylene blue and analyzed by light microscopy. Ultrathin sections (80 nm) were mounted to copper grids, counterstained with lead citrate, and analyzed by electron microscopy.

4.5 Immunohistochemistry

For identification of endogenous antibodies on nerve cross-sections or teased fibers, PFA-fixed samples were blocked for 30 min with 10% bovine serum albumin (BSA) and 1% normal goat serum (NGS) in 0.1M PBS, followed by incubation with Cy3-conjugated goat anti-mouse IgG-Fc antibodies in 1% BSA and 1% NGS in 0.1M PBS for 1 h at room temperature (RT). Alternatively, samples were incubated over night with non-coupled rabbit anti-mouse IgG-Fc antibodies at 4°C. After washing steps with PBS corresponding Cy3-conjugated secondary antibodies were added for 1 h at RT.

To investigate if antibodies are bound to extra- or intracellular domains, unfixed and non-permeabilized native sciatic nerves were incubated free floating in a 96-well plate (Klein et al., 2015). IgG-Fc staining was performed equally as described above. To control for intracellular antibody binding, nerve fibers were permeabilized by repeated cycles of freezing in liquid nitrogen and thawing. Incubation with rabbit anti-mouse β -III-Tubulin and detection with the corresponding Cy3-conjugated secondary antibodies for 1 h was performed as a positive control.

Complement deposition was identified on teased fiber preparations as described elsewhere (Klein et al., 2015). Briefly, samples were fixed in acetone (10 min, -20°C), blocked with 5% NGS with 0.3% TritonX-100 in 0.1M PBS, and incubated with FITC-conjugated goat anti-mouse C3 antibodies in 1% NGS with 0.3% TritonX-100 in 0.1M PBS for 1 h at RT. As positive controls, single teased fibers from distal parts of lesioned sciatic nerves (3 days after crush) were identically treated. As another positive control, diaphragms, incubated *ex vivo* with anti-ganglioside monoclonal antibodies and normal human serum (Goodyear et al., 1999) (provided by Dr. Rhona McGonigal) were investigated for complement deposition in the same way, whereby postsynaptic terminals were identified with Alexa Fluor 555-conjugated α -Bungarotoxin.

For staining of endoneurial macrophages, fresh-frozen samples were fixed in acetone, blocked with 5% BSA in 0.1M PBS followed by an avidin-biotin blocking step. Afterwards biotinylated rat anti-F4/80 primary antibodies in 1% BSA in 0.1M PBS were applied for 1 h at RT and detected by Cy3-conjugated Streptavidin (1:100, CED-CLCSA1010, Biozol).

For identification of macrophage polarization, immunohistochemical stainings against CD86 (M1-marker) or CD206 (M2-marker) were performed on fresh frozen nerve samples. Sections were fixed in acetone followed by blocking with 5% BSA in 0.1 M PBS. After incubation over night at 4°C, primary antibodies (in 0.1 M PBS containing 1% BSA) were detected by the corresponding Cy3-conjugated secondary antibodies. In case of CD206 labeling, 0.3% TritonX-100 was added to the blocking and antibody solutions.

To quantify T-lymphocytes, fresh frozen nerve sections were treated the same way as described before (see section CD86) with primary antibodies (CD4, CD8) over night and detection with corresponding Cy3-conjugated secondary antibodies the next day.

In all cases nuclei were visualized by incubation with DAPI (1:500000, D9542, Sigma-Aldrich) for 10 min at RT.

Immunohistochemical stainings against B-lymphocytes were performed on cross-sections of the spleen. Therefore, fresh-frozen samples were fixed in acetone, blocked with 5% BSA in 0.1M PBS and incubated with rat anti-B220/CD45R primary antibodies in 1% BSA in 0.1M PBS over night at 4°C and detected by Cy3-conjugated secondary antibodies.

Immunohistochemistry for SMI32 (recognizing non-phosphorylated neurofilaments) as a marker for axonal perturbation was performed on femoral nerve cross-sections as previously described (Klein et al., 2014). Briefly, after acetone fixation and blocking with 5% BSA and 5% NGS with 0.2% TritonX-100 in 0.1M PBS (30 min at RT) respective primary antibodies (SMI32, P0) were incubated over night at 4°C in 1% BSA 1% NGS with 0.2% TritonX-100 in 0.1M PBS and detected by corresponding secondary antibodies.

To study muscle innervation, flexor digitorum brevis cross-sections were blocked with 5% BSA with 0.3% TritonX-100 in 0.1M PBS and, for visualization of presynaptic terminals, incubated with a guinea pig anti-synaptophysin primary antibody at 4°C over night in 1% BSA with 0.3% TritonX-100 in 0.1M PBS followed by incubation with Cy3-conjugated donkey anti-guinea pig IgG secondary antibodies. Postsynapses were labeled with Alexa Fluor 488-conjugated α -Bungarotoxin (1:300, B-13422, Molecular Probes). At least 80 neuromuscular junctions per animal were quantified and categorized as being either innervated or denervated/partially denervated.

All samples were embedded after a final washing step with either Aqua-Poly/Mount[®] (Polysciences) or DABCO and encircled with Vitro-Clud[®] (Langenbrinck). Detailed information about the antibodies used in this study can be found in appendix 8.5.

Digital fluorescence microscopic images were acquired using an Axiophot 2 microscope (Zeiss) equipped with a CCD camera (Visitron Systems) and afterwards processed with Photoshop CS3 (Adobe). In case of P0/SMI32 immunohistochemistry, images were acquired on a FluoView FV1000 confocal microscope and processed using FluoView software (Olympus Germany). For quantification of immune cells (CD4, CD8, CD86, CD206, F4/80), whole nerve cross-sections were analyzed and the mean number of corresponding cells per section in seven to ten consecutive sections per animal was calculated. IgG fluorescence intensity in the endoneurium of femoral quadriceps nerve cross-sections was measured with ImageJ (NIH) as described elsewhere (Klein et al., 2015). Images were converted to 32 bit grayscale images and the mean gray value of the endoneurium was calculated to determine immunoreactive signals, taking the mean gray value of P0wt nerves as a reference value of '1'. Data is shown as the mean of n = 2 per genotype of three repeated stainings. At least three sections per animal and experiment were analyzed.

4.6. RNA extraction and semi-quantitative real-time PCR

RNA extraction and semi-quantitative real-time PCR (qRT-PCR) were performed as previously described (Fischer et al., 2008a). Briefly, snap frozen femoral quadriceps nerves were homogenized (ART Labortechnik) in TRIzol[®] reagent (Invitrogen). Total RNA was isolated by Phenol-Chloroform extraction, phase separation and subsequent precipitation according to the guidelines of manufacturer. Additionally, 20 µg of Glycogen (Roche) was added to each sample before RNA-precipitation. Precipitated RNA was subsequently solubilized in 10 µl DEPC-H₂O and incubated at 60°C for 10 min. Afterwards the concentration and the quality of RNA were measured using a photometer (Eppendorf).

0.5 µg of RNA was reverse transcribed in a 100 µl reaction using random hexamer primers and MuLV reverse transcriptase (Applied Biosystems) according to the guidelines of manufacturer with the following cycler conditions: 10 min at 25°C; 60 min at 37°C; 5 min at 95°C. 1.5 µl of the resulting complementary DNA (cDNA) was analyzed in duplicates or triplicates by semi-quantitative real-time PCR using pre-developed TaqMan[®] assays

(eukaryotic 18s rRNA, 4319413E; murine Arginase1, Mm00475988_m1; CD86, Mm00444543; CD206, Mm00485148_m1; CSF-1, Mm00432688_m1, FcγRI, Mm00438874_m1; FcγRIIB, Mm00438875_m1; FIZZ1, Mm00445109; IFNγ, Mm01168134_m1; IL-1β, Mm00434228_m1; IL-6, Mm00446190_m1; iNOS, Mm00440485_m1; LIF, Mm00434761_m1; CCL2/MCP-1, Mm99999056_m1; TGF-β, Mm00441724_m1; TNFα, Mm00443258_m1; TREM-2, Mm00451744_m1; Ym1, Mm00657880_mH) and TaqMan® universal PCR master mix (Applied Biosystems) according to the instructions of the manufacturers (10 μl per sample). Data sets were analyzed with the $\Delta\Delta C_T$ method in relation to the corresponding 18s RNA content and were related to a wildtype sample.

4.7. Western blot analysis

Dissected femoral quadriceps nerves were snap frozen in liquid nitrogen. After sonification (Sonoplus HD60, Bandelin electronic) in 100 μL RIPA lysis buffer per 10 mg tissue, protein concentrations were determined by a Lowry assay (Sigma-Aldrich) using BSA as standard (Lowry et al., 1951). Samples were combined with 6x Laemmli sample buffer (Laemmli, 1970) and denatured for 5 min at 95°C. Equal amounts of proteins were resolved by sodium dodecyl sulfate-polyacrylamide gel electrophoresis (SDS-PAGE with 10% acrylamide) using a Mini-PROTEAN3 module (Bio-RAD). Afterwards, samples were transferred to a nitrocellulose membrane (Hartenstein) using a Mini-Trans-Blot® module (Bio-RAD) at 400 mA with the addition of an ice-cooling unit and visualized with Ponceau S (Carl Roth). After three washing steps in PBST, membranes were blocked with 5% skimmed milk in PBST and incubated with either goat anti-C3 (1:500, 0855500, MP Biomedicals) or rabbit anti-ERK1/2 (1:10000, sc-94, Santa Cruz) antibody solution overnight at 4°C. After several washing steps in PBST the corresponding horseradish peroxidase (HRP)-conjugated secondary antibodies (anti-goat: 1:10000, 705-035-147, Jackson ImmunoResearch; anti-rabbit: 1:5000, NA9340V, GE Healthcare) were probed for 1 h at RT. After final incubation in PBST immune reactions were determined by incubation with ECL reagents for 1 min and chemiluminescence detected by ECL hyperfilm (GE Healthcare). Endogenous antibodies were detected by directly labelled HRP-anti-mouse IgG-Fc antibodies (1:5000, 115-035-008, Dianova) overnight at 4°C or for 2 h at room temperature. To determine IgG- or C3-immunoreactivity in nerve lysates, densitometric analyses were performed with Image J (NIH). The specific band for C3-

immunoreactivity was detectable at approximately 65kDa, the estimated molecular size of the C3b fragment (α -chain), an activated form of C3. P0wt nerves were taken as a reference. Results from two experiments are shown and depicted as the ratio of IgG or C3 to ERK1/2, respectively.

4.8. Electron microscopy and morphological analysis

Samples were processed as described above and multiple image alignments were acquired. Abnormally myelinated fibers, consisting of thinly and demyelinated axons, onion bulbs, periaxonal vacuoles and foamy macrophages were quantified in relation to the total number of axons in cross-sections of the femoral quadriceps nerve. The g-ratio was determined by dividing the diameter of the axon by the fiber diameter (axon including its myelin sheath). At least 125 fibers per animal were randomly selected and measured. Analysis was performed using a ProScan Slow Scan CCD camera mounted to a Leo 906E electron microscope (Zeiss) with corresponding iTEM software (Olympus Soft Imaging Solutions GmbH).

4.9. Reconstitution experiments

150 μ g of mouse IgGs (PMP01, Serotec) or mouse anti-keyhole limpet hemocyanin (KLH)-antibody (orb11067, Biorbyt) or 50 μ g mouse IgG Fc-fragments (31205, Pierce) were injected into the tail vein (i.v.) once or at four consecutive weeks followed by analysis one week later. After dissection and tissue processing, specific binding of antibodies in peripheral nerves was controlled by immunohistochemistry and Western blot analysis (see above).

4.10. Nerve conduction studies

Mice were anesthetized by an intraperitoneal injection of a mixture of ketavet and xylavet (10 μ l per g body weight), placed under a heating lamp to avoid hypothermia and body temperature was controlled before and after measurements (34-36°C). Neurological properties of the left sciatic nerve were measured as described previously (Zielasek et al., 1996). In short, after supramaximal stimulation of the tibial nerve at the ankle (distal) and the sciatic nerve at the sciatic notch (proximal) with monopolar needle electrodes compound muscle action potential (CMAP) amplitudes [mV] were recorded at the hind

paw muscles using steel needle electrodes. Furthermore, distal, proximal and F-wave latencies [ms] were measured as well as the distance between stimulation sites and the corresponding nerve conduction velocity (NCV) [ms] was calculated. All neurographic recordings were performed with a digital Neurosoft-Evidence 3102 electromyograph (Schreiber & Tholen Medizintechnik). Nerve conduction studies were approved by the local authorities.

4.11. Statistical analysis

Data sets were controlled for normal distribution by the Shapiro-Wilk test, and variance homology was determined by the Levene test. The comparison of more than two groups with normally distributed data (parametric) was performed by a one-way ANOVA, followed by Tukey's *post hoc*-test or Bonferroni-Holm correction. In case of non-normally distributed data sets, the nonparametric Kruskal-Wallis-test with Bonferroni-Holm correction was applied. Significance levels (*, # $P < 0.05$; **, ## $P < 0.01$; ***, ### $P < 0.001$) are indicated together with the applied statistical tests within the figure legends. Measurements and quantifications are shown as mean + SD unless otherwise mentioned. Statistical analyses were performed using PASW Statistics 18 (SPSS, IBM) software and diagrams were generated with Microsoft Excel 2007. All experiments were performed by investigators unaware of the genotypes of the analyzed mice.

5. Results

5.1. Antibodies accumulate in peripheral nerves of P0het myelin mutant mice

Several studies revealed the pathogenic role of secondary low grade inflammation - implicating macrophages and lymphocytes - in mouse models for CMT1 (Martini et al., 2013). Whereas macrophages were clearly identified as robust disease modifiers, the exact function of the adaptive immune system in the pathogenesis of CMT1B is not clearly understood. Interestingly, a previous study demonstrated that endogenous antibodies bound to injured myelinated fibers act as important co-mediators for Wallerian degeneration after peripheral nerve injury, contributing to the activation of macrophages and rapid clearance of myelin (Vargas et al., 2010). Based on these observations, the pathogenic impact of endogenous antibodies in a mouse model for CMT1B (P0het mice) was investigated.

To detect possible antibody depositions in peripheral nerves, immunohistochemical stainings for IgGs on femoral nerve cross-sections from 6-month-old P0het mutant mice and wildtype (P0wt) littermates were performed. A strong IgG-immunoreactivity was detectable in the perineurium of femoral quadriceps nerves from both P0wt mice and P0het mutants (Fig. 1A). In contrast, the endoneurium of mutant nerves revealed a higher antibody deposition compared to wildtype littermates. This could be confirmed by measuring the signal intensity of IgG-immunoreactivity in P0het and P0wt mice (Fig. 1B). Of note, in the saphenous nerve, the non-affected sensory branch of the femoral nerve (Carenini et al., 2001; Fischer et al., 2008b), this prominent antibody deposition could not be detected in P0het mutant mice (Fig. 1A).

Moreover, IgG-immunocytochemistry was also performed on single teased fiber preparations to detect a preferential deposition along myelinated fibers. A stronger deposition along nerve fibers could be confirmed in P0het mice compared to wildtype littermates, with strongest IgG-immunoreactivity at nodes of Ranvier (Fig. 2A). To further confirm whether endogenous antibodies bind to extra- or intracellular domains of nerves from P0het mice, fibers of unfixed and non-permeabilized sciatic nerves were separated into small fiber bundles and stained free floating for IgG and β -III-Tubulin. Endogenous antibodies could be observed along myelinated nerve fibers indicating extracellular deposition. In contrast, β -III-Tubulin-immunoreactivity was confined to some axonal profiles at nodes of Ranvier (Fig. 2B), possibly reflecting the vulnerability of this structure

by mechanical teasing and resulting in a higher accessibility to intracellular domains. To control for binding to intracellular domains, nerve fibers were repeatedly frozen in liquid nitrogen to allow permeabilization followed by incubation with antibodies to IgG or β -III-Tubulin. As expected β -III-Tubulin staining showed an extended immunoreactivity along the entire axon including internodes, while IgG-immunoreactivity was still visible along the outer margins of the myelinated fibers (Fig. 2B). These results suggest that endogenous antibodies bind to extracellular surface structures.

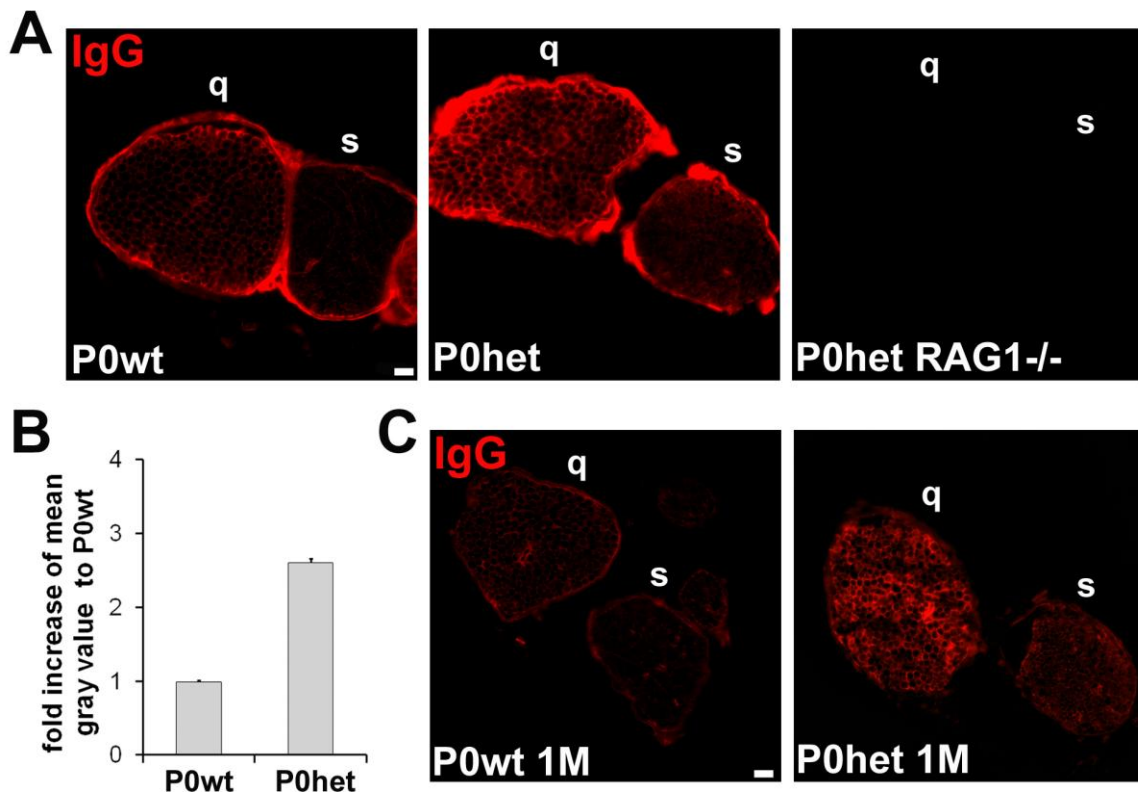


Figure 1: Antibodies accumulate in peripheral nerves of 6-month-old P0het mice. A. Immunohistochemical localization of endogenous antibodies (IgG) in femoral quadriceps (q) and saphenous nerves (s) from 6-months-old wildtype mice (P0wt) and myelin mutants (P0het). Note the prominent labeling of the endoneurium in femoral quadriceps nerve cross-sections of mutants in contrast to wildtype mice. RAG1-deficient mice (deficient for T- and B-lymphocytes) are, expectedly, devoid of antibody deposition. Scale bar, 20 μ m. B. IgG fluorescence intensity in the endoneurium of femoral quadriceps nerve cross-sections is shown as the mean gray value, taking P0wt nerves as a reference. n = 2 animals per genotype were analyzed within 3 repeated stainings and measurements. C. Immunohistochemical localization of endogenous antibodies (IgG) in femoral quadriceps (q) and saphenous nerves (s) from 1-month-old wildtype mice (P0wt) and myelin mutants (P0het). Note similar endoneurial immunoreactivity in comparison to 6-months-old mutants (see A) but the much lower intensity of the perineurium. Scale bar, 20 μ m.

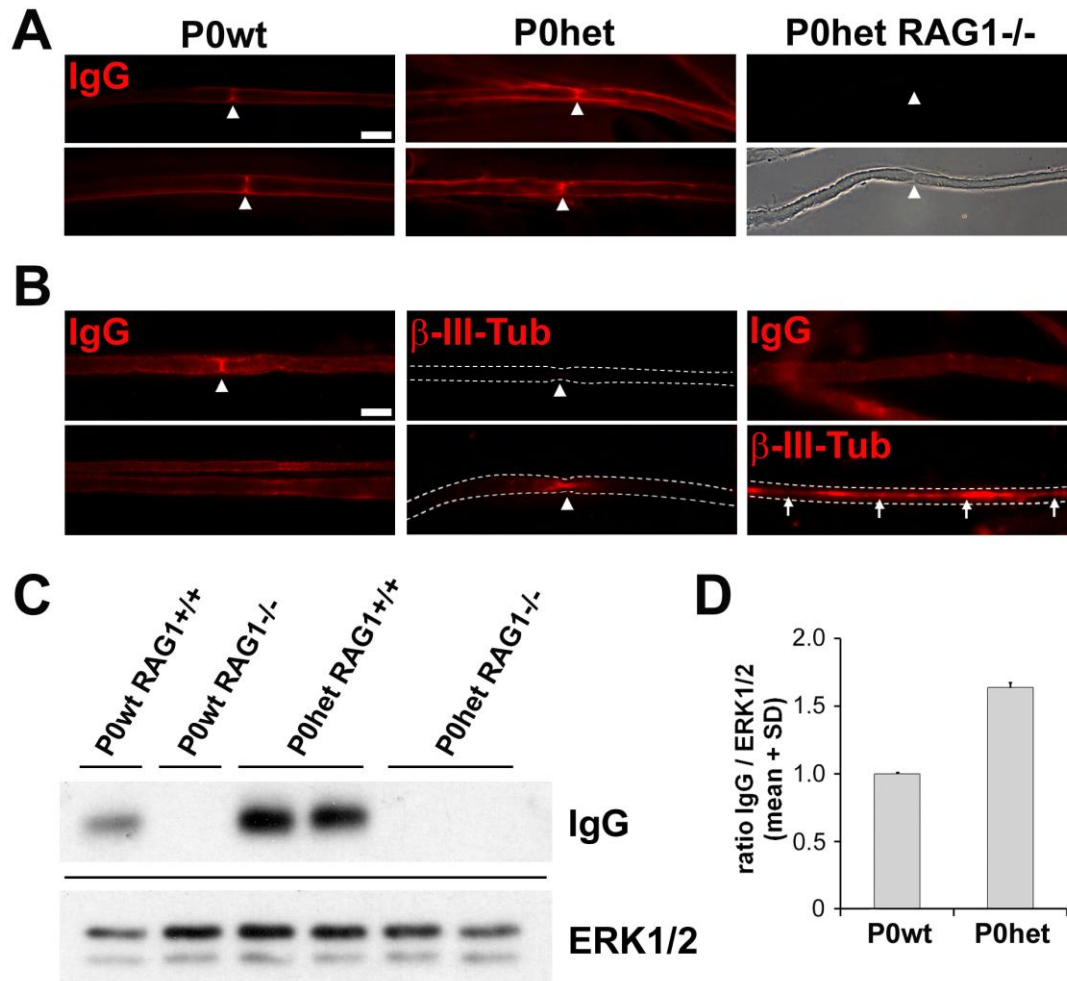


Figure 2: Antibody deposition at extracellular domains in peripheral nerves of 6-month-old P0het mice. A. Immunocytochemical staining against IgG on single teased fiber preparations. Note preferential deposition of antibodies in the nodal regions and the generally stronger signal along myelinated fibers in P0het mice compared to wildtype littermates. Nerve-specific antibodies are not detectable in RAG1-deficient mice. The corresponding phase contrast micrograph displays the teased fiber with a node of Ranvier (arrowhead). Scale bar, 20 μ m. B. Immunocytochemical staining against IgG or β -III-Tubulin on unfixed and non-permeabilized native sciatic nerve fibers of P0het mice (left and middle column). Note IgG-immunoreactivity along the outer margins of the myelinated nerve fibers and at nodes of Ranvier (arrowhead, left column) whereas β -III-Tubulin-immunoreactivity is confined to some axonal profiles at nodes of Ranvier (arrowheads, middle column), likely due to the vulnerability of this structure upon teasing. In the permeabilized sciatic nerve samples of P0het mice, β -III-Tubulin-immunoreactivity is visible along the entire axon (arrows, lower right column) and no longer confined to nodes (see middle columns), whereas IgG-immunoreactivity is still detectable along myelinated fibers (upper right column). White dashed lines indicate outer margins of myelinated nerve fibers. Scale bar, 20 μ m. C. Western blot analysis of P0wt and P0het femoral quadriceps nerve lysates showing stronger IgG signal in mutant mice. RAG1-deficient mice show no antibody signal. ERK1/2 serves as a loading control. D. Densitometric analysis of IgG-immunoreactivity in Western blots from P0het mutant mice and P0wt littermates, taking ERK1/2 signal as a reference (loading control). Results of n = 2-3 from two independent experiments are depicted.

To corroborate the immunocytochemical findings, Western blot analysis of peripheral nerve extracts were performed using antibodies to mouse IgG and IgM subtypes. An increased IgG (Fig. 2C) and IgM signal (not shown) was found in P0het mice in comparison to P0wt mice and in the respective densitometric quantification (Fig. 2D), supporting the immunocytochemical observations. Specificity of the antibody deposition was controlled by immunocytochemistry and Western blot analysis in RAG1-deficient mice, lacking T- and B-lymphocytes, and therefore antibodies. As expected, antibody deposition was undetectable in peripheral nerves (Fig. 1 and 2). Next, 1-month-old P0het and P0wt mice were investigated to determine whether endogenous antibodies are present at early disease course. At this time point in the disease, features typical for demyelination are morphologically not yet visible. Indeed, by immunohistochemistry (Fig. 1C) and Western blot analysis (not shown), already at this age a similarly elevated IgG-immunoreactivity in the mutant nerves comparable to 6 months of age was detectable. Antibody deposition was additionally investigated by immunohistochemistry on femoral nerve cross-sections from 12-month-old P0wt and P0het mice, a time point with a fully developed demyelinating phenotype. Comparable with observations in mice at the age of 6 months, a strong IgG-immunoreactivity was detectable in the perineurium of femoral nerves of both investigated groups. Similarly, the endoneurium of femoral quadriceps nerves in P0het mutant mice revealed a higher IgG-immunoreactivity compared to wildtype littermates (Fig. 3A). A stronger antibody deposition along nerve fibers could be confirmed in P0het mice compared to P0wt mice by IgG-immunocytochemistry on single teased fiber preparations (Fig. 3B). Together these data suggest that specific endogenous antibodies bind to extracellular domains of mutant Schwann cells in peripheral nerves of myelin mutant mice as a potential early prerequisite to modulate disease pathogenesis in an animal model for CMT1B.

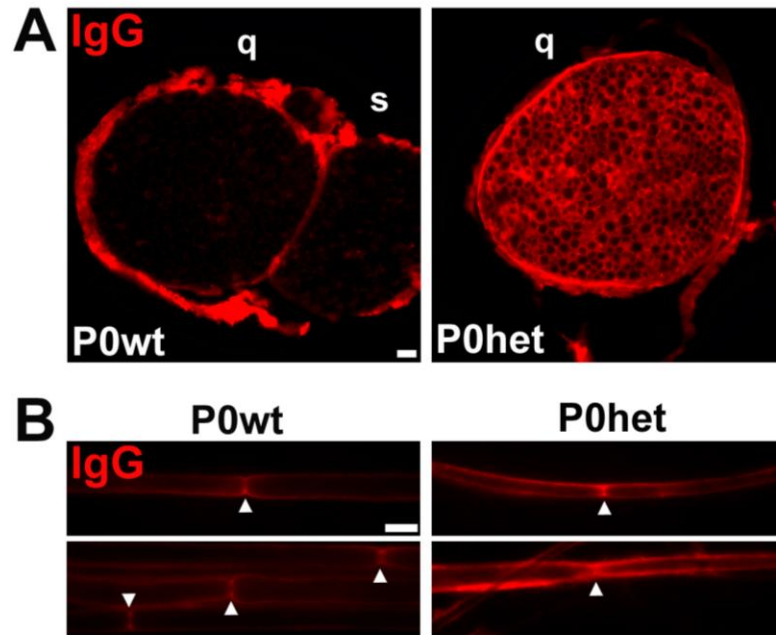


Figure 3: Antibodies accumulate in peripheral nerves of 12-month-old P0het mice. A. Immunohistochemical localization of endogenous antibodies (IgG) in femoral quadriceps (q) and saphenous nerves (s) from 12-month-old wildtype mice (P0wt) and myelin mutants (P0het). Note strong immunoreactivity in the perineurium and similarly prominent labeling of the endoneurium in P0het mutants in contrast to P0wt mice, as in 6-month-old mice (see Fig. 1). B. Immunocytochemical staining against IgG on single teased fiber preparations. Note the preferential deposition of antibodies in the nodal regions and the generally stronger immunoreactivity along myelinated fibers in P0het mice compared to wildtype mice, similar as in 6-months-old mice (see Fig. 2). Scale bars, 20 μ m.

5.2. Lack of evidence for complement deposition

Previous studies demonstrated that antibody deposition, either at the outer surface of Schwann cells, or at nodes of Ranvier, can lead to activation of the complement system to trigger subsequent nerve damage (Willison et al., 2008; Yuki and Hartung, 2012; Willison and Goodyear, 2013). Moreover, it was shown that the complement system is involved in the efficient removal of myelin and the recruitment of macrophages in Wallerian degeneration (Dailey et al., 1998; Ramaglia et al., 2007). Therefore, it was investigated if C3, a central component of the classical and alternative complement pathway, was detectable in P0het mutant nerve fibers at 6 months of age by immunocytochemistry using a C3-specific antibody. C3-deposition was strongly detectable on nerve fibers of crushed nerves and on explanted diaphragms incubated with anti-ganglioside antibodies and normal human serum (Fig. 4), which both served as a positive control for complement activation,

as previously described (Goodyear et al., 1999; Ramaglia et al., 2007). However, no complement deposition was observable on wildtype or mutant nerve fibers (Fig. 4) which could also be confirmed by Western blot analysis (Fig. 5). Activation of the complement cascade was also investigated in 12-month-old mice by Western blot analysis. Whereas C3-immunoreactivity was amply detectable in lysates of P0wt mice after sciatic nerve crush, again serving as a positive control, nerve lysates of P0het mice showed no complement activation (Fig. 5), suggesting no involvement of the complement pathway during disease pathogenesis in CMT1B mutant mice.

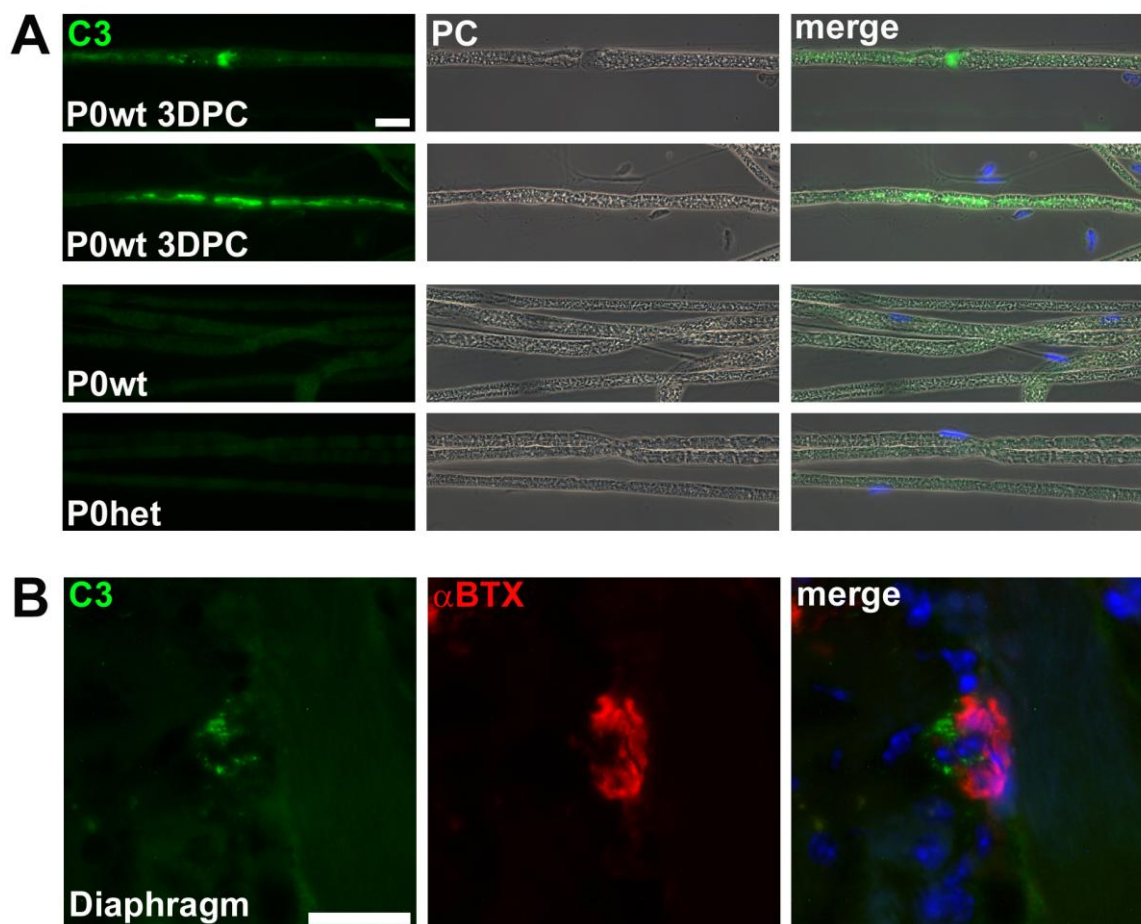


Figure 4: Lack of evidence for complement deposition in peripheral nerve fibers of 6-month-old P0het mice. A. Immunocytochemical staining against C3 on single teased fiber preparations. Complement deposition is detectable in teased fibers from crushed wildtype sciatic nerves (3 days post crush, DPC), but not in nonlesioned sciatic nerves from 6-month-old P0wt and P0het mice. Corresponding phase contrast (PC) micrographs are also shown. B. Immunohistochemical staining against C3 (green) and α -Bungarotoxin (α BTX, red, postsynapse) on diaphragm cross-section. Complement deposition is found at presynaptic terminals and perisynaptic Schwann cells (Goodyear et al., 1999). Blue profiles in merged micrographs are DAPI-labeled nuclei. Scale bars, 5 μ m.

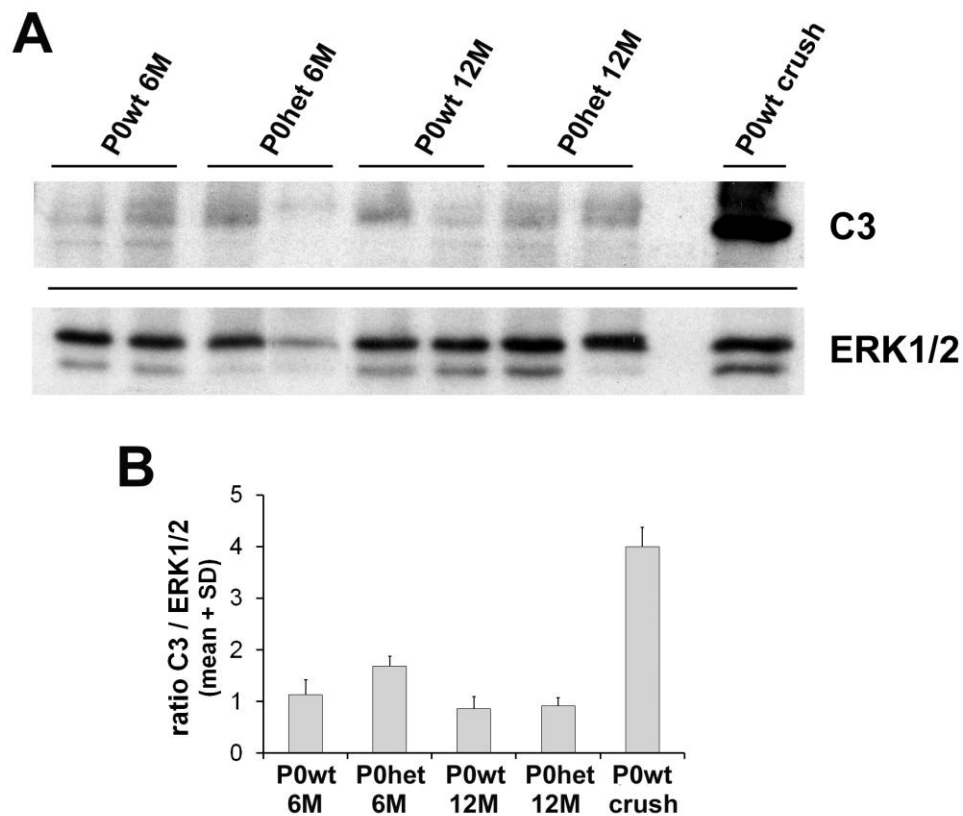


Figure 5: Lack of evidence for complement deposition in peripheral nerve fibers of 6- and 12-month-old P0het mice. A. Western blot analysis of wildtype (P0wt) and P0het mutant mice at 6 and 12 months of age. Complement activation (C3) is detectable in nerve lysates from crushed wildtype sciatic nerves (3 days post crush), but not in nonlesioned sciatic nerve lysates from 6- and 12-month-old P0wt and P0het mice. ERK1/2 serves as a loading control. B. Densitometric analysis of C3-immunoreactivity in Western blots from P0het mutant mice and P0wt littermates at 6 and 12 months of age, taking ERK1/2 signal as a reference (loading control). Results of $n = 2$ per group from two experiments are depicted.

5.3. Reduced macrophage numbers in peripheral nerves of 6-month-old P0het JHD^{-/-} mice

As a next step, P0het mice were crossbred with JHD-deficient mutants that specifically lack B-lymphocytes and are incapable to produce antibodies in order to identify the pathogenic role of endogenous antibodies in a mouse model for CMT1B. As expected, JHD^{-/-} mice lacked B-lymphocytes in the spleen and antibodies in peripheral nerves as demonstrated by immunohistochemistry and Western blot analysis (Fig. 6).

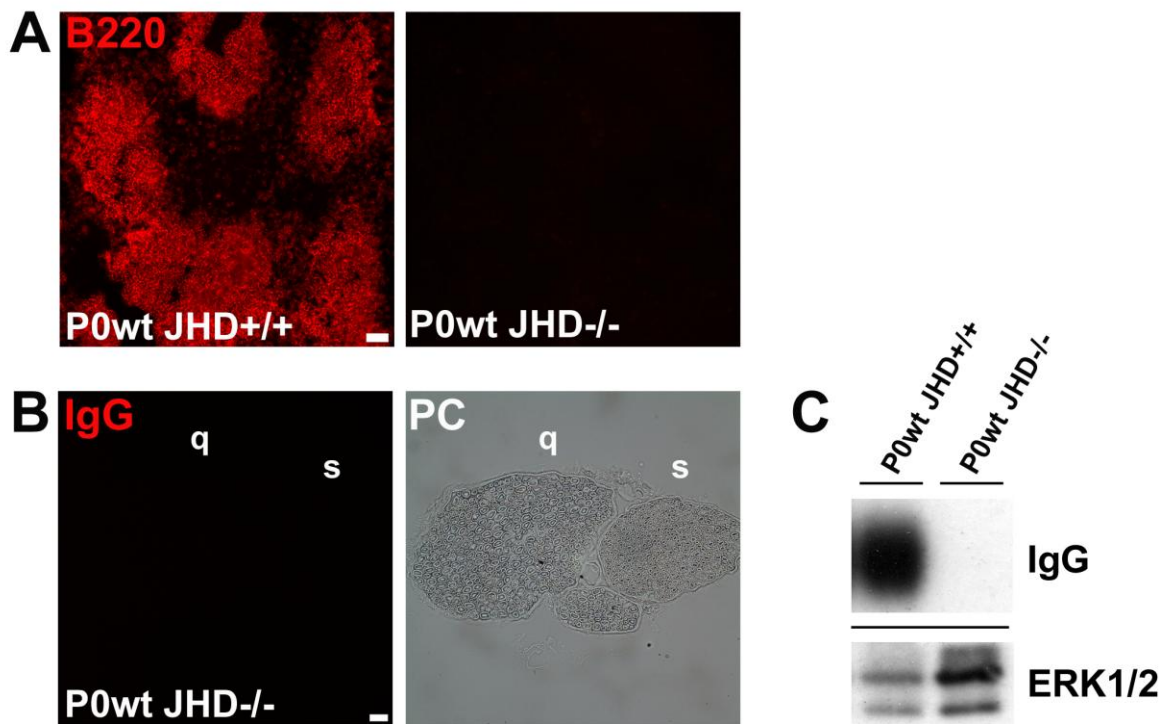


Figure 6: JHD-deficient mice lack B-lymphocytes and antibodies. A. Immunohistochemical staining against B220-positive B-lymphocytes in wildtype (P0wt JHD^{+/+}) and JHD-deficient mice. Note lack of immunoreactivity in JHD-deficient mice. Scale bar, 50 μ m. B. IgG deposition was not detectable in 6-month-old femoral quadriceps (q) and saphenous nerves (s) from JHD-deficient mice. The corresponding phase contrast (PC) micrograph is also shown. Scale bar, 20 μ m. C. Western blot analysis confirms the lack of endogenous antibodies in JHD-deficient mice. ERK1/2 serves as a loading control.

To gain further insights into the pathogenic role of endogenous antibodies, the number of macrophages was investigated in 6-month-old wildtype, single and double mutant mice (Fig. 7). As previously shown, increased macrophage numbers and subsequent demyelination occur in femoral quadriceps nerves of P0het mice (Carenini et al., 2001; Fischer et al., 2008b). Corroborating these results, the number of macrophages was significantly elevated in femoral quadriceps nerves of P0het mice at 6 months of age compared with age-matched wildtype littermates (Fig. 7A, B). Whereas no effect on macrophage numbers was detectable in P0wt JHD^{-/-} mice, P0het JHD^{-/-} mice revealed a significantly attenuated elevation of F4/80-positive macrophages (Fig. 7A, B). In pathologically non-affected cutaneous saphenous nerves that also lack extensive antibody deposition (see Fig. 1) the number of macrophages was not altered in single and double mutant mice (Fig. 7A, B). Moreover, macrophage activation, represented by a myelin-

laden ('foamy') appearance, was investigated by electron microscopy. A substantial number of activated macrophages was only detectable in P0het JHD^{+/+} mice, whereas all other genotypes, including P0het JHD^{-/-} mice lacked these foamy macrophages (Fig. 7C).

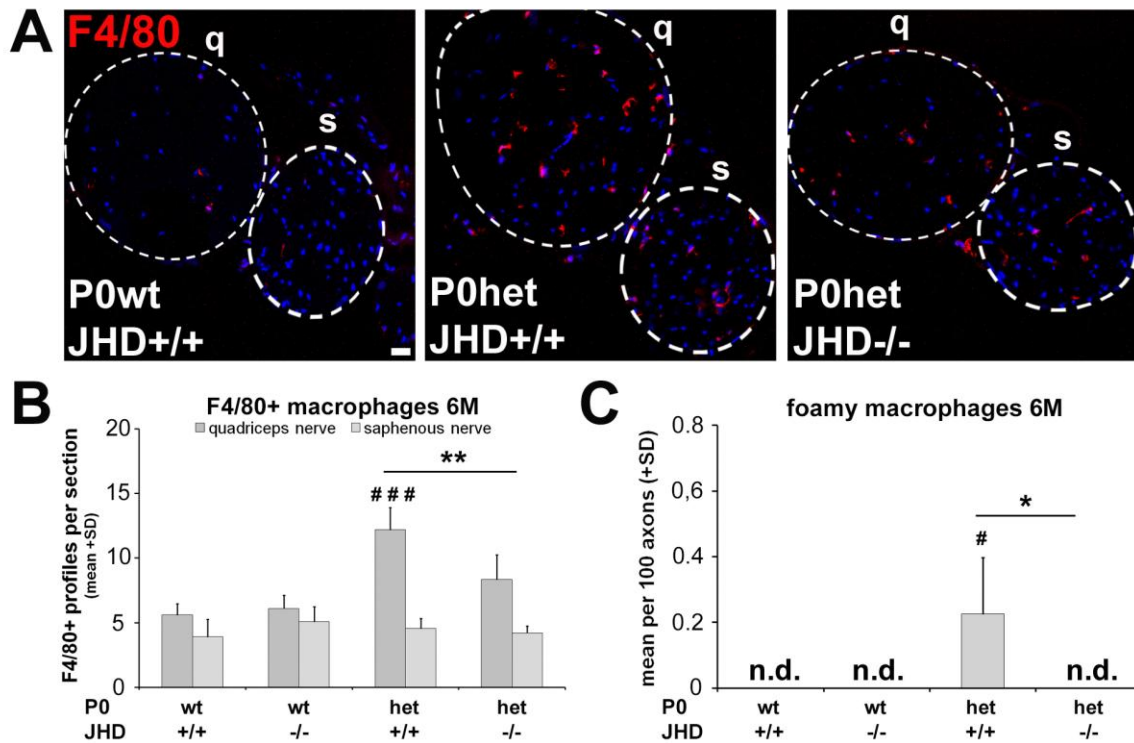


Figure 7: Reduced macrophage numbers in 6-month-old P0het JHD^{-/-} mice. A. Immunohistochemistry against macrophages (F4/80) in femoral nerve cross-sections from 6-month-old wildtype (P0wt JHD^{+/+}), single (P0het JHD^{+/+}) and double mutant mice (P0het JHD^{-/-}). Representative micrographs are shown. Dashed circles indicate femoral quadriceps (q) and saphenous nerves (s). Scale bar, 20 μ m. B. Quantification of F4/80-positive profiles showing a significant reduction of macrophage numbers in the femoral quadriceps nerve from P0het JHD^{-/-} double mutants in comparison to single mutants. In the saphenous nerve the number of macrophages is not increased in mutants. n = 4 - 5; one-way ANOVA with Tukey *post hoc* test. # (significant difference to P0wt JHD^{+/+}), * (significant difference between P0het mutant groups). #, * P < 0.05; ##, ** P < 0.01; ###, *** P < 0.001. C. Quantification of foamy macrophages in femoral quadriceps nerve cross-sections reveals an absence of phagocytosing macrophages in nerves from P0het JHD^{-/-} mice. n = 4 - 5; Kruskal-Wallis test with Bonferroni-Holm correction. # (significant difference to P0wt JHD^{+/+}), * (significant difference between P0het mutant groups). #, * P < 0.05. n.d. (not detected).

In order to determine the polarization status of macrophages immunohistochemical stainings were performed against CD86 and CD206 (mannose receptor), markers for M1- or M2-activation, respectively (Kigerl et al., 2009). In femoral quadriceps nerve cross-

sections from 6-month-old P0het JHD^{+/+} mice the number of CD86-positive cells was significantly increased compared to wildtype littermates (Fig. 8A). Interestingly, the numbers of M1-polarized, CD86-positive cells was significantly reduced in P0het JHD^{-/-} mice (Fig. 8A). In contrast, CD206-positive cells were not elevated in numbers in P0het JHD^{+/+} mice compared to wildtype littermates and did not significantly differ between P0het JHD^{+/+} and P0het JHD^{-/-} mice (Fig. 8B). These results suggest that the reduced number of F4/80-positive macrophages in P0het JHD^{-/-} mice at 6 months of age is preferentially due to a reduced number of CD86-positive, M1-polarized cells.

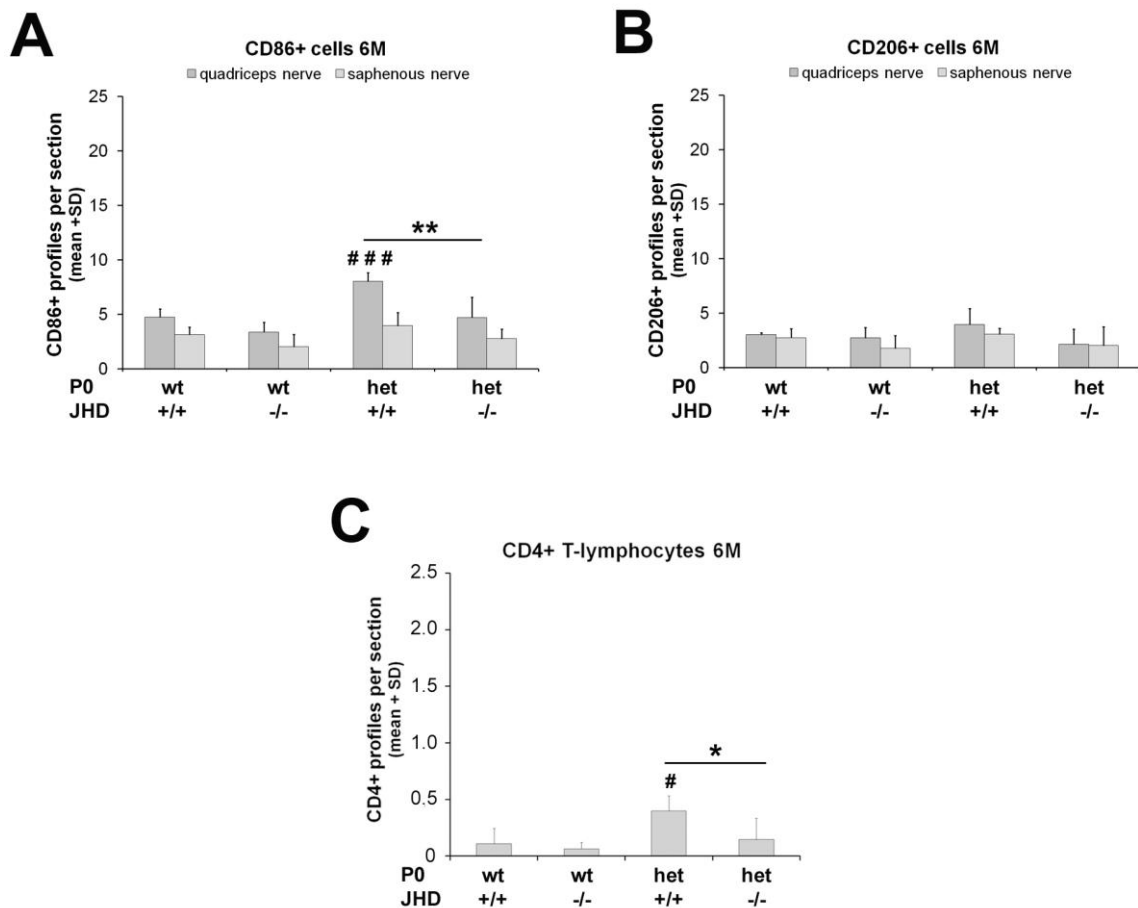


Figure 8: Altered macrophage polarization and reduced number of CD4-positive T-lymphocytes in 6-month-old P0het JHD^{-/-} mice. A. Quantification of CD86-positive cells (M1) in femoral quadriceps nerve cross-sections of 6-month-old mice. P0het JHD^{+/+} mice show significantly increased number of CD86-positive cells compared to P0wt JHD^{+/+} mice. Consistent with macrophage numbers, M1-polarized cells are significantly reduced in P0het JHD^{-/-} mice compared to P0het JHD^{+/+} single mutants. B. Quantification of CD206-positive cells (M2) in femoral quadriceps nerve cross-sections of 6-month-old mice. No significant alterations in the number of CD206-positive cells can be detected in the investigated groups at 6 months of age. n =

3 - 5; one way ANOVA with Bonferroni-Holm correction, # (significant difference to P0wt JHD+/+), * (significant difference between P0het mutant groups). #, * P < 0.05; ##, ** P < 0.01; ###, *** P < 0.001. C. Quantification of CD4-positive T-lymphocytes in femoral quadriceps nerve cross-sections of 6-month-old mice. CD4-positive lymphocytes are significantly elevated in P0het JHD+/+ mutant mice compared to wildtype littermates, but significantly reduced in P0het JHD-/- mice. n = 3 - 6; Kruskal-Wallis test with Bonferroni-Holm correction, # (significant difference to P0wt JHD+/+), * (significant difference between P0het mutant groups). #, * P < 0.05.

As a next step, T-lymphocytes as possible mediators of the pathogenesis were investigated. CD8-positive T-lymphocytes were scarcely detectable in peripheral nerves of P0het JHD+/+ and P0het JHD-/- mice at 6 months of age (not shown) and therefore not further considered to contribute to disease progression. However, quantification of CD4-positive T-lymphocytes revealed a significant elevated number in P0het JHD+/+ mice compared to wildtype littermates and P0het JHD-/- double mutants (Fig. 8C), suggesting that JHD deficiency results in a reduction of immune-related cells in P0het mice.

5.4. JHD deficiency ameliorates the demyelinating phenotype in 6-months-old P0het mutant mice

Demyelination is a typical feature in the P0het CMT1B mouse model (Carenini et al., 2001; Fischer et al., 2008b). Therefore, it was investigated whether the absence of antibodies in P0het JHD-/- mice leads to reduced signs of demyelination. Quantification by electron microscopy demonstrated a significant reduction of abnormally myelinated fibers (comprising de- and thinly myelinated axons) and supernumerary Schwann cells ('onion bulbs') in P0het JHD-/- mice compared to P0het JHD+/+ mice at 6 months of age (Fig. 9A-C). Of note, JHD deficiency had no effect on the nerve structure in P0wt mice (Fig. 9B-C). Moreover, calculation of the g-ratio (axon diameter/fiber diameter) revealed a significantly less reduced myelin thickness in P0het JHD-/- compared to P0het JHD+/+ mice (Fig. 9D) further supporting the hypothesis that endogenous antibodies might contribute to macrophage-mediated demyelination in a mouse model for CMT1B.

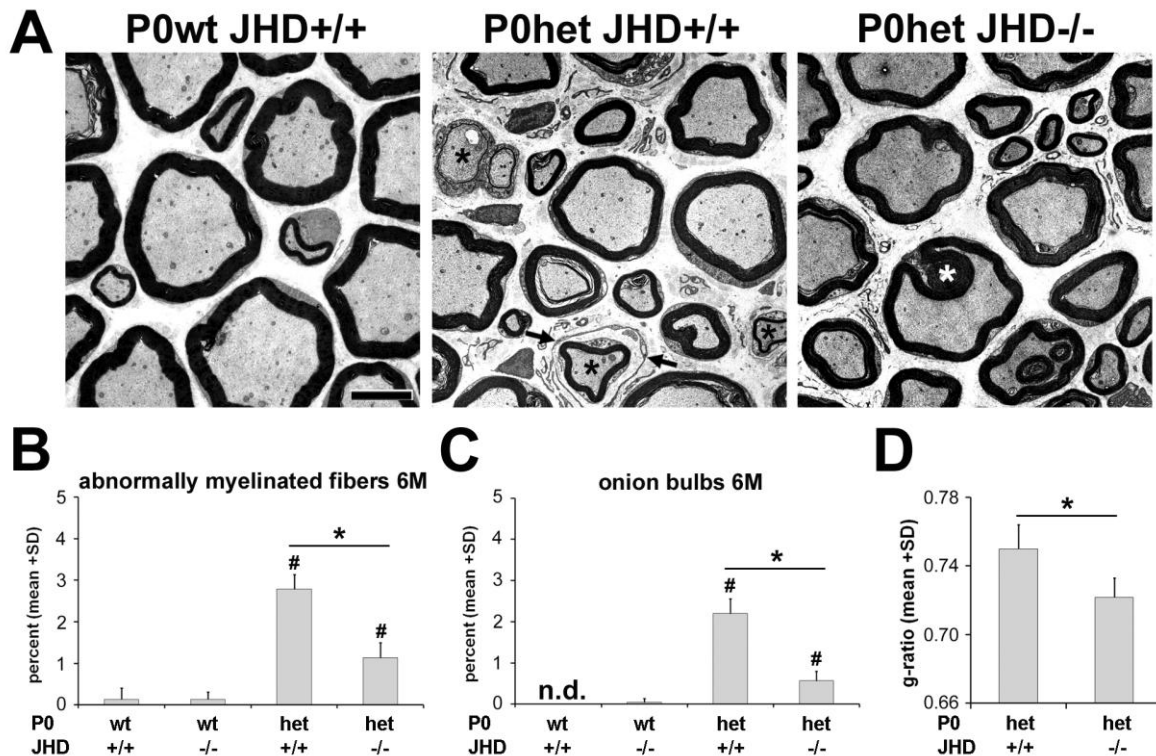


Figure 9: Ameliorated myelin degeneration in 6-month-old P0het JHD-/- mice. A. Representative ultrathin sections of femoral quadriceps nerves from 6-month-old wildtype (P0wt JHD+/+), single (P0het JHD+/+) and double mutant mice (P0het JHD-/-). Black asterisks indicate abnormally myelinated fibers, and arrows supernumerary Schwann cells ('onion bulbs'). Note an asymmetric inclusion of compacted myelin, likely at the juxtaparanode, in P0het JHD-/- mice (white asterisk) as described previously (Martini et al., 1995). Scale bar, 5µm. B. - C. Quantification of abnormally myelinated fibers (B) and onion bulbs (C) demonstrate significantly ameliorated demyelination and improved myelin integrity in P0het JHD-/- double mutants in comparison to P0het JHD+/+ mice. n = 4 - 5; Kruskal-Wallis test with Bonferroni-Holm correction, # (significant difference to P0wt JHD+/+), * (significant difference between P0het mutant groups). #, * P < 0.05. n.d. (not detected). D. Quantification of the g-ratio (axon diameter/fiber diameter) demonstrates a significant increase in myelin thickness in P0het JHD-/- compared to P0het JHD+/+ mice. n = 4 (125-135 axons per animal); two-tailed Student's t-test. * P < 0.05.

5.5. Passive transfer of antibodies reverts the ameliorated demyelinating phenotype in 6-month-old P0het JHD-/- mice

To further validate the hypothesis and clarify the role of endogenous antibodies in the pathogenesis of CMT1B, reconstitution experiments into P0het JHD-/- mice were performed in order to study if antibodies are capable to reverse the observed beneficial effects of JHD deficiency. Mice at the age of 6 months received i.v. injections of IgGs either once or on four consecutive weeks and were analyzed afterwards. As detected by

immunohistochemistry, passive transfer into P0wt JHD^{-/-} and P0het JHD^{-/-} mice led to an accumulation of IgGs in peripheral nerves comparable to corresponding JHD-positive controls, although at a weaker level. This indicates that injected IgGs are capable to enter the nerve and bind to their respective targets (Fig. 10A). Expectedly, P0het JHD^{-/-} mice that received four weekly IgG-injections showed a stronger IgG deposition in the endoneurium compared to mice that received only a single passive transfer (Fig. 10A).

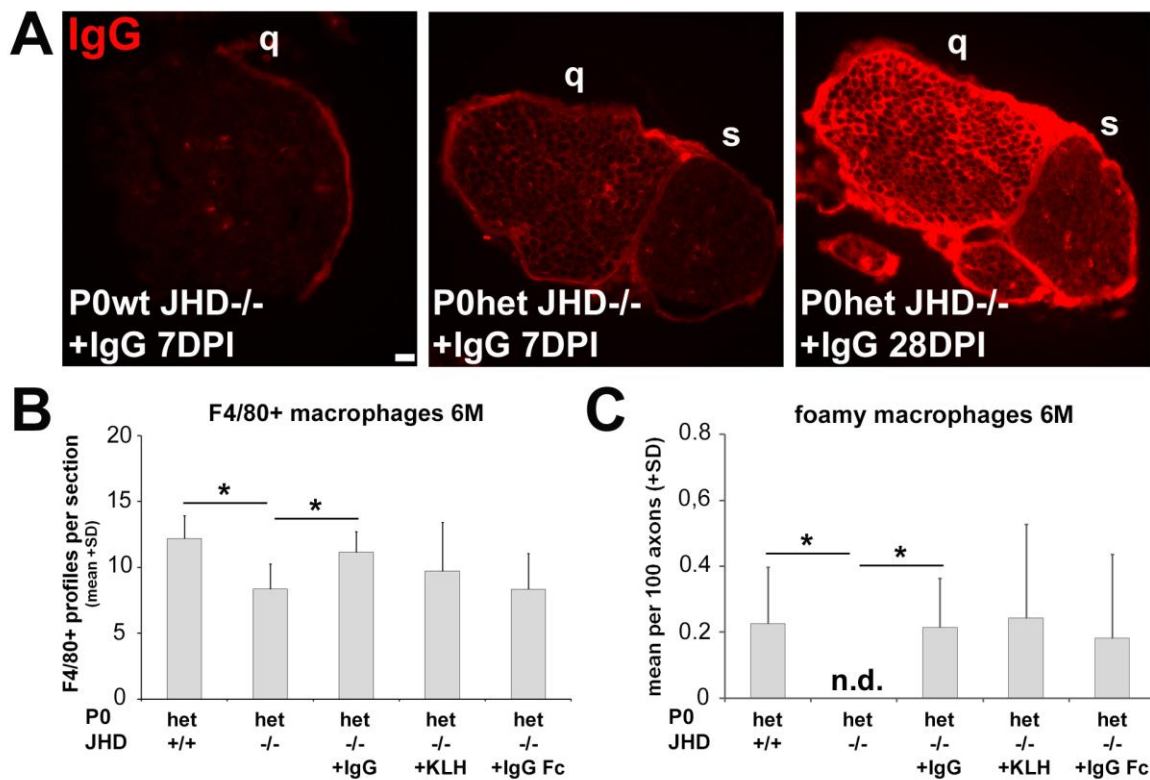


Figure 10: Antibodies accumulate in peripheral nerves after passive transfer and lead to increased macrophage numbers. A. Immunohistochemical localization of antibodies in femoral quadriceps (q) and saphenous nerves (s) from 6-month-old P0wt JHD^{-/-} (7 days post injection, DPI) and P0het JHD^{-/-} mice (7DPI and 28DPI) after systemic injection of IgGs. Note stronger IgG-immunoreactivity in the endoneurium of P0het JHD^{-/-} mice that received 4 weekly IgG-injections within 28 days (28DPI). Scale bar, 20 μ m. B. Quantification of F4/80-positive profiles in non-injected control and reconstituted mice showing an increase of macrophage numbers in the femoral quadriceps nerve from P0het JHD^{-/-} mutants after IgG reconstitution. n = 3 - 5; one-way ANOVA with Bonferroni-Holm correction. * P < 0.05. C. Quantification of foamy macrophages reveals an increase of phagocytosing macrophages in the femoral quadriceps nerve from P0het JHD^{-/-} mice after IgG reconstitution. Note also the presence of phagocytosing macrophages in control-reconstituted animals (+KLH, +IgG Fc). n = 3 - 5; Kruskal-Wallis test with Bonferroni-Holm correction. * P < 0.05. n.d. (not detected). For comparison, data from P0het JHD^{+/+} and P0het JHD^{-/-} mice, as shown in figure 7 are presented here again.

Consistent with an increased antibody deposition in nerve sections after passive antibody transfer, elevated numbers of F4/80-positive macrophages and foamy macrophages were detectable in P0het JHD^{-/-} mice (Fig. 10B, C). Interestingly, these numbers were comparable to numbers obtained in age-matched P0het JHD^{+/+} mutants, suggesting an activated macrophage response after IgG injections. Of note, antibody reconstitution had no effect on macrophage numbers in P0wt JHD^{-/-} mice (not shown). As a next step, nerve fiber damage was quantified by electron microscopy in order to analyse the pathogenic impact of passive antibody transfer. P0wt JHD^{-/-} showed no pathological alterations after IgG injections (Fig. 11A). However, passive antibody transfer reverted the ameliorated phenotype in P0het JHD^{-/-} mice, as determined by an increased number of abnormally myelinated fibers and supernumerary Schwann cells after IgG injections (Fig. 11B, C), suggesting that added antibodies can modulate macrophage-mediated demyelination.

To study whether antigen specificity is necessary for the detrimental effect of antibodies, passive transfer experiments into P0het JHD^{-/-} mice were performed using mouse antibodies that either show specificity for a non-mammalian antigen, like keyhole limpet hemocyanin (KLH), or antibody fragments lacking the antigen directed domain (mouse IgG Fc-fragments). As expected for both cases, no antibody deposition could be detected in peripheral nerves by immunohistochemistry (not shown). Unexpectedly, passive transfer of non-specific IgGs or mouse IgG Fc-fragments led to a slight, non-significant increase of total macrophage numbers in individual animals (Fig. 10B) together with an increase of phagocytosing macrophages (Fig. 10C). Consistent with this activated macrophage response, a mild increase in nerve fiber damage could be observed after reconstitution experiments with the above-mentioned antibodies and fragments (Fig. 11). These data suggest that non-specific IgGs can activate macrophages and contribute to demyelination in peripheral nerves of P0het mice, yet to a lesser extent.

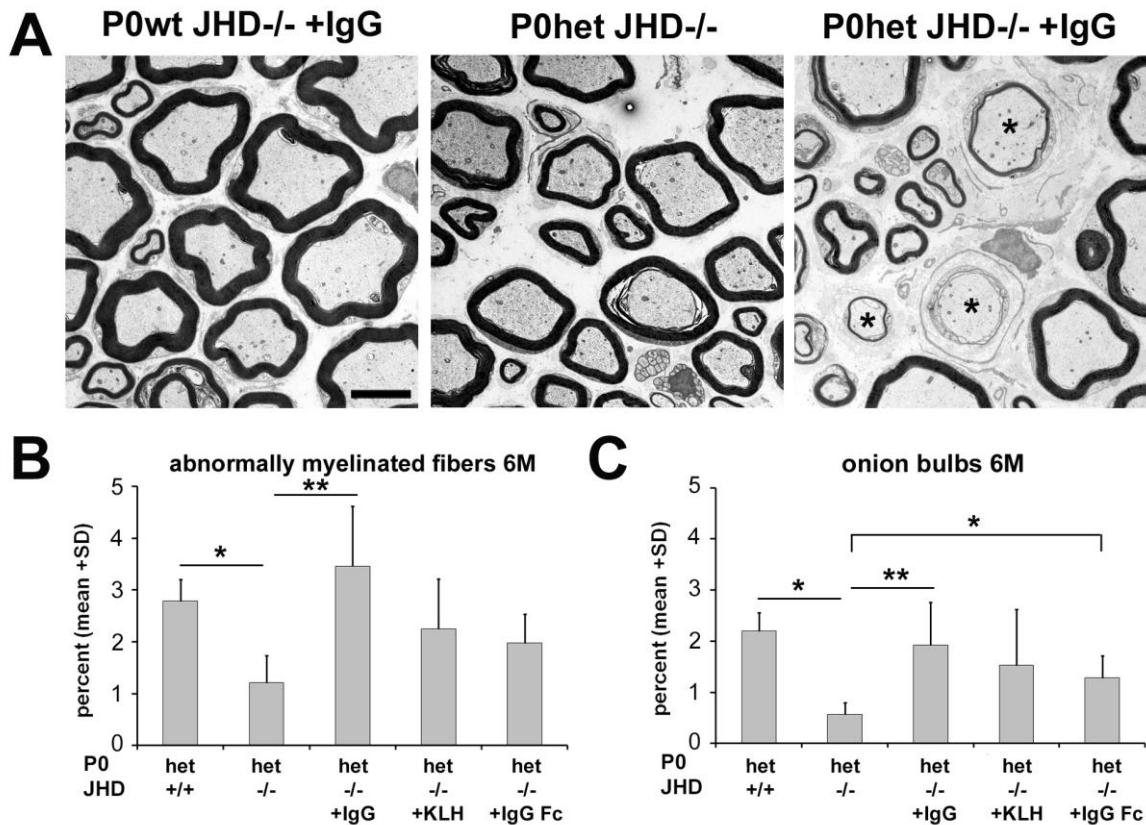


Figure 11: Antibody reconstitution reverts the ameliorated demyelinating phenotype in 6-month-old P0het JHD^{-/-} mice. A. Representative ultrathin sections of femoral quadriceps nerves from 6-month-old IgG reconstituted P0wt JHD^{-/-}, P0het JHD^{+/+} controls and IgG reconstituted P0het JHD^{-/-} mice. Asterisks indicate abnormally myelinated fibers. Scale bar, 5 μ m. B. - C. Quantification of abnormally myelinated fibers (B) and signs of demyelination (onion bulbs) (C) in control and reconstituted mice reveal a significant aggravation of myelin degeneration in IgG reconstituted P0het JHD^{-/-} mutants. Note also a non-significant trend of increased pathological alterations in control-reconstituted animals (+KLH, +IgG Fc). n = 3 - 5; Kruskal-Wallis test with Bonferroni-Holm correction. * P < 0.05; ** P < 0.01. For comparison, data from P0het JHD^{+/+} and P0het JHD^{-/-} mice, as shown in figure 9 are presented here again.

5.6. Increased macrophage numbers in peripheral nerves of 12-month-old P0het JHD^{-/-} mice

A robust and persistent reduction of macrophages and amelioration of the demyelinating phenotype could be demonstrated in P0het mice lacking both T- and B-lymphocytes at 12 months of age (Schmid et al., 2000). Therefore the number of macrophages was investigated in femoral nerve cross-sections from 12-month-old mice. Confirming previous results (Fischer et al., 2008b), P0het single mutants showed increased numbers of macrophages compared to 6 months of age, reflecting the increased inflammatory reaction

with ongoing disease development (Fig. 12A, B). Unexpectedly, in P0het JHD^{-/-} double mutants the number of macrophages was further elevated in the femoral quadriceps nerve (Fig. 12A, B), contrary to the observations at 6 months of age. This was also in line with electron microscopic analysis, as foamy macrophages were amply detectable in peripheral nerves of P0het JHD^{-/-} mice (Fig. 12C), suggesting distinct effects on macrophage activation upon JHD deficiency during disease progression. Notably, in pathologically non-affected cutaneous saphenous nerves the number of macrophages was not altered in single and double mutant mice (Fig. 12A, B).

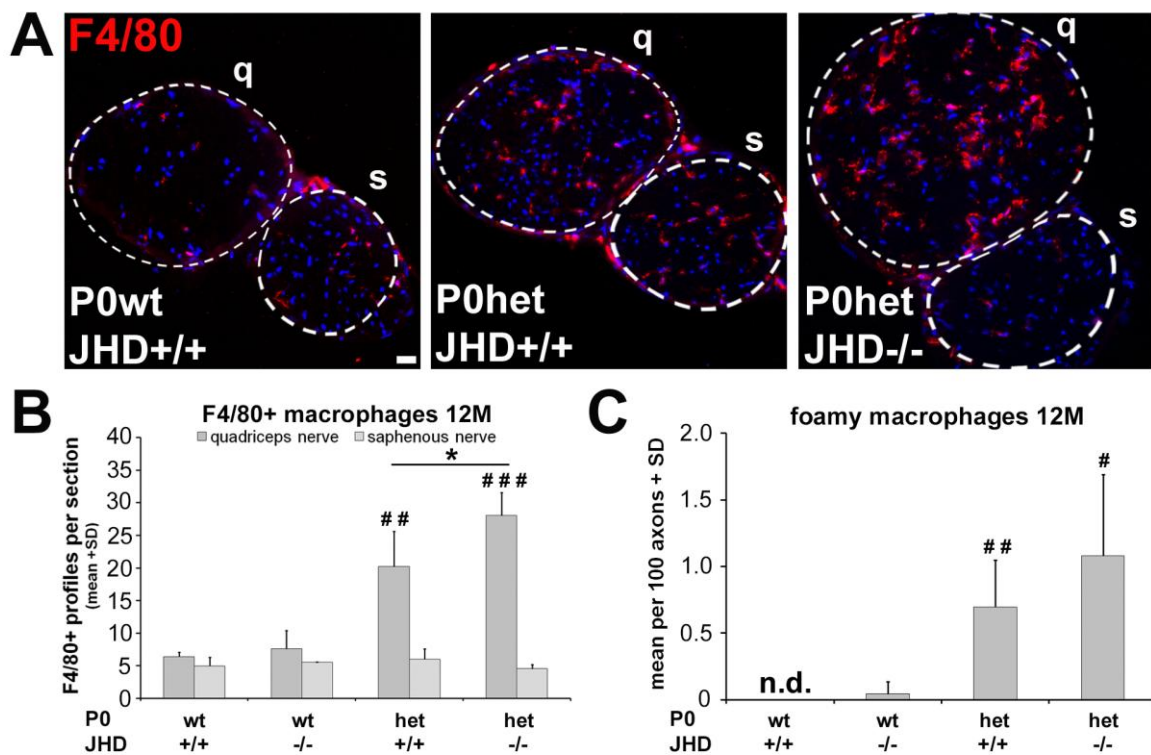


Figure 12: Increased macrophage numbers in 12-month-old P0het JHD^{-/-} mice. A. Immunohistochemistry against macrophages (F4/80) in cross-sections of femoral nerves from 12-month-old wildtype (P0wt JHD^{+/+}), single (P0het JHD^{+/+}) and double mutant mice (P0het JHD^{-/-}). Representative micrographs are shown. Dashed circles indicate femoral quadriceps (q) and saphenous nerves (s). Note increased number of macrophages in P0het JHD^{-/-} mice. Scale bar, 20 μ m. B. Quantification of F4/80-positive profiles showing a significant increase of macrophage numbers in the femoral quadriceps nerve from P0het JHD^{-/-} double mutants in comparison to P0het JHD^{+/+} single mutants. In the saphenous nerve the number of macrophages is not increased in mutants (n = 3 - 5); one-way ANOVA with Tukey *post hoc* test. # (significant difference to P0wt JHD^{+/+}), * (significant difference between P0het mutant groups). #, * P < 0.05; ##, ** P < 0.01; ###, *** P < 0.001. C. Quantification of foamy macrophages reveals the presence of phagocytosing macrophages in femoral quadriceps nerves from P0het JHD^{-/-} mice. n = 4 - 7; Kruskal-Wallis test with Bonferroni-Holm correction. # (significant difference to P0wt JHD^{+/+}), # P < 0.05; ## P < 0.01. n.d. (not detected).

5.7. JHD deficiency aggravates the demyelinating phenotype in 12-month-old P0het mutant mice

Next, it was investigated whether the increased macrophage activation is reflected by augmented pathological alterations. Myelin degeneration was quantified in femoral quadriceps nerves by electron microscopy. Nerve fiber damage was increased in P0het JHD^{+/+} mice at 12 months compared to 6 months of age, reflecting the progressive disease course in the CMT1B neuropathy (Fig. 13). However, contrary to the ameliorating phenotype due to absence of endogenous antibodies at 6 months of age, the percentage of demyelinated fibers was significantly elevated in P0het JHD^{-/-} mice compared to P0het JHD^{+/+} mice at 12 months of age (Fig. 13C). Of note, no effect on the nerve structure was detectable in P0wt JHD^{-/-} mice (Fig. 13B, C). These observations suggest that JHD deficiency has an opposite effect in the disease course of P0het mice which results eventually in an aggravated phenotype.

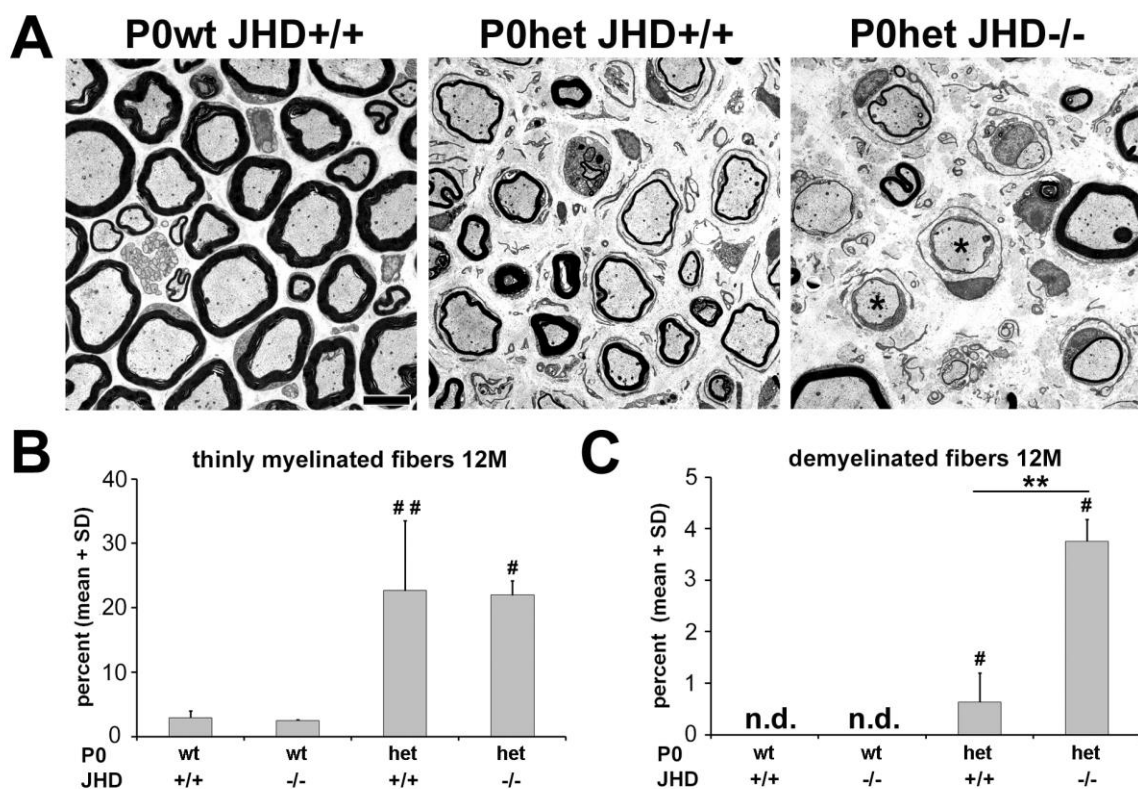


Figure 13: Aggravated myelin degeneration in 12-month-old P0het JHD^{-/-} mice. A. Representative ultrathin sections of femoral quadriceps nerves from 12-month-old wildtype (P0wt JHD^{+/+}), single (P0het JHD^{+/+}) and double mutant mice (P0het JHD^{-/-}). Asterisks indicate demyelinated fibers. Scale bar, 5 μ m. B. - C. Quantification of thinly (B) and demyelinated fibers (C)

(C) demonstrate a significant increase in demyelination and deteriorated myelin integrity in P0het JHD^{-/-} mice in comparison to P0het JHD^{+/+} mice. $n = 4 - 7$; Kruskal-Wallis test with Bonferroni-Holm correction, # (significant difference to P0wt JHD^{+/+}), * (significant difference between P0het mutant groups). #, * $P < 0.05$; ##, ** $P < 0.01$. n.d. (not detected).

It is assumed that Schwann cells can support axonal integrity and that prolonged demyelination or an impaired Schwann cell phenotype might lead to axonal perturbation (Martini, 2001; Nave, 2010). In order to study axonal damage, immunohistochemical stainings against non-phosphorylated neurofilaments (SMI32) (Groh et al., 2010) were performed on femoral nerve cross-sections of 12-month-old wildtype, single and double mutant mice. In P0het JHD^{+/+} mutants the number of SMI32-immunoreactive profiles was only slightly increased compared to P0wt JHD^{+/+} mice, reflecting the rather mild axonopathic phenotype in peripheral nerves of CMT1B mice at this age (Fig 14). However, P0het JHD^{-/-} double mutants revealed a stronger SMI32-immunoreactivity of irregular shaped axons (Fig 14), suggesting increased axonal perturbation in 12-month-old P0het JHD^{-/-} mice.

Neurological deterioration and impaired muscle strength are typical features in CMT1 and primarily caused by demyelination and impaired axon function (Scherer and Wrabetz, 2008; Nave, 2010). Therefore it was investigated whether the observed axonal perturbation (SMI32-positive axons) is reflected by an altered neurological phenotype in 12-month-old P0het JHD^{-/-} mice. P0het JHD^{+/+} mice demonstrated significantly decreased distal and proximal compound muscle action potential (CMAP) amplitudes at 12 months of age (Fig. 15A, B) and also showed slowed nerve conduction velocities (NCV) (Fig. 15C), as well as prolonged F-wave latencies (Fig. 15D) compared to wildtype mice, as previously reported (Martini et al., 1995; Zielasek et al., 1996). JHD deficiency had no significant effect on the investigated neurological parameters (Fig. 15).

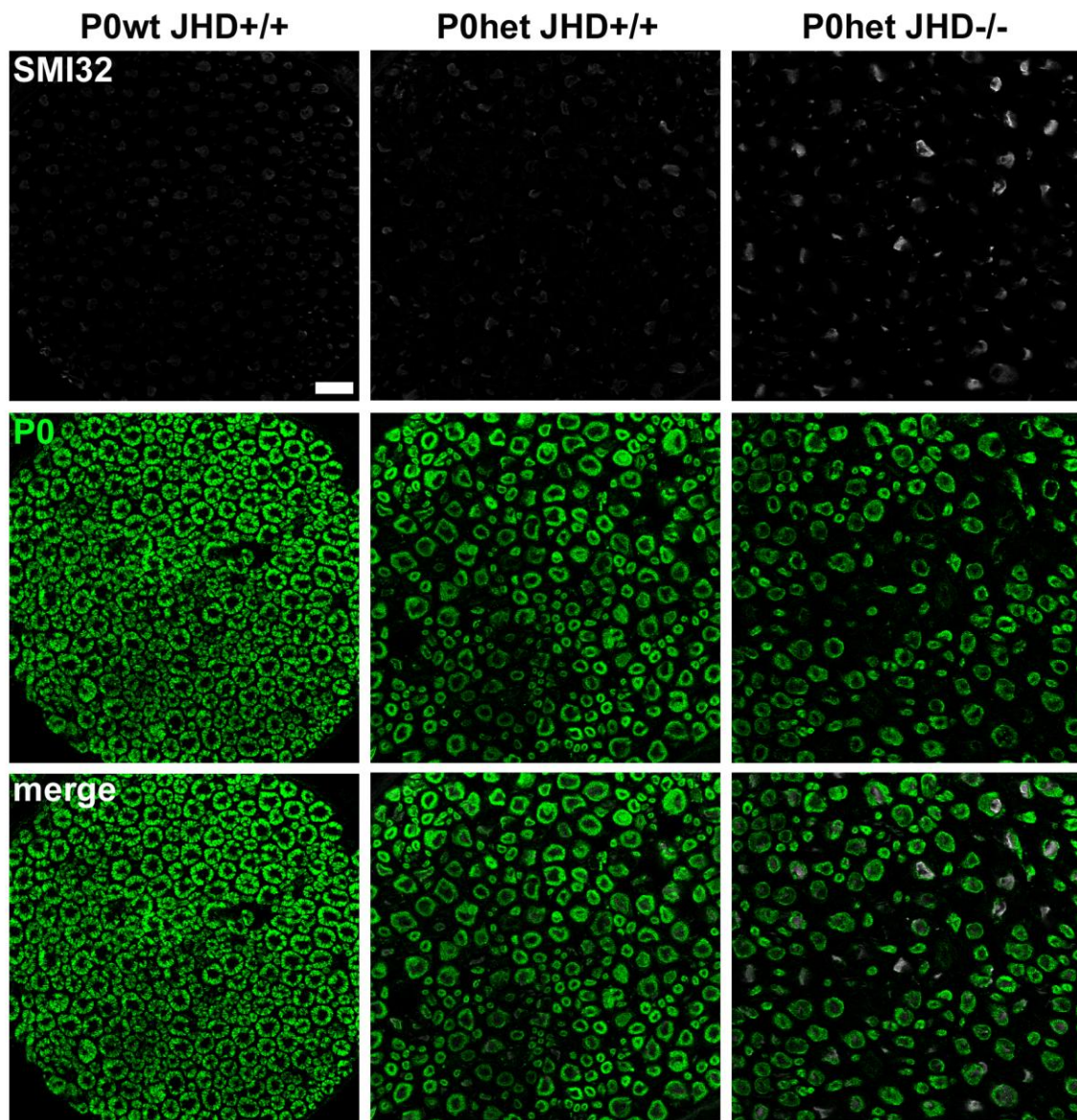


Figure 14: Increased axonal perturbation in 12-month-old P0het JHD^{-/-} mice. Immunohistochemistry against non-phosphorylated neurofilaments (SMI32; grayscale) and P0 (green) in cross-sections of femoral quadriceps nerves from 12-month-old wildtype (P0wt JHD^{+/+}), single (P0het JHD^{+/+}) and double mutant mice (P0het JHD^{-/-}). Note increased SMI32-immunoreactivity in P0het JHD^{-/-} mice compared to P0wt JHD^{+/+} and P0het JHD^{+/+} mice. Scale bar, 20 μ m.

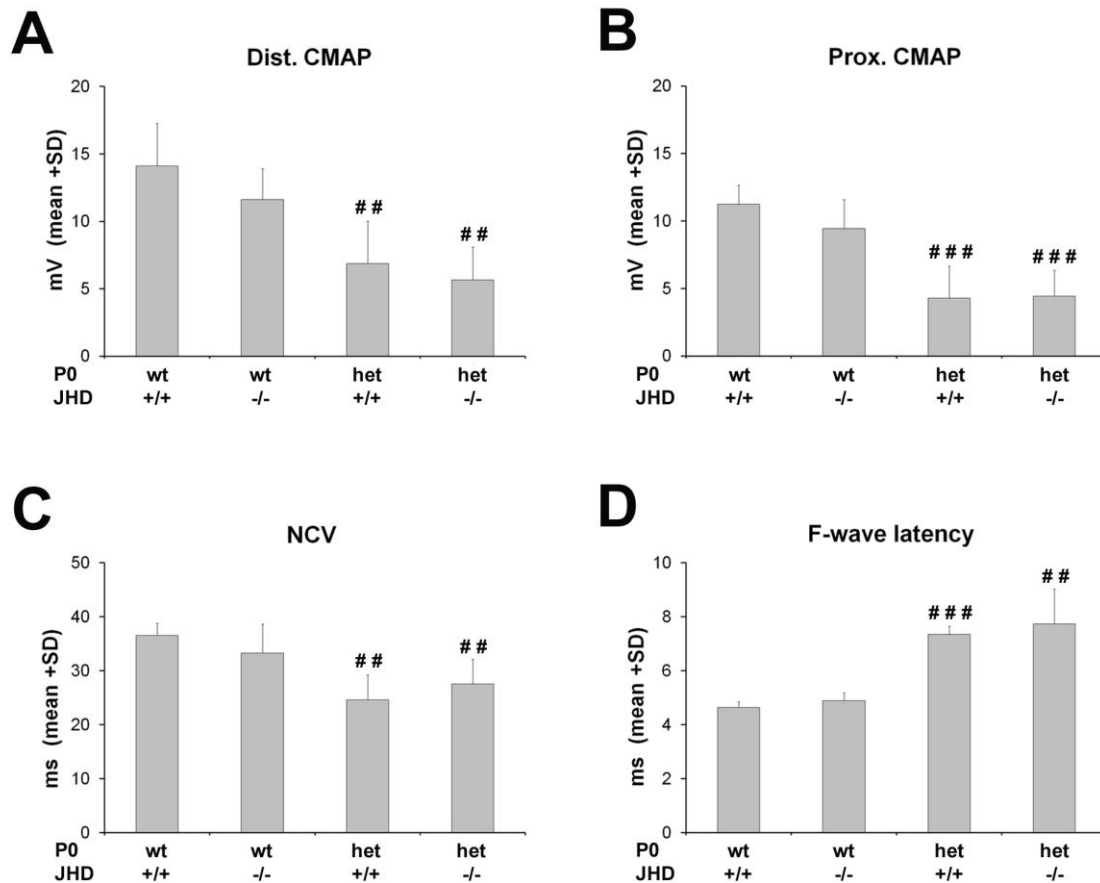


Figure 15: Impaired physiological properties in 12-month-old P0het mutants. A. - B. Distal (A) and proximal (B) compound muscle action potential (CMAP) amplitudes in 12-month-old mice. P0het JHD+/+ mice have significantly lowered amplitudes compared to wildtype littermates. JHD deficiency has no further effect on CMAP amplitudes. C. Quantification of nerve conduction velocity (NCV). JHD deficiency has no effect on NCV in P0wt mice, but is significantly reduced in P0het JHD+/+ and P0het JHD-/- mice. D. F-wave latencies are prolonged in P0het JHD+/+ mutants in comparison to P0wt JHD+/+ mice. No further prolongation in the F-wave latency is detectable in P0het JHD-/- mice. n = 5 - 8; one-way ANOVA with Bonferroni-Holm correction; # (significant difference to P0wt JHD+/+), # P < 0.05; ##, P < 0.01; ###, P < 0.001.

Consistent with the nerve conduction studies, immunohistochemical stainings against pre-synaptic (synaptophysin) and postsynaptic (α -Bungarotoxin) markers on cross-sections of the flexor digitorum brevis muscle from 12-month-old mice (Fig. 16A) displayed a significant increase in the number of denervated and partially denervated neuromuscular junctions (NMJs) in P0het JHD+/+ mice compared to wildtype littermates (Fig. 16B). P0het JHD-/- mice showed similarly increased values (Fig. 16B). Moreover, electron microscopic quantification of axon numbers and periaxonal vacuoles (readout parameters for axonal damage) in femoral quadriceps nerves revealed no significant alterations between P0het

JHD^{+/+} and P0het JHD^{-/-} mice (Fig. 16C, D). Together these results suggest that P0het JHD^{-/-} mice show increased histological signs of axonal perturbation in peripheral nerves (SMI32-positive axons) without physiological consequences when standard neurographic techniques were used (CMAP amplitudes). This goes along with a lack of increased numbers of periaxonal vacuoles and denervation of NMJs.

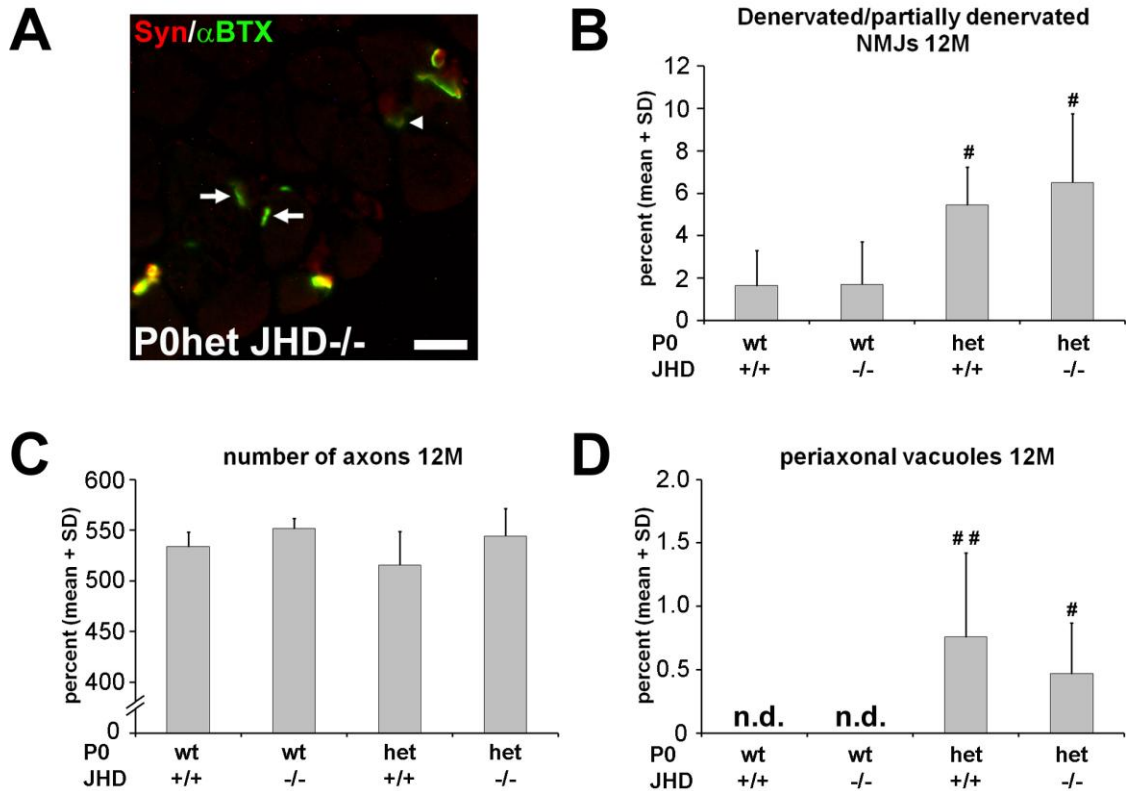


Figure 16: JHD deficiency has no impact on axonal loss and muscle denervation in 12-month-old P0het mutants. A. Representative immunohistochemical staining of synaptophysin (Syn) and labeling with α -Bungarotoxin (α BTX) to detect pre- and postsynapses, respectively, at neuromuscular junctions (NMJ) within cross-sections of the flexor digitorum brevis muscle from P0het JHD^{-/-} mice. Arrows depict completely denervated NMJs; arrowhead depicts a partially denervated NMJ. Scale bar, 20 μ m. B. Denervated/partially denervated NMJs are significantly increased in P0het JHD^{+/+} and P0het JHD^{-/-} mice compared to wildtype littermates. $n = 4$; one-way ANOVA with Bonferroni-Holm correction; # (significant difference to P0wt JHD^{+/+}), # $P < 0.05$. C. Quantification of the number of axons in femoral quadriceps nerve cross-sections reveals no significant alteration between investigated groups. $n = 4$; one-way ANOVA; $P > 0.05$. D. Quantification of periaxonal vacuoles in femoral quadriceps nerve cross-sections. The percentage of periaxonal vacuoles is significantly increased in P0het JHD^{+/+} and P0het JHD^{-/-} mice compared to wildtype littermates. $n = 4 - 7$; Kruskal-Wallis test with Bonferroni-Holm correction. # (significant difference to P0wt JHD^{+/+}). #, $P < 0.05$; ##, $P < 0.01$. n.d. (not detected).

5.8. Altered numbers of immune-related cells in 12-month-old P0het JHD^{-/-} mice

In order to get more insights into the pathomechanisms that lead to aggravated nerve damage in P0het JHD^{-/-} mice at 12 months of age, T-lymphocytes as possible amplifiers of disease progression were investigated. CD8-positive T-lymphocytes were scarcely detectable in peripheral nerves of P0het JHD^{+/+} and P0het JHD^{-/-} mice at 12 months of age (not shown) and therefore not further considered to be involved in the pathogenesis. Quantification of CD4-positive T-lymphocytes revealed a significant difference between P0het JHD^{+/+} and P0het JHD^{-/-} mice (Fig. 17). Whereas the number of CD4-positive T-lymphocytes was significantly reduced in 6-month-old P0het JHD^{-/-} mice, this number was significantly elevated at 12 months of age compared to P0het JHD^{+/+} single mutants (Fig. 17). This suggests that CD4-positive T-lymphocytes might contribute to the demyelinating phenotype in 12-month-old P0het JHD^{-/-} mice.

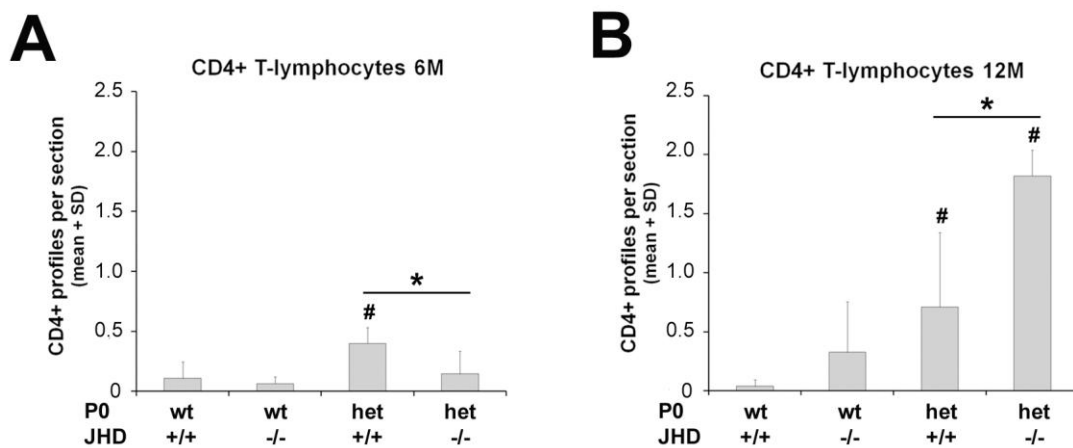


Figure 17: Increased number of CD4-positive T-lymphocytes in 12-month-old P0het JHD^{-/-} mice. A. - B. Quantification of CD4-positive T-lymphocytes in femoral quadriceps nerve cross-sections from 6- (A) and 12-month-old mice (B). A. CD4-positive lymphocytes are significantly elevated in P0het JHD^{+/+} mutant mice compared to wildtype littermates, but significantly reduced in P0het JHD^{-/-} mice. B. At 12 months of age the number of CD4-positive T-lymphocytes is significantly elevated in P0het JHD^{-/-} mice compared to P0het JHD^{+/+} and wildtype littermates. n = 3 - 6; Kruskal-Wallis test with Bonferroni-Holm correction, # (significant difference to P0wt JHD^{+/+}), * (significant difference between P0het mutant groups). #, * P < 0.05. For comparison, data from 6-month-old mice, as shown in figure 8 are presented here again.

As a next step, immunohistochemical stainings were performed against CD86 and CD206, to determine the polarization status of macrophages at 12 months of age. In femoral quadriceps nerve cross-sections from P0het JHD^{+/+} mice the number of CD86-positive cells increased from 6 to 12 months of age and was significantly elevated compared to wildtype littermates (Fig. 18A, B). In contrast to 6 months of age this number was further augmented in 12-month-old P0het JHD^{-/-} mice (Fig. 18A, B). The number of CD206-positive cells was elevated in P0het JHD^{+/+} mice compared to wildtype littermates at 12 months of age but did not significantly differ between P0het JHD^{+/+} and P0het JHD^{-/-} mice (Fig. 18C, D). Consistent with F4/80-positive macrophage numbers (see Fig. 7 and Fig. 12) the number of both M1- and M2-polarized cells was not altered in cutaneous saphenous nerves in all genotypes at both investigated ages (Fig. 18A - D). To further substantiate and extend these findings, double immunohistochemistry was performed against CD86 and F4/80 to determine M1-polarized macrophages. Indeed, both phenotypes could be observed in femoral quadriceps nerves (Fig. 18E). Most interestingly, macrophages with an activated, myelin-phagocytosing appearance were found either positive or negative for the M1 associated marker CD86 (Fig. 18E). These results suggest that JHD deficiency leads to a shift of macrophage polarization during disease progression in P0het mice and that the increased number of macrophages in P0het JHD^{-/-} mice at 12 months of age is preferentially due to an elevated number of CD86-positive, M1-polarized cells that most likely contribute to myelin degeneration.

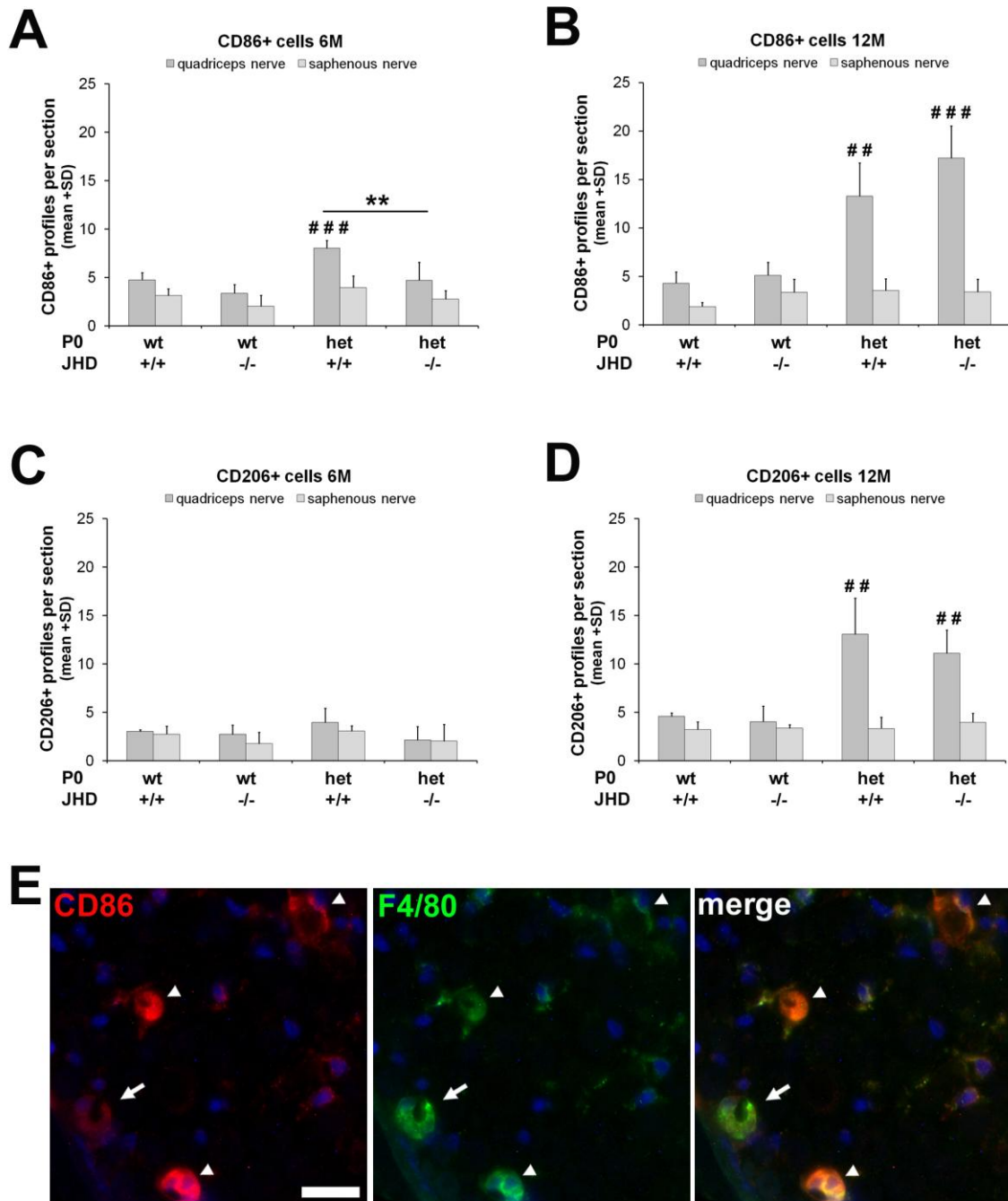


Figure 18: Altered macrophage polarization in 6 and 12-month-old P0het JHD-/- mice. A. - B. Quantification of CD86-positive cells (M1) in 6- (A) and 12-month-old mice (B). A. P0het JHD+/+ mice show significantly increased number of CD86-positive cells compared to P0wt JHD+/+ mice at 6 months of age. Consistent with macrophage numbers, M1-polarized cells are significantly reduced in P0het JHD-/- mice compared to P0het JHD+/+ single mutants. B. In 12-month-old P0het JHD+/+ mice the number of CD86-positive cells is further increased. P0het JHD-/- mutants show further augmented numbers of CD86-positive cells. C. - D. Quantification of CD206-positive cells (M2) in 6- (C) and 12-month-old mice (D). No alteration in the number of CD206-positive cells can be detected in P0het JHD+/+ and P0het JHD-/- mice at 6 months of age (C). At 12 months of age the number of CD206-positive cells is significantly increased in both P0het JHD+/+ and P0het JHD-/- mice compared to wildtype littermates (D). n = 3 - 5; one-way ANOVA with

Bonferroni-Holm correction, # (significant difference to P0wt JHD+/+), * (significant difference between P0het mutant groups). #, * P < 0.05; ##, ** P < 0.01; ###, *** P < 0.001. For comparison, data from 6-month-old mice, as shown in figure 8 are presented here again. E. Representative micrographs of an immunohistochemical staining against M1-polarized, CD86-positive (red) and F4/80-positive macrophages (green) in cross-sections from 12-month-old P0het JHD-/- mice. Nuclei are labeled with DAPI. Note two different phenotypes of activated, myelin-phagocytosing macrophages in the endoneurium. M1-polarized macrophages (CD86^{hi}-positive) are indicated by arrowheads, a possible M2-polarized macrophage (CD86^{low}-positive) is indicated by an arrow. Scale bar = 20 μ m.

To further characterize macrophage polarization in peripheral nerves of 12-month-old single and double mutants, the expression of M1 and M2 associated markers as well as pro- and anti-inflammatory cytokines (Biswas and Mantovani, 2010; Ydens et al., 2012) was analyzed by semi-quantitative real-time PCR (qRT-PCR) (Fig. 19 and 20). Consistent with the immunohistochemical observations (Fig. 18B), CD86 mRNA expression was significantly increased in P0het JHD-/- mice (Fig. 19A). Interestingly, the majority of M2-associated genes, like CD206, TREM-2, FIZZ, Ym1, and Arginase-1 were also elevated in their expression in P0het JHD-/- mice compared to P0het JHD+/+ single mutants and wildtype littermates (Fig. 19B - F). Moreover, JHD deficiency resulted also in increased mRNA expression of Fc γ receptors (Fig. 19G, H).

Furthermore, an altered cytokine profile could be detected in peripheral nerves upon JHD deficiency. The expression of several known immune mediators, like CCL2/MCP-1, CSF-1, LIF or IL-1 β (Martini et al., 2008) was increased in P0het JHD-/- double mutants compared to P0het JHD+/+ single mutants and wildtype littermates (Fig. 20A - D). Of note, none of the characteristic M1 associated pro-inflammatory cytokines such as IL-6, iNOS or IFN γ (not detectable) were elevated in their expression in P0het JHD+/+ and P0het JHD-/- mice (Fig. 20E, F). TNF α levels were increased both in P0het JHD+/+ and P0het JHD-/- mutants compared to wildtype mice (Fig. 20G). On the other hand, the expression of the M2 associated anti-inflammatory cytokine TGF- β was significantly increased in P0het JHD-/- mice (Fig. 20H). Together these results suggest that JHD deficiency triggers an enhanced M2-polarized (alternative) macrophage response in 12-month-old P0het mice, similar to observations after acute nerve injury (Ydens et al., 2012).

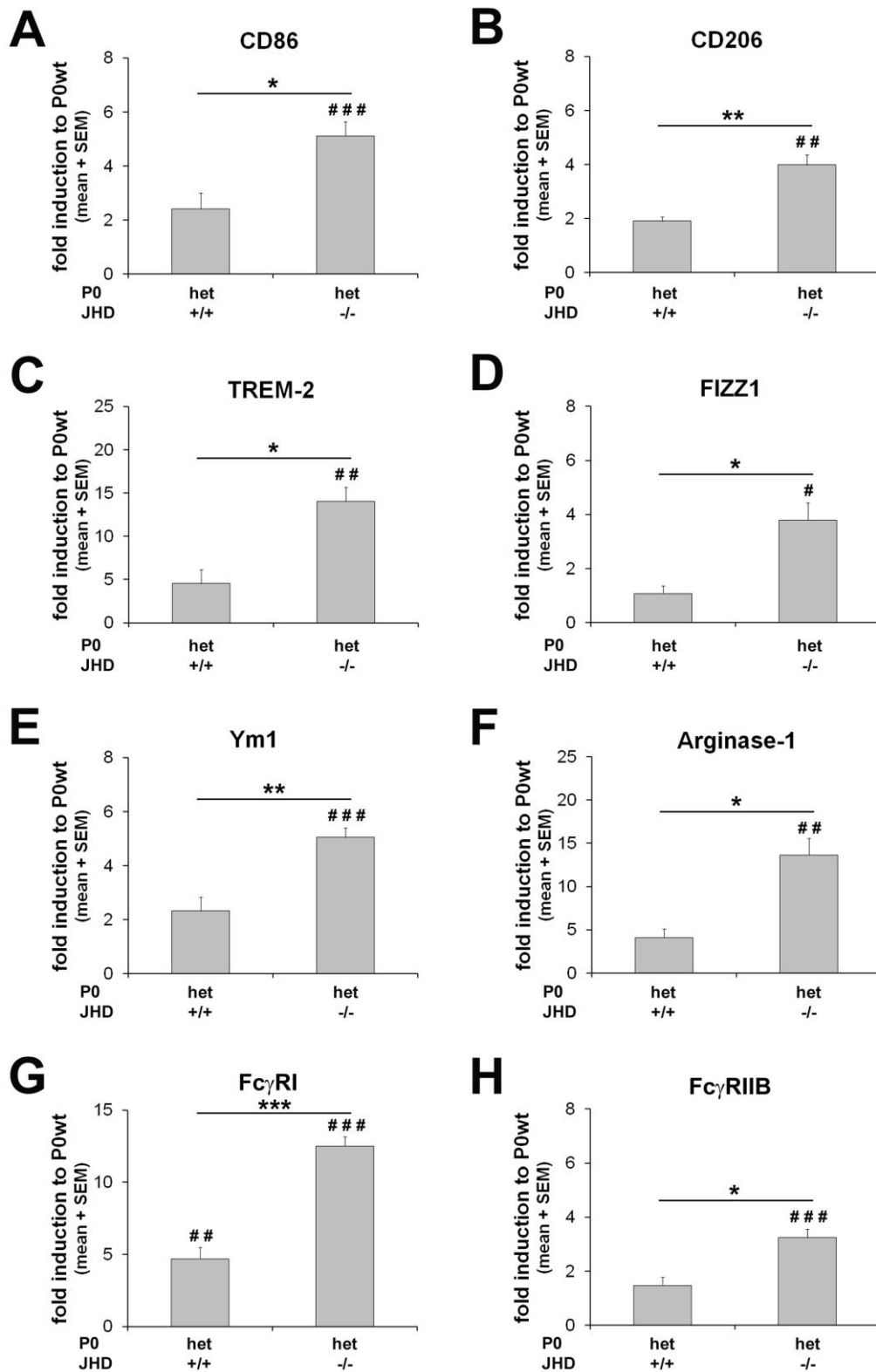


Figure 19: JHD deficiency triggers an M2-polarized (alternative) macrophage response in 12-month-old P0het mice. A. - H. mRNA expression of M1 (A) and M2 (B - F) associated genes in femoral quadriceps nerves from 12-month-old wildtype (P0wt JHD^{+/+}), single (P0het JHD^{+/+}) and double mutant mice (P0het JHD^{-/-}) was analyzed by qRT-PCR. mRNA expression levels are shown as fold induction to P0wt JHD^{+/+} and are all significantly increased in P0het JHD^{-/-} mice

compared to P0het JHD+/+ single mutants and wildtype littermates. G. - H. mRNA expression levels for Fc γ receptors are also significantly increased in P0het JHD-/- mice. n = 3 - 4; mean + SEM (standard error of mean); one-way ANOVA with Bonferroni-Holm correction, # (significant difference to P0wt JHD+/+), * (significant difference between P0het mutant groups). #, * P < 0.05; ##, ** P < 0.01; ###, *** P < 0.001.

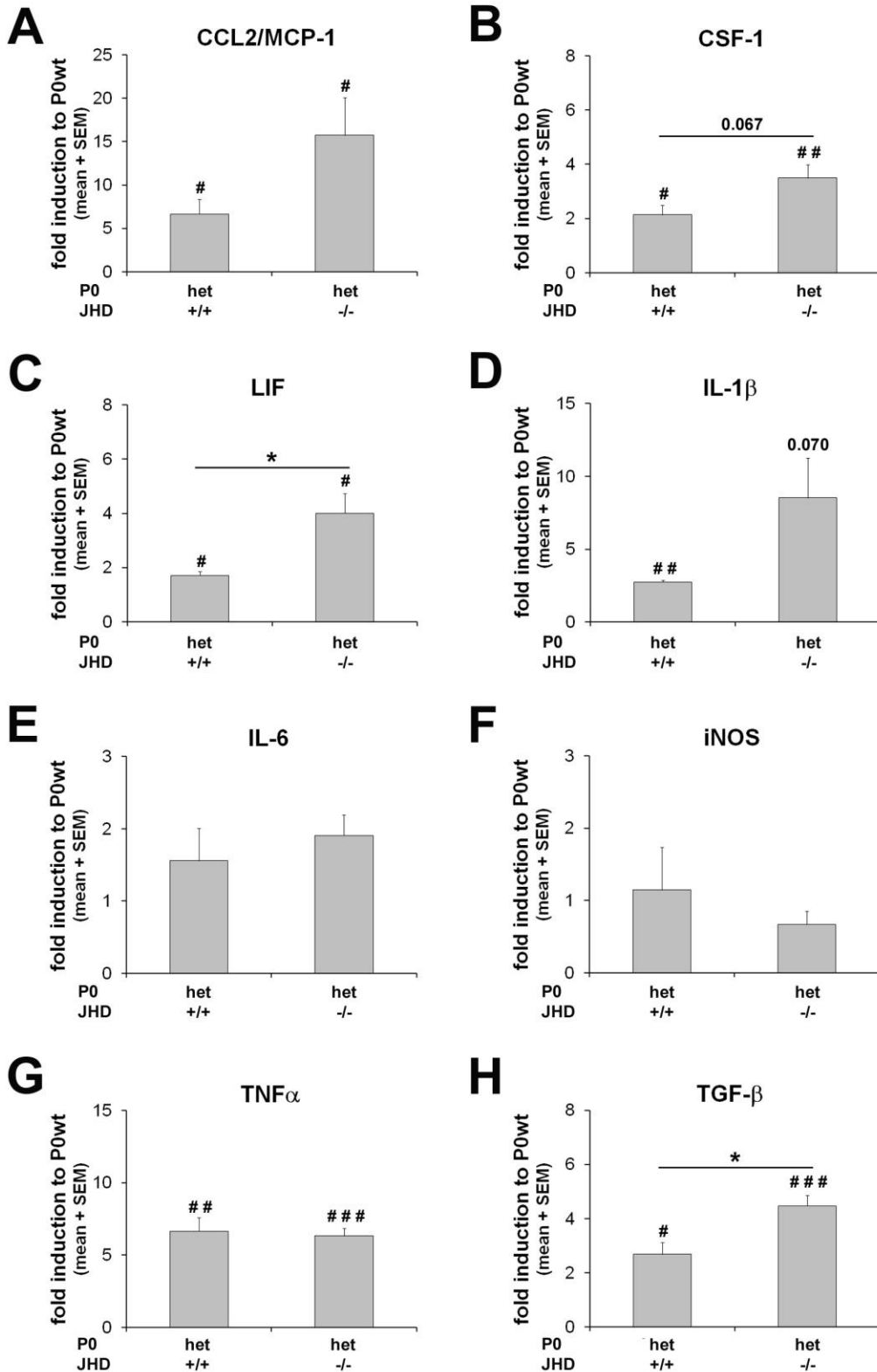


Figure 20: JHD deficiency leads to an increased cytokine production in 12-month-old P0het mice. A. - H. The mRNA expression of immune mediators (A - D), M1 (E - G), and M2 associated (H) cytokines in femoral quadriceps nerves from 12-month-old wildtype (P0wt JHD+/+), single (P0het JHD+/+) and double mutant mice (P0het JHD-/-) was analyzed by qRT-PCR. mRNA expression levels are shown as fold induction to P0wt JHD+/+. Several immune mediators (A - D) are significantly increased in their expression in P0het JHD-/- mice compared to P0het JHD+/+ single mutants and wildtype littermates, whereas the expression of typical M1 associated pro-inflammatory cytokines is not altered (E - G). H. mRNA expression of the M2 associated anti-inflammatory cytokine TGF- β is significantly increased in P0het JHD-/- mice. n = 3 - 4; mean + SEM (standard error of mean); one-way ANOVA with Bonferroni-Holm correction, # (significant difference to P0wt JHD+/+), * (significant difference between P0het mutant groups). #, * P < 0.05; ##, ** P < 0.01; ###, *** P < 0.001.

6. Discussion

Several previous results highlighted the important role of secondary low grade inflammation - implicating macrophages and lymphocytes - as a disease amplifier in mouse models for primarily genetically-induced nerve disorders (Martini et al., 2013). However, the exact function of the adaptive immune system in the pathogenesis of CMT1B is not completely understood. Interestingly, a previous study demonstrated that endogenous antibodies - as a part of the adaptive immune system - bound to myelin components contribute to the activation of macrophages and rapid myelin clearance during Wallerian degeneration (Vargas et al., 2010). Based on these observations, the pathogenic impact of endogenous antibodies was investigated in peripheral nerves of a mouse model for CMT1B (P0het mice).

6.1. Endogenous antibodies accumulate in peripheral nerves of P0het myelin mutant mice

This study demonstrates for the first time that endogenous antibodies strongly accumulate in the endoneurium of femoral quadriceps nerves from P0het mice compared to wildtype littermates. By immunohistochemistry and Western blot analysis it could be shown that these antibodies comprise both IgG and IgM subtypes. Moreover, immunocytochemical investigations on single teased fiber preparations revealed that endogenous antibodies are associated with the extracellular domains of endoneurial tubes and also located at the nodes of Ranvier. Furthermore, IgG-immunoreactivity was not only detectable in 6- and 12-month-old P0het mice, but already at 1 month of age, an early time point in disease before demyelinating features are morphologically visible, suggesting that endogenous antibodies probably contribute to early pathogenesis in an animal model for CMT1B. Supporting this view, the non-affected sensory branch of the femoral nerve (saphenous nerve) lacked this prominent antibody deposition in P0het mutant mice.

Similar observations have been gained after peripheral nerve injury, where endogenous antibodies accumulate along endoneurial tubes of lesioned nerves (Vargas et al., 2010). Of note, intact nerves revealed a similarly weak labeling as in wildtype mice in this study. Moreover, at least a subpopulation of systemic antibodies recognized the myelin component P0 (MPZ) (Vargas et al., 2010). Based on the similar staining pattern and the

systemic presence of such antibodies even in wildtype mice, it is very likely that the antibodies accumulating in the endoneurium of P0het mice share the same or similar epitopes. Interestingly, in both P0wt and P0het mice at 6 and 12 months of age a strong antibody deposition was detectable in the perineurium of femoral nerves, whereas a much lower IgG-immunoreactivity was visible in the perineurium of 1-month-old mice. The relevance of this observation is enigmatic.

The question emerges why endogenous, preexisting antibodies bind to myelin components in P0het mutants and do not accumulate in wildtype mice. It is likely that an intact blood-nerve barrier explains the diminished antibody deposition (Bouldin et al., 1990; Vargas et al., 2010). Additionally, it might be possible that some epitopes are only accessible under pathological conditions and ‘hidden’ in normal myelin. Supporting the latter hypothesis, an interrupted blood-nerve barrier was not observed in young CMT1B mice (Martini, unpublished observations). Furthermore, previous results demonstrated the presence of anti-PMP22 antibodies in sera from CMT1 patients, but immunohistochemical analysis revealed that myelinated fibers of healthy controls were not stained when they were incubated with isolated anti-PMP22 IgGs (Ritz et al., 2000).

Another important mediator for pattern recognition is the complement system which can be activated by three different pathways. Notably, antibody deposition is necessary for the initial activation of the classical pathway (Ramaglia et al., 2008). Previous studies demonstrated that the complement system exerts a similar role as antibodies in models for Wallerian degeneration, because its activation contributes to the efficient removal of myelin debris and recruitment and activation of macrophages after nerve lesion (Dailey et al., 1998; Ramaglia et al., 2007; Ramaglia et al., 2009). Therefore activation of the complement cascade might be another potential mechanism which could provide a link between the innate and adaptive immune system in models for CMT1. Interestingly, both immunocytochemistry and Western blot analysis showed no indications for the activation of C3, a central component in the complement system, in the disease progression of P0het myelin mutant mice, suggesting that an involvement in the pathogenesis is rather unlikely. These observations might also favor the possibility that complement deposition is related to axonal damage, a pathogenic feature that is rather mild in P0het mice. However, further crossbreeding experiments with mice that lack specific complement components are

necessary to determine the exact function of the complement system in the pathogenesis of other CMT1 mouse models in detail.

6.2. Crucial role for endogenous antibodies in early macrophage-mediated demyelination

In order to investigate the functional role of antibodies in a mouse model for CMT1B, P0het mutant mice were crossbred with JHD-deficient mice that lack B-lymphocytes, and therefore antibodies. In 6-month-old P0het mice, the lack of antibodies resulted in a reduced elevation of macrophage numbers in femoral quadriceps nerves. Furthermore, the demyelinating phenotype was substantially ameliorated in P0het JHD^{-/-} mice. Reconstitution with murine antibodies (IgG fraction) restored antibody deposition in peripheral nerves and reverted the neuropathy in P0het JHD^{-/-} mice, thereby confirming the potentially pathogenic role of endogenous antibodies at this stage of the disease. Of note, passive transfer into P0wt JHD^{-/-} mice had no effect on macrophage activation and nerve structure. This implies that the deterioration after passive antibody transfer is dependent on the susceptibility of mutated Schwann cells in P0het mice. Corroborating this hypothesis, passive antibody transfer had no effect in P0wt RAG1^{-/-} mice, but led to a substantial disease aggravation in P0het RAG1^{-/-} double mutants at 8 months of age (Klein and Martini, unpublished observations). Taken together, these data suggest that myelin bound antibodies might serve as a recognition signal for activated macrophages, thereby directly contributing to early macrophage-mediated demyelination. A similar role was described for accumulating antibodies in Wallerian degeneration, as JHD-deficient mice showed slightly delayed macrophage recruitment, impaired phagocytic activity and subsequent myelin removal. In addition, passive transfer of antibodies reconstituted early macrophage activation and rapid myelin clearance in JHD^{-/-} mice (Vargas et al., 2010).

How might antibody deposition and macrophage-mediated demyelination be linked? A broad range of receptors are responsible for target recognition and the phagocytic activation of macrophages (Taylor et al., 2005). The best characterized among these are Fc γ receptors for immunoglobulins and the complement receptor 3 (CR3, also known as CD11b) for complement component C3bi which both can act synergistically on macrophages (Rotshenker, 2003; Hall et al., 2006). Since complement deposition could not

be found along P0het mutant nerve fibers, an involvement of CR3 in the pathogenesis of CMT1B is unlikely. By contrast, the expression of Fc γ receptors is increased in P0het mutants (this study) and the receptor is also amply detectable on endoneurial macrophages (Klein and Martini, unpublished observation), and might therefore be an important mediator to link innate and adaptive immune reactions in a mouse model for CMT1B. In fact, the involvement of other macrophage receptors (i.e. mannose receptor, scavenger receptor or Toll-like receptors (TLR)) in the pathogenesis of CMT1 cannot be ruled out, but this needs to be investigated in future experiments.

Interestingly, it has been reported that CSF-1 is involved in Fc receptor upregulation in peritoneal macrophages (Magee et al., 1987) and under various pathological conditions (Chitu and Stanley, 2006). As CSF-1 expression is increased in peripheral nerves of distinct CMT1 mouse models (Fischer et al., 2008b; Groh et al., 2012; Kohl and Martini, unpublished observations), it is conceivable that CSF-1 not only leads to intrinsic macrophage proliferation and activation (Müller et al., 2007), but additionally increases Fc γ receptor expression on macrophages to prime them for subsequent recognition of antibody depositions. Supporting this idea, this study shows that Fc γ receptor mRNA expression correlates with the level of CSF-1 expression in 12-month-old P0het JHD $^{+/-}$ single and P0het JHD $^{-/-}$ double mutants.

Surprisingly, reconstitution with antibodies specific to a non-mammalian antigen, keyhole limpet hemocyanin (KLH), or with murine IgG Fc-fragments resulted in an intermediate effect. Although antibody deposition was, as expected, not detectable in peripheral nerves, endoneurial macrophage numbers were elevated together with an aggravated myelin degeneration in individual animals in comparison to non-reconstituted P0het JHD $^{-/-}$ mice. Although the corresponding values in the reconstituted and non-reconstituted double mutants were not significantly different from each other, these data may suggest that not only myelin bound antibodies, but also systemic, ‘free’ antibodies might have the capacity to contribute to macrophage activation. Notably, passive transfer of unspecific anti-GFP antibodies also generated a mild, non-significant increase in the number of infiltrated macrophages in the lesion model which was not further addressed by the authors (Vargas et al., 2010).

6.3. JHD deficiency triggers increased immune reactions and disease aggravation in 12-month-old P0het mice

In previous studies it was demonstrated that the lack of T- and B-lymphocytes resulted in a substantial and persistent reduction of endoneurial macrophages and amelioration of the demyelinating phenotype in two models of CMT1 (Schmid et al., 2000; Kobsar et al., 2003), similar to the findings of 6-month-old P0het JHD^{-/-} mice which lack B-lymphocytes and antibodies solely. Thus, P0het JHD^{-/-} double mutants were also investigated at the age of 12 months and compared to the findings from P0het RAG1^{-/-} mice. P0het single mutants showed increased numbers of macrophages compared to 6 months of age, confirming previous results (Fischer et al., 2008b) and reflecting the increased inflammatory reaction during the progressive disease development. Unexpectedly, JHD-deficient P0het mice presented more macrophages in peripheral nerves, contrary to the observations at 6 months of age. Furthermore, double mutants revealed an aggravated demyelinating phenotype compared to P0het JHD^{+/+} single mutants. This could be a consequence of myelin-phagocytosing macrophages that were also amply detectable in P0het JHD^{-/-} double mutants, corroborating the correlation between the total number of endoneurial macrophages and subsequent nerve fiber damage. These results clearly demonstrate that JHD deficiency has, in contrast to RAG1 deficiency, opposite effects in the disease course of P0het mice.

How is target recognition in the absence of antibody and complement deposition regulated, and myelin phagocytosis possible in 12-month-old P0het JHD^{-/-} mice? Despite Fc γ and complement receptor-mediated myelin removal (Kuhlmann et al., 2002; Rotshenker, 2003), several studies demonstrated the involvement of other receptors expressed on macrophages/microglia under various pathological conditions, like scavenger receptor (Reichert and Rotshenker, 2003; Rotshenker et al., 2008; Hendrickx et al., 2013), Galectin-3 (Rotshenker et al., 2008; Mietto et al., 2013), and Toll-like receptors (TLR) (Mietto et al., 2013). However, if these receptors contribute to myelin degeneration in mouse models for CMT1 is not known and needs to be investigated in future studies.

Considering typical symptoms in CMT1 patients, axonal damage and subsequent muscular atrophy are crucial factors that determine the clinical outcome (Scherer and Wrabetz, 2008). As an indicator for axonal perturbation, immunohistochemical stainings against

non-phosphorylated neurofilaments (SMI32) (Groh et al., 2010) were investigated in this study. The rather mild axonopathic phenotype in peripheral nerves of P0het mice at 12 months of age was reflected by only slightly increased SMI32-immunoreactive profiles compared to wildtype littermates. Interestingly, P0het JHD^{-/-} mice had elevated numbers of SMI32-positive, irregular shaped axons. This does not stringently reflect axonal degeneration or injury, as axon numbers and the percentage of periaxonal vacuoles were unchanged between P0het JHD^{+/+} single and P0het JHD^{-/-} double mutants. Therefore, the reason for the increased number of SMI32-positive axons remains elusive.

How might JHD deficiency result in these divergent effects during pathogenesis in P0het mutant mice? In contrast to RAG1 deficiency, T-lymphocytes are still present in JHD-deficient mice. Of note, CD8-positive T-lymphocytes were barely detectable in peripheral nerves of P0het JHD^{+/+} and P0het JHD^{-/-} mice at 6 and 12 months of age, and therefore not further considered to contribute to disease progression. Quantification of CD4-positive T-lymphocytes revealed significant differences between P0het JHD^{+/+} and P0het JHD^{-/-} mice. In 6-month-old P0het JHD^{-/-} mice the number of CD4-positive T-lymphocytes was substantially reduced compared to P0het JHD^{+/+} mice. In contrast, CD4-positive T-lymphocytes were significantly increased at 12 months of age compared to P0het single mutants, thus correlating with the respective degree of demyelination. Despite the overall low absolute numbers, these results suggest that CD4-positive T-lymphocytes might contribute to the demyelinating phenotype in 12-month-old P0het JHD^{-/-} mice. It is plausible to assume that T-lymphocytes might modulate the activation of macrophages (Mäurer et al., 2002; Ip et al., 2006). This might also explain the distinct nerve phenotype between JHD⁻ and RAG1-deficient P0het mutants at 12 months of age, as the latter lack this potential disease-amplifying effect of T-lymphocytes.

Several recent studies have demonstrated that macrophages can become polarized to pro- and anti-inflammatory states (Gordon, 2003; Shechter and Schwartz, 2013). These ‘classically-activated’ (M1) or ‘alternatively activated’ (M2) macrophages possess different functional properties and can be either detrimental or beneficial for nervous tissue (Gordon, 2003; Kigerl et al., 2009; David and Kroner, 2011). To further elucidate differences in the inflammatory response in peripheral nerves of 12-month-old single and double mutants, the activation state of macrophages was investigated by immunohistochemistry against CD86 or CD206, typical markers for M1-polarized or M2-

polarized macrophages, respectively (Gordon, 2003; Kigerl et al., 2009). During disease progression the number of CD86-positive cells increased in P0het JHD^{+/+} mice compared to wildtype littermates. Interestingly, P0het JHD^{-/-} double mutants at 6 months of age had reduced numbers of M1-polarized macrophages, whereas 12-month-old P0het JHD^{-/-} double mutants showed further increased numbers of CD86-positive cells. In contrast, the number of CD206-positive cells did not differ between P0het JHD^{+/+} and P0het JHD^{-/-} mice and was only significantly increased compared to wildtype mice at the age of 12 months. Consistent with macrophage numbers the number of both M1- and M2-polarized cells was not altered in the cutaneous saphenous nerve in all genotypes. These results suggest that JHD deficiency leads to a shift of macrophage polarization during disease development in P0het mice and that the elevated number of macrophages in P0het JHD^{-/-} mice at 12 months of age is preferentially due to an increased number of CD86-positive cells that most likely contribute to the demyelinating phenotype.

To further corroborate these findings, the expression levels of several pro- and anti-inflammatory cytokines, as well as M1- and M2-associated genes (Biswas and Mantovani, 2010; Ydens et al., 2012) were investigated by qRT-PCR. This was performed in order to elucidate the ‘inflammatory milieu’ in peripheral nerves of wildtype and mutant mice at the age of 12 months. The increased number of inflammatory cells in P0het JHD^{-/-} double mutants compared to P0het JHD^{+/+} single mutants that could be detected by immunohistochemistry was consistent with an elevated expression of several characteristic immune mediators, like CCL2/MCP-1, CSF-1, LIF or IL-1 β (Martini et al., 2008). Confirming the immunohistochemical data, CD86 mRNA expression was significantly increased in P0het JHD^{-/-} compared to P0het JHD^{+/+} mice. However, other M1 associated genes, like iNOS, IL-6 or IFN γ , showed no elevated expression in P0het JHD^{+/+} and P0het JHD^{-/-} mice. On the other hand, the expression of the M2 associated, anti-inflammatory cytokine TGF- β was significantly increased in P0het JHD^{-/-} mice. Additionally, the expression of prototypical M2 associated genes, like TREM2, Arginase1, FIZZ1, CD206, and YM1, was substantially elevated in P0het JHD^{-/-} mice compared to P0het JHD^{+/+} single mutants. Interestingly, TGF- β , CCL2, and CSF-1, which are all increased in their expression in P0het JHD^{-/-} mice, have been described to foster M2-polarization in tumor associated macrophages (TAM) (Biswas and Mantovani, 2010; Van Overmeire et al., 2014), proposing similar mechanisms in endoneurial macrophages. It was also reported that Galectin-3 expression is induced in M2-polarized macrophages

(MacKinnon et al., 2008), again suggesting that other receptors might compensate - in the absence of endogenous antibodies - for target recognition and Fc γ receptor-mediated myelin removal.

On the first glance, the qRT-PCR data might be in disagreement with the immunohistochemical observations. However, M1- and M2-activation are only 'the extremes of a continuum' (Mantovani et al., 2004). Thus, it was shown that M2b/M2-like-polarized macrophages share the expression of some M2 associated markers, but can also express M1 associated genes, like CD86 (Mosser, 2003; Mantovani et al., 2004). Supporting this view, F4/80-positive macrophages with a myelin-phagocytosing appearance that are thought to be M2-polarized were also found to be positive for CD86.

Taken together, JHD deficiency triggers enhanced immune reactions and an altered cytokine profile, as well as an M2-polarized macrophage response in 12-month-old P0het mice, similar to observations in Wallerian degeneration (Ydens et al., 2012). Although M2-polarized macrophages mediate tissue repair, and are considered to be beneficial under various disease conditions (Gordon, 2003; Kigerl et al., 2009; Mantovani et al., 2013), they seem to have a detrimental function in mouse models for CMT1 disorders when they are chronically activated under nonlesion conditions. Presently it is difficult to decide whether the absence of accumulating antibodies or the altered cytokine profile due to JHD deficiency is responsible for the aggravated demyelinating phenotype at 12 months of age. Notably, another possible function of antibodies was demonstrated in distinct CNS disorders, as they bind to the surface of oligodendrocytes and modulate their intracellular signaling, thereby promoting remyelination, interestingly, in the absence of Fc function (Ciric et al., 2003; Warrington and Rodriguez, 2008; Wright et al., 2009). There is no evidence that accumulating antibodies in the PNS might exert similar effects on mutant Schwann cells, but it is tempting to speculate that they can also directly modulate intracellular signaling or cytokine expression. Supporting this hypothesis, antibody depositions are preferentially detectable in the femoral quadriceps as opposed to the saphenous nerve, as the latter lacks an increased cytokine expression (MCP-1/CCL2, CSF-1) and is protected from inflammatory reactions and myelin degeneration.

6.4. The immune system as a therapeutic target for CMT1

Despite the remarkable progress in CMT research in the last years, there is still no causative cure available for affected patients and only rehabilitative strategies or surgeries are available as therapeutic approaches (Schenone et al., 2011). Therefore, novel approaches are needed to determine beneficial therapies to treat inherited peripheral neuropathies. Several potential therapeutic agents demonstrated improvement in animal models for CMT1A, like ascorbic acid (Passage et al., 2004) or neurotrophin-3 (NT3) (Sahenk et al., 2005; Sahenk et al., 2014), but clinical trials failed to translate an unequivocal beneficial effect in humans (Pleasure and Chance, 2005; Burns et al., 2009; Micallef et al., 2009; Verhamme et al., 2009; Pareyson et al., 2011).

To identify new therapies, disease mechanisms in preclinical animal models, that additionally have implications for CMT1 patients, must be determined. Considering the data from this study, lack of endogenous antibodies revealed beneficial effects in 6-month-old P0het mice. Notably, endoneurial antibody deposition was also detectable in a sural nerve biopsy of a CMT1A patient (Klein, Sommer and Martini, unpublished observation) and autoantibodies were present in sera from CMT1 patients (Ritz et al., 2000), suggesting that B-lymphocytes and endogenous antibodies - as part of the adaptive immune system - might be a reasonable target for a therapeutic approach. However, JHD deficiency led to aggravated nerve fiber damage in 12-month-old P0het mice, arguing against this possible therapeutic approach. Currently it is hard to decipher whether the lack of endogenous antibodies or B-lymphocytes is responsible for the observed phenotype, and if they also possess a neuroprotective function in 12-month-old P0het JHD^{-/-} mice. Interestingly, a neuroprotective role for the adaptive immune system was described in a dysmyelinating mutant, as RAG1-deficient P0 null double mutants showed increased axonal loss, maybe due to the constantly elevated numbers of potentially cytotoxic endoneurial macrophages (Berghoff et al., 2005).

In human biopsies, prominent inflammation in peripheral nerves was reported only in some cases (for review see Martini and Toyka, 2004). However, some of these atypical forms of CMT that also presented features typical for chronic inflammatory demyelinating polyneuropathy (CIDP), reacted positively upon immunomodulation, like corticosteroid treatment (Dyck et al., 1982; Bird and Sladky, 1991; Rajabally et al., 2000; Watanabe et al., 2002), plasmapheresis (Malandrini et al., 1999) or intravenous immunoglobulin (IVIg)

treatment (Ginsberg et al., 2004; Desurkar et al., 2009; Schneider-Gold et al., 2010; Miki et al., 2013). It is possible that those cases that clearly show an implication of immune cells reflect a strong inflammatory reaction superimposed on the primarily hereditary demyelinating neuropathy (Martini and Toyka, 2004). Additionally, it is plausible to assume that macrophages were not detectable in the majority of cases, because the active phase of demyelination in many forms of CMT1 occurs in early pathogenesis during childhood (Gabreels-Festen et al., 1992; Vital et al., 1992; Garcia et al., 1998; Thomas, 1999), when nerve biopsies are usually not performed. Supporting this hypothesis, aged mice (24-month-old) display also reduced numbers of macrophages in distinct CMT1 mutants (Klein and Martini, unpublished observations), but this requires further investigations.

Nevertheless, immunomodulation appears as a suitable therapeutic approach to treat CMT1. Tacrolimus (FK506) is frequently used as an immunosuppressant in patients receiving organ transplantations. Moreover, neuroprotective effects were described in various disease models (Sulaiman et al., 2002; Gold et al., 2004). However, treatment of P0het mice with FK506 did not reduce the number of endoneurial CD8-positive T-lymphocytes and led to an aggravated demyelinating phenotype, excluding the drug for the treatment of CMT1 patients (Ip et al., 2009).

Taking these observations into account, directly targeting the innate immune system might be a more promising approach to reduce nerve fiber damage, as myelin degeneration is more efficiently blocked by the absence of macrophage-activating cytokines, like CCL2/MCP-1 or CSF-1 (Carenini et al., 2001; Fischer et al., 2008b). Moreover, the adaptive immune system seems not to be pathogenetically relevant in PMP22tg mice, a model for CMT1A which represent the most common form of CMT1 (Kohl et al., 2010b). Especially CSF-1, a crucial mediator in macrophage activation, has a substantial role in disease progression as shown by genetic ablation in three CMT1 mouse models (Carenini et al., 2001; Groh et al., 2012; Groh and Martini, unpublished observations). Activation of macrophages by CSF-1-producing fibroblasts was also recently observed in nerve biopsies of distinct CMT1 patients (Groh et al., 2012). CSF-1 signaling has additionally been shown to be involved in Fc receptor upregulation in murine peritoneal macrophages (Magee et al., 1987), suggesting that blocking this pathway might be a promising therapeutic approach to reduce neuroinflammation and subsequent nerve damage in patients. Indeed, in a

preclinical experiment, mice that were treated with a highly selective CSF-1 receptor (CSF-1R) inhibitor (provided by Plexxikon Inc.) showed a robust decline in nerve macrophages. Moreover, the systemic inhibition of the CSF-1R resulted in a substantial reduction of typical histopathological features, and also functional improvement (Klein and Martini, unpublished observations), offering a clinically highly relevant and potent treatment option for CMT1 neuropathies.

6.5. Synopsis

In summary, this study extends the understanding about pathomechanisms in inherited neuropathies. Moreover, it demonstrates that endogenous antibodies contribute to initial mechanisms in macrophage-mediated demyelination in a mouse model for CMT1B. Furthermore, this study identifies endogenous antibodies as a possible link in the interaction between the innate and adaptive immune system in P0het mutant mice (Fig. 21). Antibodies have also been shown to contribute to macrophage activation and rapid myelin clearance after peripheral nerve lesion. Therefore, this study supports the view that CMT1 disorders and Wallerian degeneration share common pathomechanisms that are beneficial after nerve injury, but detrimental under nonlesion conditions.

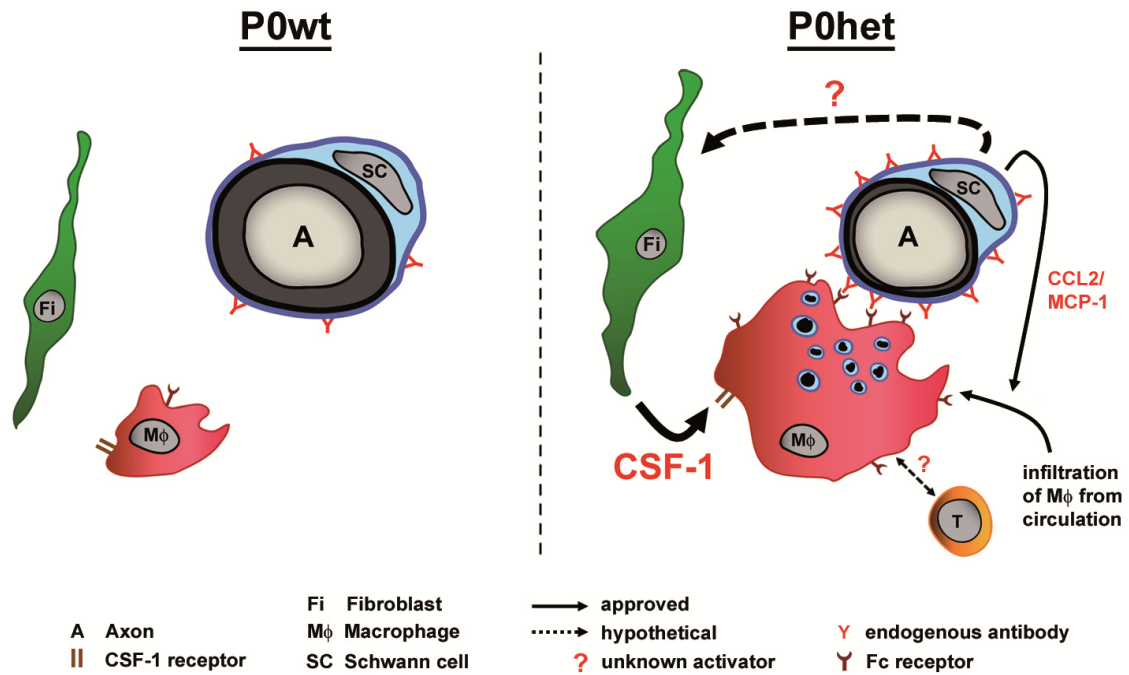


Figure 21: Synoptic view on the proposed pathomechanisms in P0het mice. Important mediators are hierarchically represented by their size in the scheme. In wildtype mice (P0wt, left) myelinating Schwann cells (SC) show only mild deposition of endogenous antibodies. Nerve resident fibroblasts (Fi) and macrophages (M ϕ) are not activated. In CMT1B myelin mutant mice (P0het, right), impaired SC display an elevated expression of several pathogenic cytokines. Upregulation of the chemokine CCL2/MCP-1 fosters the recruitment of macrophages/monocytes from the circulation, thereby contributing to an increase in numbers of endoneurial macrophages. In contrast, fibroblasts become activated by a (possible) Schwann cell derived, so far unknown, cytokine to trigger subsequent expression of CSF-1. Increased CSF-1 levels lead to proliferation and activation of endoneurial macrophages. Moreover, a CSF-1 dependent upregulation of Fc receptors on macrophages facilitates the recognition of antibody depositions at the outer aspects of Schwann cells, leading to myelin phagocytosis and demyelination. Additionally, macrophages can be modulated by T-lymphocytes. However, activation of fibroblasts and subsequent CSF-1-dependent activation of macrophages are thought to act as the major disease amplifier in the pathogenesis of a mouse model for CMT1B.

7. References

- Anzini P, Neuberg DH, Schachner M, Nelles E, Willecke K, Zielasek J, Toyka KV, Suter U, Martini R (1997) Structural abnormalities and deficient maintenance of peripheral nerve myelin in mice lacking the gap junction protein connexin 32. *J Neurosci* 17:4545-4551.
- Berghoff M, Samsam M, Muller M, Kobsar I, Toyka KV, Kiefer R, Maurer M, Martini R (2005) Neuroprotective effect of the immune system in a mouse model of severe dysmyelinating hereditary neuropathy: enhanced axonal degeneration following disruption of the RAG-1 gene. *Mol Cell Neurosci* 28:118-127.
- Bird SJ, Sladky JT (1991) Corticosteroid-responsive dominantly inherited neuropathy in childhood. *Neurology* 41:437-439.
- Biswas SK, Mantovani A (2010) Macrophage plasticity and interaction with lymphocyte subsets: cancer as a paradigm. *Nat Immunol* 11:889-896.
- Bouldin TW, Earnhardt TS, Goines ND (1990) Sequential changes in the permeability of the blood-nerve barrier over the course of ricin neuropathy in the rat. *Neurotoxicology* 11:23-34.
- Brennan KM, Bai Y, Shy ME (2015) Demyelinating CMT-what's known, what's new and what's in store? *Neurosci Lett* 596:14-26.
- Burns J, Ouvrier RA, Yiu EM, Joseph PD, Kornberg AJ, Fahey MC, Ryan MM (2009) Ascorbic acid for Charcot-Marie-Tooth disease type 1A in children: a randomised, double-blind, placebo-controlled, safety and efficacy trial. *Lancet Neurol* 8:537-544.
- Carenini S, Maurer M, Werner A, Blazycza H, Toyka KV, Schmid CD, Raivich G, Martini R (2001) The role of macrophages in demyelinating peripheral nervous system of mice heterozygously deficient in p0. *J Cell Biol* 152:301-308.
- Casasnovas C, Cano LM, Alberti A, Cespedes M, Rigo G (2008) Charcot-Marie-tooth disease. *Foot Ankle Spec* 1:350-354.
- Chen J, Trounstein M, Kurahara C, Young F, Kuo CC, Xu Y, Loring JF, Alt FW, Huszar D (1993) B cell development in mice that lack one or both immunoglobulin kappa light chain genes. *Embo J* 12:821-830.
- Chitu V, Stanley ER (2006) Colony-stimulating factor-1 in immunity and inflammation. *Curr Opin Immunol* 18:39-48.
- Ciric B, Howe CL, Paz Soldan M, Warrington AE, Bieber AJ, Van Keulen V, Rodriguez M, Pease LR (2003) Human monoclonal IgM antibody promotes CNS myelin repair independent of Fc function. *Brain Pathol* 13:608-616.

- Dailey AT, Avellino AM, Benthem L, Silver J, Kliot M (1998) Complement depletion reduces macrophage infiltration and activation during Wallerian degeneration and axonal regeneration. *J Neurosci* 18:6713-6722.
- David S, Kroner A (2011) Repertoire of microglial and macrophage responses after spinal cord injury. *Nat Rev Neurosci* 12:388-399.
- Desurkar A, Lin JP, Mills K, Al-Sarraj S, Jan W, Jungbluth H, Wraige E (2009) Charcot-Marie-Tooth (CMT) disease 1A with superimposed inflammatory polyneuropathy in children. *Neuropediatrics* 40:85-88.
- Dyck PJ, Swanson CJ, Low PA, Bartleson JD, Lambert EH (1982) Prednisone-responsive hereditary motor and sensory neuropathy. *Mayo Clin Proc* 57:239-246.
- Fischer S, Weishaupt A, Troppmair J, Martini R (2008a) Increase of MCP-1 (CCL2) in myelin mutant Schwann cells is mediated by MEK-ERK signaling pathway. *Glia* 56:836-843.
- Fischer S, Kleinschnitz C, Muller M, Kobsar I, Ip CW, Rollins B, Martini R (2008b) Monocyte chemoattractant protein-1 is a pathogenic component in a model for a hereditary peripheral neuropathy. *Mol Cell Neurosci* 37:359-366.
- Fledrich R, Stassart RM, Sereda MW (2012) Murine therapeutic models for Charcot-Marie-Tooth (CMT) disease. *Br Med Bull* 102:89-113.
- Gabreels-Festen AA, Joosten EM, Gabreels FJ, Jennekens FG, Janssen-van Kempen TW (1992) Early morphological features in dominantly inherited demyelinating motor and sensory neuropathy (HMSN type I). *J Neurol Sci* 107:145-154.
- Gabreels-Festen AA, Hoogendijk JE, Meijerink PH, Gabreels FJ, Bolhuis PA, van Beersum S, Kulkens T, Nelis E, Jennekens FG, de Visser M, van Engelen BG, Van Broeckhoven C, Mariman EC (1996) Two divergent types of nerve pathology in patients with different P0 mutations in Charcot-Marie-Tooth disease. *Neurology* 47:761-765.
- Garcia A, Combarros O, Calleja J, Berciano J (1998) Charcot-Marie-Tooth disease type 1A with 17p duplication in infancy and early childhood: a longitudinal clinical and electrophysiologic study. *Neurology* 50:1061-1067.
- Giese KP, Martini R, Lemke G, Soriano P, Schachner M (1992) Mouse P0 gene disruption leads to hypomyelination, abnormal expression of recognition molecules, and degeneration of myelin and axons. *Cell* 71:565-576.
- Ginsberg L, Malik O, Kenton AR, Sharp D, Muddle JR, Davis MB, Winer JB, Orrell RW, King RH (2004) Coexistent hereditary and inflammatory neuropathy. *Brain* 127:193-202.
- Gold BG, Voda J, Yu X, Gordon H (2004) The immunosuppressant FK506 elicits a neuronal heat shock response and protects against acrylamide neuropathy. *Exp Neurol* 187:160-170.

- Goodyear CS, O'Hanlon GM, Plomp JJ, Wagner ER, Morrison I, Veitch J, Cochrane L, Bullens RW, Molenaar PC, Conner J, Willison HJ (1999) Monoclonal antibodies raised against Guillain-Barre syndrome-associated *Campylobacter jejuni* lipopolysaccharides react with neuronal gangliosides and paralyze muscle-nerve preparations. *J Clin Invest* 104:697-708.
- Gordon S (2003) Alternative activation of macrophages. *Nat Rev Immunol* 3:23-35.
- Groh J, Weis J, Zieger H, Stanley ER, Heuer H, Martini R (2012) Colony-stimulating factor-1 mediates macrophage-related neural damage in a model for Charcot-Marie-Tooth disease type 1X. *Brain* 135:88-104.
- Groh J, Klein I, Hollmann C, Wettmarshausen J, Klein D, Martini R (2015) CSF-1-activated macrophages are target-directed and essential mediators of schwann cell dedifferentiation and dysfunction in Cx32-deficient mice. *Glia* 63:977-988.
- Groh J, Heidl K, Kohl B, Wessig C, Greeske J, Fischer S, Martini R (2010) Attenuation of MCP-1/CCL2 expression ameliorates neuropathy in a mouse model for Charcot-Marie-Tooth 1X. *Hum Mol Genet* 19:3530-3543.
- Guenard V, Montag D, Schachner M, Martini R (1996) Onion bulb cells in mice deficient for myelin genes share molecular properties with immature, differentiated non-myelinating, and denervated Schwann cells. *Glia* 18:27-38.
- Hall AB, Gakidis MA, Glogauer M, Wilsbacher JL, Gao S, Swat W, Brugge JS (2006) Requirements for Vav guanine nucleotide exchange factors and Rho GTPases in FcγR- and complement-mediated phagocytosis. *Immunity* 24:305-316.
- Hayasaka K, Takada G, Ionasescu VV (1993a) Mutation of the myelin P0 gene in Charcot-Marie-Tooth neuropathy type 1B. *Hum Mol Genet* 2:1369-1372.
- Hayasaka K, Ohnishi A, Takada G, Fukushima Y, Murai Y (1993b) Mutation of the myelin P0 gene in Charcot-Marie-tooth neuropathy type 1. *Biochem Biophys Res Commun* 194:1317-1322.
- Hayasaka K, Himoro M, Sato W, Takada G, Uyemura K, Shimizu N, Bird TD, Conneally PM, Chance PF (1993c) Charcot-Marie-Tooth neuropathy type 1B is associated with mutations of the myelin P0 gene. *Nat Genet* 5:31-34.
- Hendrickx DA, Koning N, Schuurman KG, van Strien ME, van Eden CG, Hamann J, Huitinga I (2013) Selective upregulation of scavenger receptors in and around demyelinating areas in multiple sclerosis. *J Neuropathol Exp Neurol* 72:106-118.
- Himoro M, Yoshikawa H, Matsui T, Mitsui Y, Takahashi M, Kaido M, Nishimura T, Sawaishi Y, Takada G, Hayasaka K (1993) New mutation of the myelin P0 gene in a pedigree of Charcot-Marie-Tooth neuropathy 1. *Biochem Mol Biol Int* 31:169-173.
- Huxley C, Passage E, Manson A, Putzu G, Figarella-Branger D, Pellissier JF, Fontes M (1996) Construction of a mouse model of Charcot-Marie-Tooth disease type 1A by pronuclear injection of human YAC DNA. *Hum Mol Genet* 5:563-569.

- Huxley C, Passage E, Robertson AM, Youl B, Huston S, Manson A, Saberan-Djoniedi D, Figarella-Branger D, Pellissier JF, Thomas PK, Fontes M (1998) Correlation between varying levels of PMP22 expression and the degree of demyelination and reduction in nerve conduction velocity in transgenic mice. *Hum Mol Genet* 7:449-458.
- Ip CW, Kroner A, Kohl B, Wessig C, Martini R (2009) Tacrolimus (FK506) causes disease aggravation in models for inherited peripheral myelinopathies. *Neurobiol Dis* 33:207-212.
- Ip CW, Kroner A, Fischer S, Berghoff M, Kobsar I, Maurer M, Martini R (2006) Role of immune cells in animal models for inherited peripheral neuropathies. *Neuromolecular Med* 8:175-190.
- Jerath NU, Shy ME (2015) Hereditary motor and sensory neuropathies: Understanding molecular pathogenesis could lead to future treatment strategies. *Biochim Biophys Acta* 1852:667-678.
- Kigerl KA, Gensel JC, Ankeny DP, Alexander JK, Donnelly DJ, Popovich PG (2009) Identification of two distinct macrophage subsets with divergent effects causing either neurotoxicity or regeneration in the injured mouse spinal cord. *J Neurosci* 29:13435-13444.
- Klein D, Groh J, Wettmarshausen J, Martini R (2014) Nonuniform molecular features of myelinating Schwann cells in models for CMT1: Distinct disease patterns are associated with NCAM and c-Jun upregulation. *Glia* 62:736-750.
- Klein D, Groh J, Weishaupt A, Martini R (2015) Endogenous antibodies contribute to macrophage-mediated demyelination in a mouse model for CMT1B. *J Neuroinflammation* 12:267.
- Kleopa KA, Scherer SS (2006) Molecular genetics of X-linked Charcot-Marie-Tooth disease. *Neuromolecular Med* 8:107-122.
- Kobsar I, Maurer M, Ott T, Martini R (2002) Macrophage-related demyelination in peripheral nerves of mice deficient in the gap junction protein connexin 32. *Neurosci Lett* 320:17-20.
- Kobsar I, Hasenpusch-Theil K, Wessig C, Muller HW, Martini R (2005) Evidence for macrophage-mediated myelin disruption in an animal model for Charcot-Marie-Tooth neuropathy type 1A. *J Neurosci Res* 81:857-864.
- Kobsar I, Oetke C, Kroner A, Wessig C, Crocker P, Martini R (2006) Attenuated demyelination in the absence of the macrophage-restricted adhesion molecule sialoadhesin (Siglec-1) in mice heterozygously deficient in P0. *Mol Cell Neurosci* 31:685-691.
- Kobsar I, Berghoff M, Samsam M, Wessig C, Maurer M, Toyka KV, Martini R (2003) Preserved myelin integrity and reduced axonopathy in connexin32-deficient mice lacking the recombination activating gene-1. *Brain* 126:804-813.

- Kohl B, Fischer S, Groh J, Wessig C, Martini R (2010a) MCP-1/CCL2 modifies axon properties in a PMP22-overexpressing mouse model for Charcot-Marie-tooth 1A neuropathy. *Am J Pathol* 176:1390-1399.
- Kohl B, Groh J, Wessig C, Wiendl H, Kroner A, Martini R (2010b) Lack of evidence for a pathogenic role of T-lymphocytes in an animal model for Charcot-Marie-Tooth disease 1A. *Neurobiol Dis* 38:78-84.
- Kroner A, Schwab N, Ip CW, Sommer C, Wessig C, Wiendl H, Martini R (2009) The co-inhibitory molecule PD-1 modulates disease severity in a model for an inherited, demyelinating neuropathy. *Neurobiol Dis* 33:96-103.
- Kuhlmann T, Wendling U, Nolte C, Zipp F, Maruschak B, Stadelmann C, Siebert H, Bruck W (2002) Differential regulation of myelin phagocytosis by macrophages/microglia, involvement of target myelin, Fc receptors and activation by intravenous immunoglobulins. *J Neurosci Res* 67:185-190.
- Kulkens T, Bolhuis PA, Wolterman RA, Kemp S, te Nijenhuis S, Valentijn LJ, Hensels GW, Jennekens FG, de Visser M, Hoogendijk JE, et al. (1993) Deletion of the serine 34 codon from the major peripheral myelin protein P0 gene in Charcot-Marie-Tooth disease type 1B. *Nat Genet* 5:35-39.
- Laemmli UK (1970) Cleavage of structural proteins during the assembly of the head of bacteriophage T4. *Nature* 227:680-685.
- Lowry OH, Rosebrough NJ, Farr AL, Randall RJ (1951) Protein measurement with the Folin phenol reagent. *J Biol Chem* 193:265-275.
- MacKinnon AC, Farnworth SL, Hodgkinson PS, Henderson NC, Atkinson KM, Leffler H, Nilsson UJ, Haslett C, Forbes SJ, Sethi T (2008) Regulation of alternative macrophage activation by galectin-3. *J Immunol* 180:2650-2658.
- Magee DM, Wing EJ, Ampel NM, Waheed A, Shadduck RK (1987) Macrophage colony-stimulating factor enhances the expression of Fc receptors on murine peritoneal macrophages. *Immunology* 62:373-378.
- Malandrini A, Villanova M, Dotti MT, Federico A (1999) Acute inflammatory neuropathy in Charcot-Marie-Tooth disease. *Neurology* 52:859-861.
- Mantovani A, Biswas SK, Galdiero MR, Sica A, Locati M (2013) Macrophage plasticity and polarization in tissue repair and remodelling. *J Pathol* 229:176-185.
- Mantovani A, Sica A, Sozzani S, Allavena P, Vecchi A, Locati M (2004) The chemokine system in diverse forms of macrophage activation and polarization. *Trends Immunol* 25:677-686.
- Martini R (1997) Animal models for inherited peripheral neuropathies. *J Anat* 191 (Pt 3):321-336.
- Martini R (2001) The effect of myelinating Schwann cells on axons. *Muscle Nerve* 24:456-466.

- Martini R, Toyka KV (2004) Immune-mediated components of hereditary demyelinating neuropathies: lessons from animal models and patients. *Lancet Neurol* 3:457-465.
- Martini R, Klein D, Groh J (2013) Similarities between inherited demyelinating neuropathies and Wallerian degeneration: an old repair program may cause myelin and axon perturbation under nonlesion conditions. *Am J Pathol* 183:655-660.
- Martini R, Fischer S, Lopez-Vales R, David S (2008) Interactions between Schwann cells and macrophages in injury and inherited demyelinating disease. *Glia* 56:1566-1577.
- Martini R, Zielasek J, Toyka KV, Giese KP, Schachner M (1995) Protein zero (P0)-deficient mice show myelin degeneration in peripheral nerves characteristic of inherited human neuropathies. *Nat Genet* 11:281-286.
- Mäurer M, Kobsar I, Berghoff M, Schmid CD, Carenini S, Martini R (2002) Role of immune cells in animal models for inherited neuropathies: facts and visions. *J Anat* 200:405-414.
- Mäurer M, Schmid CD, Bootz F, Zielasek J, Toyka KV, Oehen S, Martini R (2001) Bone marrow transfer from wild-type mice reverts the beneficial effect of genetically mediated immune deficiency in myelin mutants. *Mol Cell Neurosci* 17:1094-1101.
- Mauri C, Bosma A (2012) Immune regulatory function of B cells. *Annu Rev Immunol* 30:221-241.
- Micallef J et al. (2009) Effect of ascorbic acid in patients with Charcot-Marie-Tooth disease type 1A: a multicentre, randomised, double-blind, placebo-controlled trial. *Lancet Neurol* 8:1103-1110.
- Mietto BS, Jurgensen S, Alves L, Pecli C, Narciso MS, Assuncao-Miranda I, Villa-Verde DM, de Souza Lima FR, de Menezes JR, Benjamim CF, Bozza MT, Martinez AM (2013) Lack of galectin-3 speeds Wallerian degeneration by altering TLR and pro-inflammatory cytokine expressions in injured sciatic nerve. *Eur J Neurosci* 37:1682-1690.
- Miki Y, Tomiyama M, Haga R, Nishijima H, Suzuki C, Kurihara A, Sugimoto K, Hashiguchi A, Takashima H, Baba M (2013) A family with IVIg-responsive Charcot-Marie-Tooth disease. *J Neurol* 260:1147-1151.
- Mombaerts P, Iacomini J, Johnson RS, Herrup K, Tonegawa S, Papaioannou VE (1992) RAG-1-deficient mice have no mature B and T lymphocytes. *Cell* 68:869-877.
- Mosser DM (2003) The many faces of macrophage activation. *J Leukoc Biol* 73:209-212.
- Müller M, Berghoff M, Kobsar I, Kiefer R, Martini R (2007) Macrophage colony stimulating factor is a crucial factor for the intrinsic macrophage response in mice heterozygously deficient for the myelin protein P0. *Exp Neurol* 203:55-62.
- Nave KA (2010) Myelination and the trophic support of long axons. *Nat Rev Neurosci* 11:275-283.

- Nelis E, Timmerman V, De Jonghe P, Muylle L, Martin JJ, Van Broeckhoven C (1994) Linkage and mutation analysis in an extended family with Charcot-Marie-Tooth disease type 1B. *J Med Genet* 31:811-815.
- Oetke C, Vinson MC, Jones C, Crocker PR (2006) Sialoadhesin-deficient mice exhibit subtle changes in B- and T-cell populations and reduced immunoglobulin M levels. *Mol Cell Biol* 26:1549-1557.
- Pareyson D, Reilly MM, Schenone A, Fabrizi GM, Cavallaro T, Santoro L, Vita G, Quattrone A, Padua L, Gemignani F, Visioli F, Laura M, Radice D, Calabrese D, Hughes RA, Solari A (2011) Ascorbic acid in Charcot-Marie-Tooth disease type 1A (CMT-TRIAAL and CMT-TRAUK): a double-blind randomised trial. *Lancet Neurol* 10:320-328.
- Passage E, Norreel JC, Noack-Fraissignes P, Sanguedolce V, Pizant J, Thirion X, Robaglia-Schlupp A, Pellissier JF, Fontes M (2004) Ascorbic acid treatment corrects the phenotype of a mouse model of Charcot-Marie-Tooth disease. *Nat Med* 10:396-401.
- Patzko A, Shy ME (2011) Update on Charcot-Marie-Tooth disease. *Curr Neurol Neurosci Rep* 11:78-88.
- Philpott KL, Viney JL, Kay G, Rastan S, Gardiner EM, Chae S, Hayday AC, Owen MJ (1992) Lymphoid development in mice congenitally lacking T cell receptor alpha beta-expressing cells. *Science* 256:1448-1452.
- Pleasure DE, Chance PF (2005) Neurotrophin-3 therapy for Charcot-Marie-Tooth disease type 1A. *Neurology* 65:662-663.
- Rajabally Y, Vital A, Ferrer X, Vital C, Julien J, Latour P, Vandenberghe A, Lagueny A (2000) Chronic inflammatory demyelinating polyneuropathy caused by HIV infection in a patient with asymptomatic CMT 1A. *J Peripher Nerv Syst* 5:158-162.
- Ramaglia V, Daha MR, Baas F (2008) The complement system in the peripheral nerve: friend or foe? *Mol Immunol* 45:3865-3877.
- Ramaglia V, King RH, Morgan BP, Baas F (2009) Deficiency of the complement regulator CD59a exacerbates Wallerian degeneration. *Mol Immunol* 46:1892-1896.
- Ramaglia V, King RH, Nourallah M, Wolterman R, de Jonge R, Ramkema M, Vigar MA, van der Wetering S, Morgan BP, Troost D, Baas F (2007) The membrane attack complex of the complement system is essential for rapid Wallerian degeneration. *J Neurosci* 27:7663-7672.
- Reichert F, Rotshenker S (2003) Complement-receptor-3 and scavenger-receptor-AI/II mediated myelin phagocytosis in microglia and macrophages. *Neurobiol Dis* 12:65-72.
- Reilly MM, Shy ME (2009) Diagnosis and new treatments in genetic neuropathies. *J Neurol Neurosurg Psychiatry* 80:1304-1314.

- Reilly MM, Murphy SM, Laura M (2011) Charcot-Marie-Tooth disease. *J Peripher Nerv Syst* 16:1-14.
- Ritz MF, Lechner-Scott J, Scott RJ, Fuhr P, Malik N, Erne B, Taylor V, Suter U, Schaeren-Wiemers N, Steck AJ (2000) Characterisation of autoantibodies to peripheral myelin protein 22 in patients with hereditary and acquired neuropathies. *J Neuroimmunol* 104:155-163.
- Rotshenker S (2003) Microglia and macrophage activation and the regulation of complement-receptor-3 (CR3/MAC-1)-mediated myelin phagocytosis in injury and disease. *J Mol Neurosci* 21:65-72.
- Rotshenker S, Reichert F, Gitik M, Haklai R, Elad-Sfadia G, Kloog Y (2008) Galectin-3/MAC-2, Ras and PI3K activate complement receptor-3 and scavenger receptor-AI/II mediated myelin phagocytosis in microglia. *Glia* 56:1607-1613.
- Sahenk Z, Nagaraja HN, McCracken BS, King WM, Freimer ML, Cedarbaum JM, Mendell JR (2005) NT-3 promotes nerve regeneration and sensory improvement in CMT1A mouse models and in patients. *Neurology* 65:681-689.
- Sahenk Z, Galloway G, Clark KR, Malik V, Rodino-Klapac LR, Kaspar BK, Chen L, Braganza C, Montgomery C, Mendell JR (2014) AAV1.NT-3 gene therapy for charcot-marie-tooth neuropathy. *Mol Ther* 22:511-521.
- Saporta MA, Shy ME (2013) Inherited peripheral neuropathies. *Neurol Clin* 31:597-619.
- Schenone A, Nobbio L, Monti Bragadin M, Ursino G, Grandis M (2011) Inherited neuropathies. *Curr Treat Options Neurol* 13:160-179.
- Scherer SS, Wrabetz L (2008) Molecular mechanisms of inherited demyelinating neuropathies. *Glia* 56:1578-1589.
- Scherer SS, Xu YT, Nelles E, Fischbeck K, Willecke K, Bone LJ (1998) Connexin32-null mice develop demyelinating peripheral neuropathy. *Glia* 24:8-20.
- Schmid CD, Stienekemeier M, Oehen S, Bootz F, Zielasek J, Gold R, Toyka KV, Schachner M, Martini R (2000) Immune deficiency in mouse models for inherited peripheral neuropathies leads to improved myelin maintenance. *J Neurosci* 20:729-735.
- Schneider-Gold C, Kotting J, Epplen JT, Gold R, Gerding WM (2010) Unusual Charcot-Marie-Tooth phenotype due to a mutation within the intracellular domain of myelin protein zero. *Muscle Nerve* 41:550-554.
- Sereda M, Griffiths I, Puhlhofer A, Stewart H, Rossner MJ, Zimmerman F, Magyar JP, Schneider A, Hund E, Meinck HM, Suter U, Nave KA (1996) A transgenic rat model of Charcot-Marie-Tooth disease. *Neuron* 16:1049-1060.
- Shechter R, Schwartz M (2013) Harnessing monocyte-derived macrophages to control central nervous system pathologies: no longer 'if' but 'how'. *J Pathol* 229:332-346.

- Shy ME, Patzko A (2011) Axonal Charcot-Marie-Tooth disease. *Curr Opin Neurol* 24:475-483.
- Shy ME, Arroyo E, Sladky J, Menichella D, Jiang H, Xu W, Kamholz J, Scherer SS (1997) Heterozygous P0 knockout mice develop a peripheral neuropathy that resembles chronic inflammatory demyelinating polyneuropathy (CIDP). *J Neuropathol Exp Neurol* 56:811-821.
- Shy ME, Jani A, Krajewski K, Grandis M, Lewis RA, Li J, Shy RR, Balsamo J, Lilien J, Garbern JY, Kamholz J (2004) Phenotypic clustering in MPZ mutations. *Brain* 127:371-384.
- Sulaiman OA, Voda J, Gold BG, Gordon T (2002) FK506 increases peripheral nerve regeneration after chronic axotomy but not after chronic schwann cell denervation. *Exp Neurol* 175:127-137.
- Suter U, Scherer SS (2003) Disease mechanisms in inherited neuropathies. *Nat Rev Neurosci* 4:714-726.
- Taylor PR, Martinez-Pomares L, Stacey M, Lin HH, Brown GD, Gordon S (2005) Macrophage receptors and immune recognition. *Annu Rev Immunol* 23:901-944.
- Thomas PK (1999) Overview of Charcot-Marie-Tooth disease type 1A. *Ann N Y Acad Sci* 883:1-5.
- Timmerman V, Strickland AV, Zuchner S (2014) Genetics of Charcot-Marie-Tooth (CMT) Disease within the Frame of the Human Genome Project Success. *Genes (Basel)* 5:13-32.
- Van Overmeire E, Laoui D, Keirse J, Van Ginderachter JA, Sarukhan A (2014) Mechanisms driving macrophage diversity and specialization in distinct tumor microenvironments and parallelisms with other tissues. *Front Immunol* 5:127.
- Vargas ME, Watanabe J, Singh SJ, Robinson WH, Barres BA (2010) Endogenous antibodies promote rapid myelin clearance and effective axon regeneration after nerve injury. *Proc Natl Acad Sci U S A* 107:11993-11998.
- Verhamme C, de Haan RJ, Vermeulen M, Baas F, de Visser M, van Schaik IN (2009) Oral high dose ascorbic acid treatment for one year in young CMT1A patients: a randomised, double-blind, placebo-controlled phase II trial. *BMC Med* 7:70.
- Vital A, Vital C, Julien J, Fontan D (1992) Occurrence of active demyelinating lesions in children with hereditary motor and sensory neuropathy (HMSN) type I. *Acta Neuropathol* 84:433-436.
- Warrington AE, Rodriguez M (2008) Remyelination-promoting human IgMs: developing a therapeutic reagent for demyelinating disease. *Curr Top Microbiol Immunol* 318:213-239.

- Watanabe M, Yamamoto N, Ohkoshi N, Nagata H, Kohno Y, Hayashi A, Tamaoka A, Shoji S (2002) Corticosteroid- responsive asymmetric neuropathy with a myelin protein zero gene mutation. *Neurology* 59:767-769.
- Williams LL, Shannon BT, Wright FS (1993) Circulating cytotoxic immune components in dominant Charcot-Marie-Tooth syndrome. *J Clin Immunol* 13:389-396.
- Williams LL, Shannon BT, O'Dougherty M, Wright FS (1987) Activated T cells in type I Charcot-Marie-Tooth disease: evidence for immunologic heterogeneity. *J Neuroimmunol* 16:317-330.
- Willison HJ, Goodyear CS (2013) Glycolipid antigens and autoantibodies in autoimmune neuropathies. *Trends in immunology* 34:453-459.
- Willison HJ, Halstead SK, Beveridge E, Zitman FM, Greenshields KN, Morgan BP, Plomp JJ (2008) The role of complement and complement regulators in mediating motor nerve terminal injury in murine models of Guillain-Barre syndrome. *J Neuroimmunol* 201-202:172-182.
- Wrabetz L, D'Antonio M, Pennuto M, Dati G, Tinelli E, Fratta P, Previtali S, Imperiale D, Zielasek J, Toyka K, Avila RL, Kirschner DA, Messing A, Feltri ML, Quattrini A (2006) Different intracellular pathomechanisms produce diverse Myelin Protein Zero neuropathies in transgenic mice. *J Neurosci* 26:2358-2368.
- Wright BR, Warrington AE, Edberg DD, Rodriguez M (2009) Cellular mechanisms of central nervous system repair by natural autoreactive monoclonal antibodies. *Arch Neurol* 66:1456-1459.
- Ydens E, Cauwels A, Asselbergh B, Goethals S, Peeraer L, Lornet G, Almeida-Souza L, Van Ginderachter JA, Timmerman V, Janssens S (2012) Acute injury in the peripheral nervous system triggers an alternative macrophage response. *J Neuroinflammation* 9:176.
- Yoshida H, Hayashi S, Kunisada T, Ogawa M, Nishikawa S, Okamura H, Sudo T, Shultz LD (1990) The murine mutation osteopetrosis is in the coding region of the macrophage colony stimulating factor gene. *Nature* 345:442-444.
- Yuki N, Hartung HP (2012) Guillain-Barre syndrome. *N Engl J Med* 366:2294-2304.
- Zielasek J, Martini R, Toyka KV (1996) Functional abnormalities in P0-deficient mice resemble human hereditary neuropathies linked to P0 gene mutations. *Muscle Nerve* 19:946-952.

8. Appendices

8.1. Technical equipment

BioPhotometer 6131	Eppendorf (Hamburg, Germany)
Biosphere Filter Tips	Sarstedt (Nuernbrecht, Germany)
Centrifuges	
Biofuge 15R	Heraeus (Hanau, Germany)
Biofuge Pico	Heraeus (Hanau, Germany)
Centrifuge 5424	Eppendorf (Hamburg, Germany)
Cryostat CM 3050S	Leica (Wetzlar, Germany)
Dry block thermostat TDB-120	Hartenstein (Wuerzburg, Germany)
Dry block thermostat TDB-100	Hartenstein (Wuerzburg, Germany)
ELISA reader Original Multiskan	EX Labsystems (Helsinki, Finland)
Freezer	Liebherr (Biberach, Germany)
Gel chambers	
Horizontal Mini Gel System	Peqlab (Erlangen, Germany)
Mini-PROTEAN3 [®] cell	Bio-Rad (Munich, Germany)
Mini-Trans-Blot [®] cell	Bio-Rad (Munich, Germany)
Gel imager	Intas (Goettingen, Germany)
Heating plate	Medax (Neumuenster, Germany)
Homogenizer MICCRA D-8	ART (Muehlheim, Germany)
Hyperfilm ECL	GE Healthcare (Buckinghamshire, UK)
MicroAmp [®] Fast 96-well reaction plate	Applied Biosystems (Darmstadt, Germany)
Microscopes	
Axiophot 2	Zeiss (Oberkochen, Germany)
FluoView FV1000	Olympus (Hamburg, Germany)
LEO 906 E	Zeiss (Oberkochen, Germany)
Stemi 200 with KL 200	Zeiss (Oberkochen, Germany)
Neurosoft-Evidence 3102 electromyograph	Schreiber & Tholen Medizintechnik (Stade, Germany)
Object slides superfrost	Langenbrinck (Teningen, Germany)
Optical adhesive covers	Applied Biosystems (Darmstadt, Germany)
PapPen	SCI (Munich, Germany)
PCR tubes	Hartenstein (Wuerzburg, Germany)

Perfusion pump Reglo	Ismatec (Glattbrugg, Switzerland)
ProScan Slow Scan CCD camera	Pro Scan (Lagerlechfeld, Germany)
Pipettes	Abimed (Berlin, Germany)
	Eppendorf (Hamburg, Germany)
	Gilson (Bad Camberg, Germany)
Power supply	Bio-RAD (Munich, Germany)
PROTRAN® Nitrocellulose Transfer Membrane	Hartenstein (Wuerzburg, Germany)
Sonication device Sonoplus HD60	Bandelin Electronic (Berlin, Germany)
Thermocycler	
Step One Plus Real Time PCR System	Applied Biosystems (Darmstadt, Germany)
Mastercycler gradient	Eppendorf (Hamburg, Germany)
Primus96 advanced	Peqlab (Erlangen, Germany)
Ultracut	Leica (Wetzlar, Germany)
Software	
Adobe Photoshop CS3	Adobe (San Jose, USA)
Evidence	Schreiber & Tholen Medizintechnik (Stade, Germany)
FluoView	Olympus (Hamburg, Germany)
iTEM	Olympus (Hamburg, Germany)
ImageJ	NIH (Bethesda, USA)
Office 2007	Microsoft (Redmond, USA)
PASW Statistics 18 SPSS	IBM (Ehningen, Germany)

8.2. Reagents

Acetone	Invitrogen (Karlsruhe, Germany)
Agarose	Carl Roth (Karlsruhe, Deutschland)
α -Bungarotoxin	Thermo Scientific (Darmstadt, Germany)
Ammonium chloride	Merck (Darmstadt, Germany)
Ammonium persulfate (APS)	Carl Roth (Karlsruhe, Deutschland)
AmpliTaq DNA Polymerase	Applied Biosystems (Darmstadt, Germany)
Aqua-Poly/Mount®	Polysciences (Eppelheim, Germany)
Avidin-Biotin blocking kit	Vector Laboratories (Burlingame, USA)

Boric acid	Merck (Darmstadt, Germany)
Bovine serum albumine (BSA) 96%	Sigma-Aldrich (Munich, Germany)
Bromphenol blue	Sigma-Aldrich (Munich, Germany)
Chloroform	Sigma-Aldrich (Munich, Germany)
DAPI	Sigma-Aldrich (Munich, Germany)
Diethylpyrocarbonate (DEPC)	Sigma-Aldrich (Munich, Germany)
1, 4-Dithiothreitol (DTT)	Sigma-Aldrich (Munich, Germany)
ECL detection reagents	Ge Healthcare (Munich, Germany)
Ethylenediaminetetraacetic acid (EDTA)	Merck (Darmstadt, Germany)
Ethanol	Sigma-Aldrich (Munich, Germany)
Folin-Ciocalteu's phenol reagent, 2N	Carl Roth (Karlsruhe, Germany)
Gel Star DNA-Dye	Lonza (Basel, Switzerland)
Glycine	Sigma-Aldrich (Munich, Germany)
Glycerol	Merck (Darmstadt, Germany)
Glycogen	Roche (Mannheim, Germany)
HD Green DNA-Dye	Intas (Goettingen, Germany)
Heparin	Ratiopharm (Ulm, Germany)
Hepes	Carl Roth (Karlsruhe, Germany)
Ketavet	Pfizer (Berlin, Germany)
Lowry powder	Sigma-Aldrich (Munich, Germany)
2-Mercaptoethanol	Thermo Scientific (Darmstadt, Germany)
Methanol	Sigma-Aldrich (Munich, Germany)
2-Methylbutane	Carl Roth (Karlsruhe, Germany)
Nonidet P-40 substitute (NP-40)	Fluka (Buchs, Swiss)
O.C.T. medium	Sakura (Alphen aan den Rijn, Netherlands)
O Range Ruler 600bp DNA ladder	Thermo Scientific (Darmstadt, Germany)
Orange Loading Dye (6x)	Thermo Scientific (Darmstadt, Germany)
Page Ruler Plus prestained protein ladder	Thermo Scientific (Darmstadt, Germany)
Primers	Sigma-Aldrich (Munich, Germany)
Potassium di-hydrogen phosphate	Merck (Darmstadt, Germany)
Potassium chloride	Merck (Darmstadt, Germany)
Potassium hydrogen carbonate	Merck (Darmstadt, Germany)
Polyacrylamid	Carl Roth (Karlsruhe, Germany)
Ponceau S	Carl Roth (Karlsruhe, Germany)

Roti [®] -Block (10x)	Carl Roth (Karlsruhe, Germany)
Protease inhibitor cocktail set	Calbiochem (Darmstadt, Germany)
Sodium chloride solution	Merck (Darmstadt, Germany)
Sodium dodecyl sulfate (SDS)	Carl Roth (Karlsruhe, Germany)
Streptavidin	Biozol (Eching, Germany)
Sucrose	Carl Roth (Karlsruhe, Germany)
Tetramethylethylenediamine (TEMED)	Sigma-Aldrich (Munich, Germany)
Tris(hydroxymethyl)aminomethane (Tris)	Merck (Darmstadt, Germany)
Tris-HCl	Merck (Darmstadt, Germany)
TritonX-100	Carl Roth (Karlsruhe, Germany)
Tween20	Carl Roth (Karlsruhe, Germany)
Vinyl/ERL4221D	ServaElectrophoresis (Heidelberg, Germany)
Vitro-Clud [®]	Langenbrinck (Teningen, Germany)
Xylavet	CP-Pharma (Burgdorf, Germany)

8.3. Buffers and solutions

Anaesthetic	1.2% Ketavet 0.08% Xylavet 0.9% NaCl
DABCO	25% PBS 75% Glycerol 25 mg/ml 1,4-diazabicyclo[2.2.2]octane Store at 4°C protected from light
DEPC-H ₂ O	0.01% diethyl pyrocarbonate (DEPC) Dissolve in distilled water, autoclave
Gel running buffer (10x)	0.25M Tris 1.92M Glycin 1% SDS Store at 4°C

Laemmli (6x)	12% Tris-HCl 12% SDS 2.4% EDTA 20% Glycerol 0.1% Bromphenol blue 4.75% 2-Mercaptoethanol Store at -20°C
Methylene blue	1% Methylene blue 1% Azure II 40% Saccharose pH 9.2
PBS (1x)	137 mM NaCl 2.7 mM KCl 1.5 mM KH ₂ PO ₄ 8.1 mM Na ₂ HPO ₄ pH 7.4
PBST (1x)	0.1% Tween 20 in PBS
Ponceau S	1% Trichloroacetic acid 0.1% Ponceau S Store protected from light
RIPA lysis buffer	25 mM Tris pH 8 10 mM Hepes pH 4.4 150mM NaCl 5mM MgCl ₂ 145 mM KCl 0.4 % EDTA 0.1 % SDS 1% Nonidet P40

	10 % Glycerol Store at 4°C
SDS PAGE buffer (10x)	0.25M Tris 1.92M Glycine 1% SDS Store at 4°C
Separating gel buffer (4x)	1.5M Tris 0.4% SDS 0.4% TEMED pH 8.8 Store at 4°C
Spurr's medium	10 g Vinyl/ERL 6 g DER 736 26 g NSA 26g 0.4 g DMAE
Stacking gel buffer (4x)	0.5M Tris 0.4% SDS 0.4% TEMED pH 6.8 Store at 4°C
Stripping-buffer	0.2M Glycine 0.1% SDS 20mM Dithiotreitol 1% Tween20 pH 2.1 Store at 4°C
TBE	89mM Tris 89mM Borate

	2mM EDTA pH 8.0
Transfer buffer (10x)	0.25M Tris 1.92M Glycine Store at 4°C.
Transfer buffer (1x)	20% Methanol Dissolve in 1x Transfer buffer

Unless otherwise mentioned, distilled water was used as solvent and solutions were stored at room temperature.

8.4. Primer sequences for genotyping

P0

S 1295 5'-TCAGTTCCTTGTCCCCCGCTCTC-3'

AS 1606 5'-GGCTGCAGGGTCGCTCGGTGTTTC-3'

AS 1772 5'-ACTTGTCTCTTCTGGGTAATCAA-3'

JHD

JH FW 5'-GAGGAGACGGTGACCGTGGTCCCTGC-3'

JH Rev 5'-GGACCAGGGGGCTCAGGTCCTC-AGG-3'

Neo FW 5'-GCCGCATTGCATCAGCCATGAT-GGA-3'

Neo Rev 5'-CCTTGCGCAGCTGTGC-TCGACGTTG-3'

RAG1

RAG-1F1 5'-GAGGTTCCGCTACGACTCTG-3'

RAG-1F2 5'-CCGGACAAGTTTTTCAT-CGT-3'

RAG-1R 5'-TGGATGTGGAATTGTTGCGAG-3'

8.5. Antibodies used in immunohistochemistry

Primary antibodies

Reactivity	Host	Catalog number	Company	Dilution	Fixation / Additives	Conjugation
B220	Rat	550286	BD Pharm.	1:100	Acetone / -	none
β -III-Tubulin	Rabbit	ab18207	Abcam	1:500	- / -	none
C3	Goat	0855500	MP Biomedicals	1:100	Acetone / 0.3% TritonX	FITC
CD4	Rat	MCA1767	Serotec	1:1000	Acetone / -	none
CD8	Rat	MCA609G	Serotec	1:500	Acetone / -	none
CD86	Rat	553688	BD Pharm.	1:100	Acetone / -	none
CD206	Rat	MCA2235	Serotec	1:2000	Acetone / 0.3% TritonX	none
F4/80	Rat	MCA497B	Serotec	1:300	Acetone / -	Biotin
IgG-Fc	Goat	715-166-150	Dianova	1:300	- / -	Cy3
IgG-Fc	Rabbit	31194	Thermo Scientific	1:1000	- / -	none
P0	Chicken	NB100-1607	Acris	1:500	Acetone / 0.2% TritonX	none
SMI32	Mouse	smi-32r	Covance	1:10000	Acetone / 0.2% TritonX	none
Synaptophysin	Guinea pig	101004	Synaptic Systems	1:500	- / 0.3% TritonX	none

Secondary antibodies

Reactivity	Host	Catalog number	Company	Dilution	Conjugation
Chicken IgG	Goat	A-11039	Invitrogen	1:300	AF488
Guinea pig IgG	Donkey	706-165-148	Dianova	1:300	Cy3
Mouse IgG	Goat	115-175-146	Dianova	1:500	Cy5
Rabbit IgG	Goat	111-165-144	Dianova	1:300	Cy3
Rat IgG	Goat	112-165-167	Serotec	1:300	Cy3

9. Abbreviations

AF	Alexa fluor
BSA	Bovine serum albumine
°C	Degree Celsius
CCL	Chemokine (C-C motif) ligand
CD	Cluster of differentiation
cDNA	Complementary DNA
CHN	Congenital hypomyelinating neuropathy
CIDP	Chronic inflammatory demyelinating polyneuropathy
CMAP	Compound muscle action potential
CMT	Charcot-Marie-Tooth
CR3 (CD11b)	Complement receptor 3
CSF-1/M-CSF	Macrophage colony stimulating factor
CSF-1R	CSF-1 receptor
Cx32/Gjb1	Connexin 32 / Gap junction protein, beta-1
Cy	Cyanine
DABCO	1,4Diazobicyclo[2.2.2]octan
DAPI	4',6-diamidino-2-phenylindole
DEPC	Diethylpyrocarbonate
DMAE	Dimethylethanolamine
DNA	Deoxyribonucleic acid
dNTP	Deoxynucleosidtriphosphate
DSN	Dejerine-Sottas neuropathy
DTT	1,4-Dithiothreitol
ECL	Enhanced chemiluminescence
EDTA	Ethylene diamine tetraacetic acid
EGR2/KROX20	Early growth response protein 2
ERK1/2	Extracellular-signal regulated kinase
ERL	Epoxycyclohexylmethyl-3,4-epoxycyclohexylcarboxylate
FcγR	Fc-gamma receptor
FIZZ1	Resistin-like molecule alpha1 (Relm alpha)

h	Hour
het	Heterozygous
HMSN	Hereditary motor and sensory neuropathy
HRP	Horseradish peroxidase
IgG	Immunoglobulin G
IgM	Immunoglobulin M
IL	Interleukin
INF γ	Interferon-gamma
iNOS	Inducible nitric oxide synthase
ITAM	Immunoreceptor tyrosine-based activation motif
i.v.	Intravenously
IVIG	Intravenous immunoglobulin
JHD	J _h -region deficient
kDa	Kilo Dalton
KLH	Keyhole limpet hemocyanin
LIF	Leukemia inhibitory factor
MCP-1/CCL2	Monocyte chemoattractant protein
MFN2	Mitofusin 2
min	Minutes
MPZ/P0	Myelin protein zero
mRNA	Messenger RNA
MTMR2	Myotubularin-related protein 2
MuLV	Murine Leukemia Virus
NCV	Nerve conduction velocity
NEFL	Neurofilament light polypeptide
NSA	Nonenylsuccinic anhydride
PBS / PBST	Phosphate buffered saline / PBS Tween
PCR	Polymerase chain reaction
PD-1	Programmed cell death 1
PFA	Paraformaldehyde
PMP22	Peripheral myelin protein-22
PNS	Peripheral nervous system
qRT-PCR	Semiquantitative real-time PCR

RAG	Recombination activating gene
RIPA	Radio-immuno precipitation assay
rRNA	Ribosomal RNA
RNA	Ribonucleic acid
RT	Room temperature
s	Seconds
SC	Schwann cell
SD	Standard deviation
SDS	Sodium dodecylsulfate
SDS-PAGE	SDS polyacrylamide gel electrophoresis
TAM	Tumor associated macrophages
TBE	Tris-borate-EDTA
TCR- α	T-cell receptor alpha
TEMED	Tetramethylethylenediamine
TGF- β	Transforming growth factor-beta
TLR	Toll-like receptor
TNF α	Tumor necrosis factor-alpha
TREM-2	Triggering receptor expressed on myeloid cells-2
Tris	Tris(hydroxymethyl)aminomethane
UPR	Unfolded protein response
wt	Wildtype
Ym1	Chitinase 3-like 3

10. Curriculum vitae

Persönliche Daten:

Name: Dennis Klein

Geburtstag und -ort: 28.02.1985 in Alzenau i. Ufr.

Familienstand: verheiratet, keine Kinder

Schule

- 09/1991 - 08/1992** Volksschule Krombach-Geiselbach
09/1992 - 08/1995 Volksschule Schöllkrippen
09/1995 - 06/2004 Spessart - Gymnasium Alzenau;
 Abschluss: allgemeine Hochschulreife

Hochschulstudium

- 10/2004 - 09/2006** Grundstudium der Biologie (Diplom) an der Universität Würzburg
10/2006 - 10/2009 Hauptstudium der Biologie (Diplom) an der Universität Würzburg
 Hauptfach: Neurobiologie
 Nebenfächer: Genetik, Zell- und Entwicklungsbiologie
12/2008 - 10/2009 Diplomarbeit in der Abteilung Experimentelle Entwicklungsneurobiologie (Prof. Rudolf Martini), Neurologische Klinik und Poliklinik, Universitätsklinikum Würzburg
 Titel: „Studien zur Charakterisierung von Makrophagen bei Myelinmutanten des peripheren Nervensystems“

Berufliche Tätigkeiten

- 10/2009 - 03/2010** Wissenschaftlicher Mitarbeiter in der Abteilung Experimentelle Entwicklungsneurobiologie (Prof. Rudolf Martini), Neurologische Klinik und Poliklinik, Universitätsklinikum Würzburg
seit 04/2010 Mitglied der GSLS, Bereich Neurowissenschaften;
 Wissenschaftlicher Mitarbeiter in der Abteilung Experimentelle Entwicklungsneurobiologie (Prof. Rudolf Martini), Neurologische Klinik und Poliklinik, Universitätsklinikum Würzburg

Ort, Datum

Unterschrift

11. Publications

Original articles in peer-reviewed international journals

Klein D, Patzkó Á, Schreiber D, van Hauwermeiren A, Baier M, Groh J, West BL, Martini R Targeting the CSF-1 receptor alleviates two forms of Charcot-Marie-Tooth disease in mice. *in preparation*

Ip CW, Isaias IU, Tekin BB, **Klein D**, Groh J, Alttoa A, Higuchi T, Toyka KV, Reif A, Volkmann J TorsinA deficiency leads to central dopaminergic malfunction in a mouse model of injury induced focal dystonia. *in preparation*

Moldovan M, Romer Rosberg M, Alvarez S, **Klein D**, Martini R, Krarup C Aging-associated motor axon Na_v1.8 channelopathy in mice. *in preparation*

Pausch J, Groh J, **Klein D**, Martini R Endoneurial macrophages show a preferential localization near nodes of Ranvier in normal and diseased nerves. *in preparation*

Klein D, Groh J, Weishaupt A, Martini R (2015) Endogenous antibodies contribute to macrophage-mediated demyelination in a mouse model for CMT1B. *J Neuroinflammation* 12:267

Groh J, Klein I, Hollmann C, Wettmarshausen J, **Klein D** and Martini R (2015) CSF-1-activated macrophages are target-directed and essential mediators of Schwann cell dedifferentiation and dysfunction in Cx32-deficient mice. *GLIA* 63:977-988.

Klein D*, Groh J*, Wettmarshausen J, Martini R (2014) Non-uniform molecular pattern of myelinating Schwann cells in models for CMT1. *GLIA* 62:736-750 (*These authors contributed equally to this work)

Ip CW, Kroner A, Groh J, Huber M, **Klein D**, Spahn I, Diem R, Williams SK, Nave KA, Edgar JM, Martini R (2012) Neuroinflammation by cytotoxic T-lymphocytes impairs retrograde axonal transport in an oligodendrocyte mutant mouse. *PLoS One* 7: e42554.

Moldovan M, Alvarez S, Pinchenko V, **Klein D**, Nielsen FC, Wood JN, Martini R, Krarup C (2011) Na(v)1.8 channelopathy in mutant mice deficient for myelin protein zero is detrimental to motor axons. *Brain* 134:585-601.

Review article

Martini R, **Klein D**, Groh J (2013) Similarities between inherited demyelinating neuropathies and Wallerian degeneration: an old repair program may cause myelin and axon perturbation under non-lesion conditions. *Am J Pathol* 183:655-660.

Book chapter

Groh J, **Klein D**, Kroner A, Martini R (2015) Inflammation in the Pathogenesis of Inherited Peripheral Neuropathies. In: *Neuroinflammation: New Insights into Beneficial and Detrimental Functions* (David S, editor). Wiley-Blackwell ISBN: 978-1-118-73282-3.

Oral presentations

Klein D et al., (2014) CMT Association Face-to-Face Meeting of the Scientific Advisory Group, Washington DC, USA: "CSF-1 Receptor Inhibition as a Treatment Option in a CMT1X model".

Klein D et al., (2014) Arbeitstagung der Bayerischen Neuromuskulären Zentren, Erlangen, Germany: "Behandlung der CMT1X (und CMT1B) im Mausmodell durch oral-induzierte Blockade des Rezeptors für das Zytokin CSF-1".

Poster presentations

Klein D et al., (2012) Graduate School of Life Sciences Symposium 2012, Wuerzburg, Germany: "The role of antibody accumulation in genetically mediated neuropathies".

Klein D et al., (2013) Current Topics in Myelin Research, Kassel, Germany: “The role of antibody accumulation in genetically mediated neuropathies”.

Klein D et al., (2014) Training course on PNS development, function, damage, regeneration and remyelination, Lecce, Italy: “Endogenous antibodies contribute to demyelination in a mouse model for CMT1B”.

12. Danksagung

Zunächst möchte ich mich bei Herrn Prof. Rudolf Martini bedanken, dass er es mir ermöglichte, meine Doktorarbeit in seiner Arbeitsgruppe anfertigen zu können. Des Weiteren möchte ich ihm für seine langjährige Betreuung und Unterstützung als Mentor aufrichtig danken. Seine Diskussions- und Gesprächsbereitschaft sowie seine hilfreichen Ratschläge haben sehr zum Gelingen dieser Arbeit beigetragen.

Zudem möchte ich mich bei meinen weiteren Betreuern, Frau Prof. Claudia Sommer und Herr Prof. Wolfgang Rössler, bedanken, die mir in meinem Promotionskomitee der GSLS ebenfalls stets mit hilfreichen Ratschlägen und neuen Ideen zur Seite standen. Weiterhin möchte ich mich zusätzlich bei Herrn Prof. Rössler für die bereitwillige Übernahme des Zweitgutachtens sowie bei Herrn Prof. Utz Fischer für den Vorsitz im Promotionskomitee bedanken.

Herrn Prof. Klaus V. Toyka und Dr. Carsten Wessig möchte ich besonders für die geduldigen Demonstrationen und das dadurch mögliche Erlernen elektrophysiologischer Ableitungen im Maus-Model danken.

Ebenso bin ich dem IZKF Würzburg und der DFG für die finanzielle Unterstützung und Förderung während meiner Doktorarbeit zu tiefstem Dank verpflichtet.

Der aktuellen Gruppe der AG Martini, Dr. Mihaela Gurgui, David Schreiber, David Stadler, Susanne Kerscher, David Komla Kessie, Xidi Yuan, Michaela Hörner und Jonas Pausch danke ich für eine wunderbare Arbeitsatmosphäre, welche die Zusammenarbeit sehr einfach machte. Besonders gilt dies für meine langjährigen Kollegen Dr. Janos Groh, seine hervorragenden wissenschaftlichen Diskussionen und Anmerkungen sowie das Einarbeiten in einige Techniken, Heinrich Blazyca, der unter anderem mit seinen Gesangskünsten in allen Sprachen der Welt immer wieder für Erheiterung sorgte, Silke Loserth, die ich sehr für ihre gewissenhafte und ordentliche Arbeit schätze und selbst nach gefühlten 10000 Färbungen und 2 Mio. geteaster Nervenfasern immer noch gut gelaunt war und freudige Diskussionen mit mir führte sowie Bettina Meyer, die nicht nur hervorragende PCR-Arbeit macht, sondern auch noch sehr guten Kaffee kocht ;-).

Nicht zu vergessen sind natürlich auch die Mitarbeiter anderer Labore der Kopfklinik. Vor allem möchte ich mich bei Dr. Andreas Weishaupt, der immer ein offenes Ohr für wissenschaftliche Fragen hatte und mich sehr mit hilfreichen Hinweisen und Anmerkungen unterstützte, und Dr. Chi Wang Ip für die Nerv-Läsions Operationen bedanken.

Weiterer Dank gebührt unseren Kollegen in Glasgow, Prof. Hugh Willison und Dr. Rhona McGonigal, die durch anregende wissenschaftliche Diskussion und Ideen ebenso zum Gelingen dieser Arbeit beigetragen haben. Besonders möchte ich hier dem leider viel zu früh verstorbenen Prof. Uwe-Karsten Hanisch (Göttingen) für die wissenschaftliche Beratung und Inspiration danken.

Ein ebenso gebührender Dank gehört unserem wunderbaren „Tierhaltungs-Team“: Helga Brüner, Anja Weidner, Jaqueline Schreiber und Jennifer Bauer, für die sehr gute Pflege unserer Mäuse und die gute Organisation beim Verpaaren der Tiere, auch bei Sonderwünschen. Hervorheben möchte ich auch den leider verstorbenen Karl-Heinz Aulenbach, dessen freudiges und engagiertes „Aber selbstverständlich!“ ich nie vergessen werde.

Ebenso danke ich meinen ehemaligen Praktikantinnen. Es war ein stets angenehmer Umgang und zuletzt konnten interessante wissenschaftliche Daten erhoben werden. Danke an Anemoon van Hauwermeiren, Michaela Baier, Anne Quatraccioni, Eva Gerten, Sina Wäldchen, Lucie Valek und besonders Marianne Huber.

Weiterhin möchte ich hier natürlich auch einige ehemalige Mitarbeiter des Labors nicht auslassen und für viele interessante Diskussion und tolle Momente während meiner Doktorarbeit danken: Dr. Ágnes Patzkó, Irene Spahn, Kristina Heinl, Ines Klein und Jennifer Wettmarshausen.

Zum Schluss gilt mein tiefster Dank meiner Frau Jenni, meiner Familie und meinen ganzen Freunden, die mich über die Jahre in allen Bereichen immer unterstützen und stets einen großen Halt darstellen. Danke dafür!